Master Thesis

Fracturing Mechanisms in Granite when Exposed to Different Modes of Microwave Irradiation

Behnam Akbari

Supervised by

Dr.mont. Philipp Hartlieb

(August / 2017)

Chair of Mining Engineering and Mineral Economics
Department Mineral Resources and Petroleum Engineering
Motanuniversitaet Leoben

A-8700 LEOBEN, Franz Josef Straße 18
Phone: +43/(0)3842-402-2001
Fax: +43/(0)3842-402-2002
bergbau@unileoben.ac.at

Declaration of authorship

I declare in lieu of oath that I wrote this thesis and performed the associated research myself, using only literature cited in this volume.

August/2017 Behnam Akbari

……

Acknowledgement

I would like to thank my research supervisor Dr. Philipp Hartlieb, for all of his valuable insights and constant support.

A further thank you to colleagues from Sandvik Company for helping us with large scale experiments as well as Mr. Klaus Lackner at the laboratory of Montanuniversität for the preparation of cores for computer tomography.

Special thanks to Dr. Bernd Oberdorfer at ÖGI Company for all his efforts in providing us with comprehensive images made by Computer Tomography system.

A great thank you to my friends Dip.Ing Fatima Fazeli and MSc Vagef Abbdolahi for their assistance in computer digitizing.

Last but not the least, I would like to express a special appreciation to my parents who gave me their love and support in every step of my life.

Abstract

Drilling and blasting is one of the most convenient and commonly used methods to break rocks in mining and civil applications. Due to numerous environmental, safety and productivity issues, the industry and contractors are looking for an alternative rock breaking system. Heating of rocks and minerals with the help of microwave treatments has therefore been the topic of many laboratory investigations and field tests since last decades.

The focus of this research is to describe the effect of microwave energy on big samples of hard Granite rocks which are not completely wave absorbent. 3 different tests were carried out using high power density radiation with magnitudes of 15 KW and 20 KW on 3 Granite blocks at Sandvik Company with the help of a 30 KW industrial microwave machine. Further on, after drilling and preparing the core and getting Computer tomography images, a complete sketch of all the cracks in small-scale and big-scale conditions were digitally made using AutoCAD software.

It was concluded that microwave energy generates high temperatures within the rocks and causes a small thermal damage on the surface that leads to a crack network underneath. By means of this investigation, it is also believed that heating is not a source directly for crack itself, but it is an initiation for thermal fracturing and later cracking.

Keywords: Drilling and blasting, Rock breakage, microwave treatments, thermal fracturing, Granite rocks, cracks

Zusammenfassung

Bohren und Sprengen ist eine der einfachsten und meistgenutzten Methoden zur Gesteinszerkleinerung im Bereich Bergbau und Bauwesen. Aufgrund zahlreicher ökologischer, sicherheits- und produktionstechnischer Schwierigkeiten wird nach alternativen Zerkleinerungsmethoden gesucht. Das Erhitzen von Gesteinen und Mineralien mithilfe von Mikrowellen war deshalb in den letzten Jahrzehnten Gegenstand vieler Labor- und Feldversuche.

Der Schwerpunkt dieser Untersuchung ist die Beschreibung des Effekts von Mikrowellenenergie auf große Granitproben, welche die Mikrowellenstrahlung nicht gänzlich absorbieren. In einer Anlage der Firma Sandvik wurden drei verschiedene Tests durchgeführt, wobei eine hohe Leistungsdichte der Strahlung von 15 und 20 kW an den drei Granitproben getestet wurde. Eingesetzt wurde dabei eine Industrie-Mikrowelle mit einer maximalen Leistung von 30 kW. Darüber hinaus wurde nach dem Bohren und der Probenvorbereitung eine Computertomographie durchgeführt. Dokumentiert wurden die Mikro- und Makro-Risse digital mithilfe von AutoCAD.

Aus den Ergebnissen wird geschlossen, dass Mikrowellenenergie hohe Temperaturen im Inneren des Gesteins und kleine thermische Schäden an der Gesteinsoberfläche erzeugen kann, welches zu einem darunterliegenden Netzwerk von Rissen führt. Im Rahmen dieser Untersuchung wird angenommen, dass das Aufheizen nicht direkt zu Rissen führt, sondern die Rissbildung durch thermische Brüche induziert wird.

Schlagworte: Bohren und Sprengen, Gesteinszerkleinerung, Mikrowellen, Thermische Rissbildung, Granitgestein, Risse

Table of contents

1 Introduction

As far as history goes, humans have increasingly used various rock breakage techniques. Today rock breakage is a common practice in mining and civil applications, presenting a number of challenges, especially in the case of extremely hard rock types. To facilitate the breaking process of hard rocks, many techniques have been developed and applied, such as 1) mechanical 2) explosive and 3) secondary methods (e.g. thermal, fluid, sonic, chemical, electrical, water jet and laser). Using explosives limitations that alter the productivity and advance rate of a project. Mechanical techniques remain the most efficient and economical, but the search for novel hard rock breakage techniques continues, particularly in light of today‘s economic factors and safety regulations.

1) Mechanical rock breakage:

Mechanical excavation refers to a method of rock breakage in which the rock is entirely removed from the mining site with the help of mechanical cutting tools. In past few years, mechanical excavation has obtained more popularity, especially in underground mining and construction. Mechanical rock excavation is conceptually compared to a drill-and-blast operation. The benefits of mechanical excavation are observed as improvements in safety, production rate, the degree of automation, minimizing damage to the walls, and control over the process, uniformity of product size and elimination of blast vibrations.

The most widely used mechanical excavators are raise boring machines, TBM, roadheaders, longwall shearers and continuous miners. However, unconventional techniques such as laser drills, microwave rock-breakage systems, projectile impact and water jets are also classified as mechanical excavation methods. (Rostami J, Mechanical rock breakage, SME Mining Engineering Handbook third edition 2011)

2) Rock breakage by blasting:

As an explosive charge detonates in a drill hole, a chemical reaction takes place, rapidly changing the solid or liquid explosive material into a hot gas. This reaction starts immediately and forms a convex shock wave on the front edge that acts on the borehole wall and further propagates through the explosives’ column. The shock

wave cracks and crushes the rock in the vicinity of the charge, also creating a network of cracks around the blast hole.

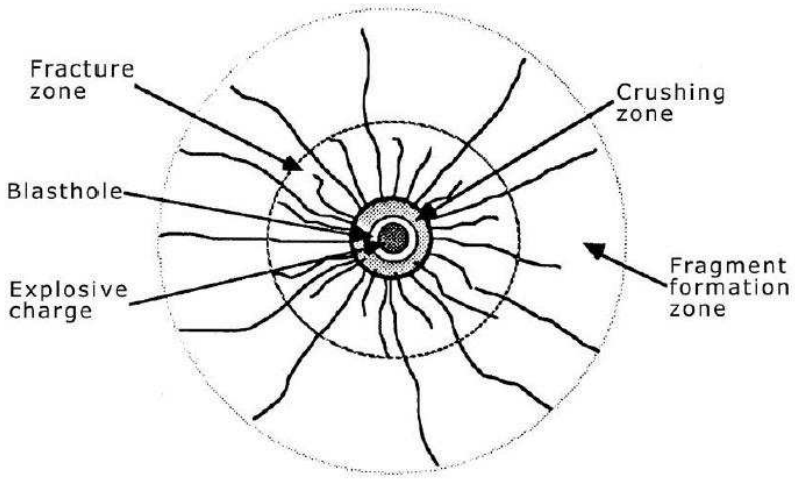

Figure 1: Schematic illustration of processes occurring in the rock around a blast hole, showing formation of crushing zones, fracture zones and fragment formation zone (Whittaker BN et al, 1992)

3) Unconventional rock breakage by Microwave (alternative rock breakage):

Microwave technology has been around for decades and has since been extensively used in the medical, food and telecommunication industries. It was found, in the early stages of development, that “an alternating electric field can alter the energy content of dipolar substances. This energy would later be released in the form of heat (Osepchuck, 1984)”. Hence, in order to predict the absorbed energy and the generated heat, research on the dielectric and thermal properties of various materials is of great importance.

Application of microwave technology as an electrical technique that does not involve mechanical tools was first proposed by Maurer in 1968. Initially, due to the high usage of energy, the technology was rendered as ‘not economically feasible’. However, the higher capital costs of microwave systems could be compensated by its lower operating costs and higher productivity especially in mine to mill process in mining applications. (Nekoovaght P, 2015)

Breaking rocks with a microwave is governed by the absorption of microwave energy combined with the conversion of electromagnetic energy to heat, by means of inducing stresses affected by differential thermal expansion. Owing to the details of the absorption process, mineralogy of rocks and heat transfer, a certain

temperature distribution is generated inside the rock which results in induced stresses. The main outcome of most industrial microwave applications is generating cracks as a result of thermal stresses which are environmentally friendly in comparison with mechanical methods and offer a safer operation with less energy intake. (Nekoovaght P, 2009)

2 Electromagnetic waves

Electromagnetic waves are waves that can travel through vacuum. The simplest example would be light waves. Mechanical waves, as opposed to electromagnetic waves, require a material medium in order to convey their energy from one location to another. Sound waves are an example of mechanical waves.

Electromagnetic waves are generally produced when an electric charge is vibrated, a vibration that creates a wave with both an electric and a magnetic component. An electromagnetic wave travels at a speed of 3.00×10^8 m/s), whereas the propagation of the same electromagnetic wave through a material medium occurs at a lower net speed.

The electromagnetic radiations are classified by their wave frequencies. They are generally ordered with increasing frequency as the amount of energy carried out by these waves increases with increasing frequency. Some common electromagnetic waves include gamma rays (with very high-frequency), x-rays, ultraviolet radiation, visible light, infrared radiation, microwaves and less energetic radio waves (with very low frequency and long wavelengths). (Scott, 2006)

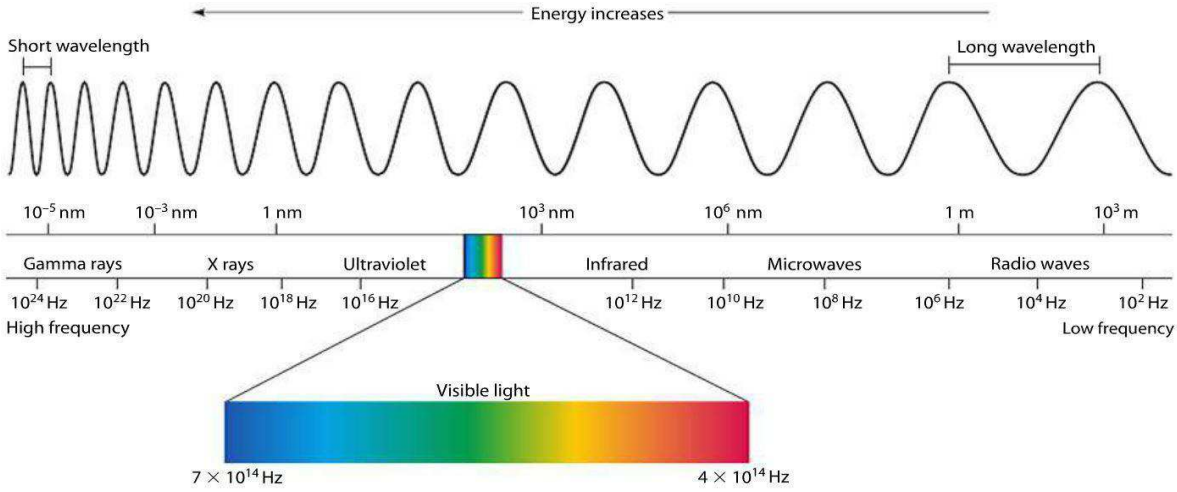

Figure 2: Electromagnetic waves spectrum (www.pinterest.com).

2.1 Microwave Energy

In 1888, Hertz managed to create the first microwave radiations with frequencies up to 500 MHz by means of oscillatory spark discharges. In 1946, Dr. P Spencer was experimenting a theory with a vacuum tube called ‘magnetron’ when he noticed a candy bar in his pocket had melted. This incident later led to the first microwave oven patent submission.

Microwaves belong to that part of the electromagnetic spectrum between the infrared range and the radio frequency range with wavelengths between 1 m and 1 mm (Stuchly, 1983). Characteristics of microwaves, like all other electromagnetic waves, as well as their wavelength and frequency, are related together by the following equation 1 (Giancoli, 1988):

$$C=\lambda*f \qquad (1)$$

Where:

- c represents the speed of light (3 × 108) in ‘m.s-1’
- λ represents the wavelength, in ‘m’
- f represents the frequency, in ‘Hz’

Microwaves lie in the frequency range of 300 to 300,000 megahertz (MHz). Within this spectrum, a frequency 2.45GHz of microwave energy is the most popular and

most commonly used. This includes the domestic and industrial use of microwave energy. The corresponding wavelength and energy for this frequency are 12.2 cm and 1.02 x 10^{-5} eV respectively (Jacob J et. al, 1995). The amount of transmitted energy is connected to the increase in frequency and reduction in the wavelength. The components of the microwave energy, just like any electromagnetic wave, are electronic and magnetic waves which travel perpendicular to each other. (Nekoovaght, 2009).

Figure 3 shows this motion in detail.

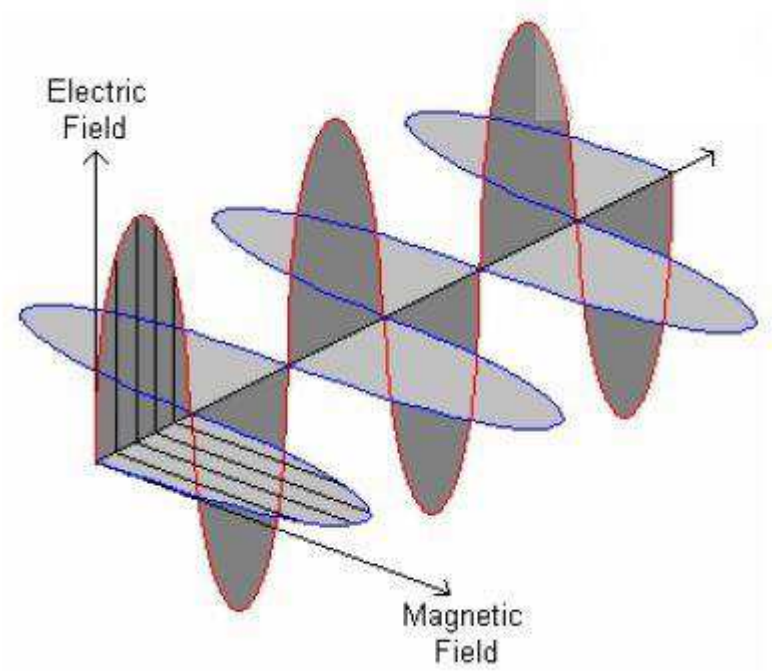

Figure 3: Electric and magnetic components in an electromagnetic wave (Scott 2006).

2.2 Properties of microwaves

Both electric and the magnetic fields obey the law of superposition. These fields can be described as vector fields, meaning that all magnetic and electric field vectors can be added together according to vector addition.

This quality recalls different phenomena like reflexion, diffraction, and refraction, all directly correlated to the wavelength and the frequency of the electromagnetic wave.

In concept, the radiation caused by an electromagnetic wave hitting a molecular structure will induce oscillation in the atoms, triggering them to emit their own electromagnetic wave.

Microwaves possess less energy in comparison to other waves within the electromagnetic spectrum. However, they are still a prime candidate for use in heating applications owing to their relatively large penetration depth into a body along with their relatively high power dissipation in certain material. Although they pass through materials like glass, paper, plastic and ceramic, they are absorbed by food and water and reflected by metals. (Scott, 2006)

2.3 Interaction of microwaves with material

Basically, all materials can be classified into three main groups:

- Conductors (reflecting microwaves)
- Insulators (allowing microwave to pass through with no effect)
- Absorbers (absorbing a part of the microwaves and producing heat in return)

As explained in the last section, microwaves are reflected from the surface of the metals, therefore, do not produce heat. Metals, in general, have high conductivity and are known to be good conductors. Such conductors are often used as conduits (waveguide) for microwaves. Furthermore, materials can be classified as insulators if they are transparent to microwaves. Insulators are frequently used in typical microwave ovens to support the material that needs to be heated. Lastly, there are dielectric materials which are excellent absorbers of microwave energy and are very easily heated.

Dielectrics own two main important properties (Oespchuck, 1984):

- Since they have the ability to let electricity to pass through, they each have their own value of electricity carriage when electricity is applied from an external source.
- The heat generated in them is a result of the dipole rotation mechanism.

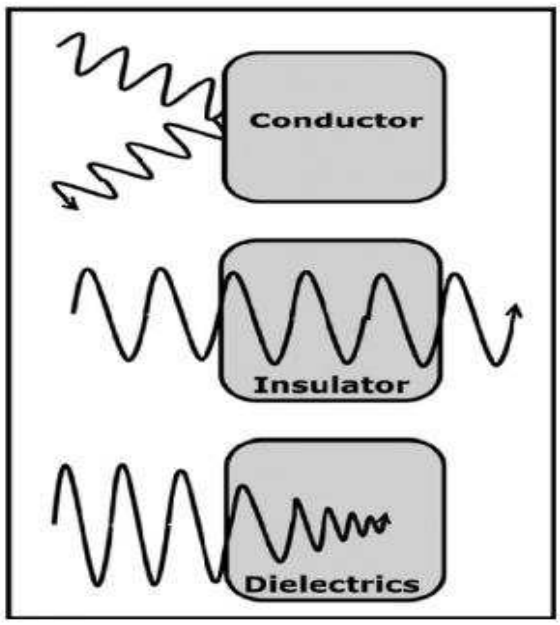

Figure 4: Interaction of different materials with microwave radiation (Manoj Tripathi 2015).

Microwaves have many applications, from being used to detect speeding cars, send telephone and radio and television communications all the way to treat muscle soreness and raise bread and doughnuts. They are also an integral part of radars, obtaining information about the location of objects.

2.4 The heating process with Microwave irradiation

Any material that is neither a perfect electrical conductor nor a perfect insulator, can be heated using high-frequency electromagnetic waves. The alternating electromagnetic field generated inside the microwave machine would stimulate the material by excitation and rotation/collision of the polar molecules and ions within the material. As a result of these molecular frictions, heat is generated which subsequently leads to temperature rise. There are two major mechanisms that explain how the heat is produced inside the material, namely dipolar and ionic interactions. (FEHD, 2005)

2.4.1 Dielectric heating

Two frequency bands can be used for dielectric heating – radio frequencies (below 300 MHz) and microwaves (above 300 MHz). In this work, dielectric heating refers to heating induced by microwave radiation only. (Vorster, 2001)

The dielectric heating is the phenomena, which leads to the heating of electrically non- conducting materials by a rapidly varying electromagnetic field.

All electromagnetic waves can be transformed into heat. There are two principal mechanisms by which an insulating material can be warmed in an electromagnetic field. Dielectric materials are heated by enforcing dipoles to rotate or by a current flow in the material induced by the oscillating electric field.

The current flow generates heat by an ohmic loss in the material. Dipole rotation works only in materials containing polar molecules having a dipole moment, which align themselves in the electric field by rotation. Because of the alternating electric field, the molecules or atoms are accelerated. (Peinsitt, 2009)

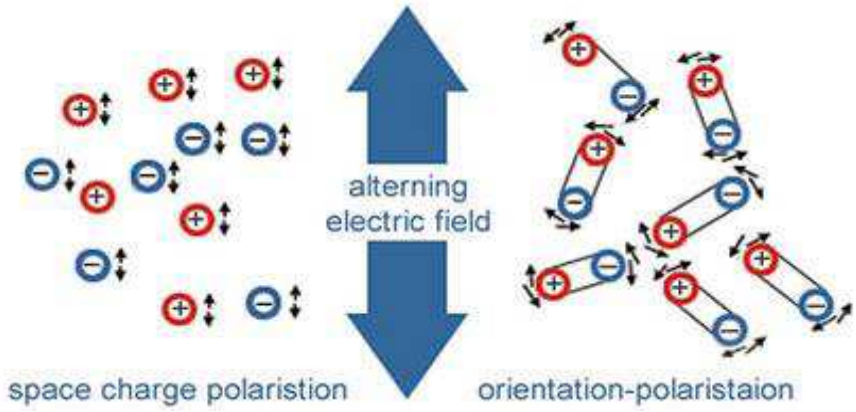

Figure 5: Principle of dipolar rotation Peinsitt (2009).

2.4.2 Factors Affecting Dielectric Heating

Dielectric properties of materials are those electrical characteristics of poorly conducting materials that determine their interaction with electric fields. These properties are important in any processes involving radio-frequency (RF) or microwave dielectric heating. They determine how well energy can be absorbed from the high-frequency alternating electric fields and thus how rapidly the materials will be heated. The dielectric properties of the load materials are also important in the design of the RF or microwave power equipment needed for the heating process. The properties effect on dielectric heating classified into (Nekoovaght, 2015):

2.4.2.1 Frequency of the Applied Field

The permittivity of a material varies with the frequency of an alternating electric field. This is due to the ability of the atoms, ions, and dipoles to align and realign with the alternating electric field. All properties of a dielectric material are connected by a complex permittivity, which is frequency-dependent, according to the Griffiths model.

2.4.2.2 Temperature of the Material

A material's loss factor determines the part of the microwave radiation that is lost into the material and transferred to heat. The loss factor is proportional to temperature and it increases as the temperature of the material increases.

2.4.2.3 Absorbency and Moisture Content of the Material

Water is known to be an excellent absorber of microwave energy, it normally has higher electrical permittivity than any other materials. Moisture within a material subjected to microwave irradiation will cause the temperature to rise significantly since water will be first to absorb microwave energy. Porosity differs among natural rocks. Hard igneous rocks have 0.5 – 1% porosity, therefore they have very low water content. Micro- and macro-factures (cracks) enhance the water retention abilities of a given rock.

2.5 Components of household microwave heating machine

Nowadays, commercial microwave machines consist of the following basic components (FEHD, 2005):

- Power supply and control: controls the input power to the magnetron and the irradiating time;
- Magnetron: a vacuum tube in which electrical energy is transformed into an oscillating electromagnetic field (frequency for household for microwave oven is 2450 MHz);
- Waveguide: a rectangular metal tube guiding the microwaves generated from the magnetron towards the cooking cavity. It prevents direct exposure of the magnetron to any spattered material that can interfere with its function;

- Cooking cavity: the space inside which the material is placed and heated by microwaves;
- Turntable: provides a rotation platform for the material through the fixed hot and cold spots inside the cooking cavity and offers the means of even exposed to microwaves;
- Stirrer: distributes microwaves from the waveguide and create a more uniform heating condition for material;
- Door and Choke: gives access to material inside the cooking cavity. They are carefully engineered so that they prevent microwaves from leaking from the gap between the door and the cooking cavity.

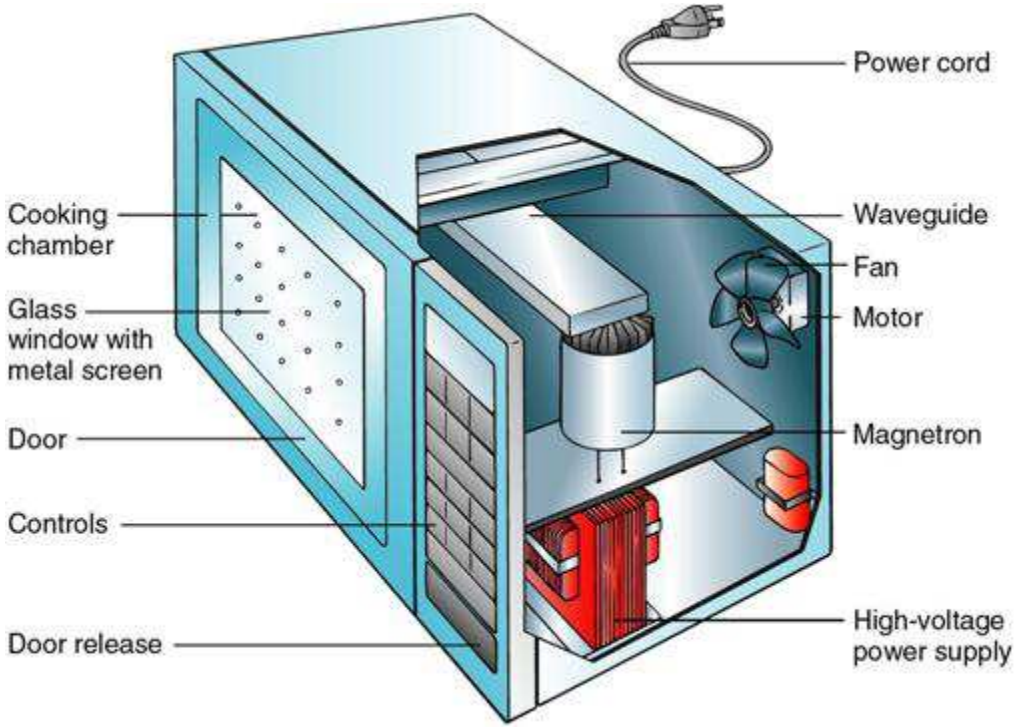

Figure 6: Components of a microwave machine in household applications.

2.5.1 How a microwave machine works

- Electrical energy, either as low-voltage alternating current or high-voltage direct current, is transformed into direct current.
- The magnetron takes the direct current and generates microwaves with a frequency of 2.45 GHz.

- The microwaves are guided into a waveguide by an antenna at the top of the magnetron.
- The waveguide channels microwave to the stirrer which scatters them inside the oven cavity.
- The microwaves then reflect off the interior metal walls of the oven and are absorbed by molecules in the material.
- The molecules in the material are jostled back and forth at a rate twice that of the microwave frequency (namely 4.9 billion times a second) due to the fact that each wave has a positive and negative component. (FEHD, 2005)

2.5.2 Application of magnetron

Magnetrons were developed in the 1950s for radar applications and are the most common type of microwave generator. They have been used for microwave heating ever since the discovery of their application for high-frequency waves. Magnetrons normally have an output power between 200 W and 60 kW and can go even higher. The majority of the magnetrons, however, are produced with an output power between 800 W and 1200 W which are commonly used in household microwave ovens. The ones with very low power are frequently used in medical applications, while the others with high power are used for research applications such as industrial heating projects. Due to the mass production of household magnetrons, the price has become comparatively low. Hence, these magnetrons are also used for industrial heating applications.

During operation, the magnetrons must be cooled every once in a while to prevent them from overheating. Magnetrons with a power up to about 2 kW are usually air-cooled, whereas those with a higher power are typically water cooled, meaning that they would require water recirculation units additionally. Moreover, such magnetrons also require some sort of special protection equipment against reflected power as it may overheat and destroy the magnetron. Low power magnetrons are evidently more robust and can be operated without the protection equipment. (L. Horst et al, 2005)

A magnetron converts electrical energy to microwave radiation. In order to do this, it must use a low-voltage alternating current and high-voltage direct current. Inside

a transformer the incoming voltage is converted into the required levels and a capacitor, in combination with a diode, separates the high voltage and changes it to a direct current.

A central terminal called ‘cathode’ emits electrons inside the magnetron while a positively charged anode surrounds the cathode and attracts these electrons. The system also includes permanent magnets that force the electrons into taking a circular path rather than traveling in a straight line. As they pass by the resonating cavities, they automatically create a continuous pulsating magnetic field also named as ‘electromagnetic radiation. (FEHD, 2005)

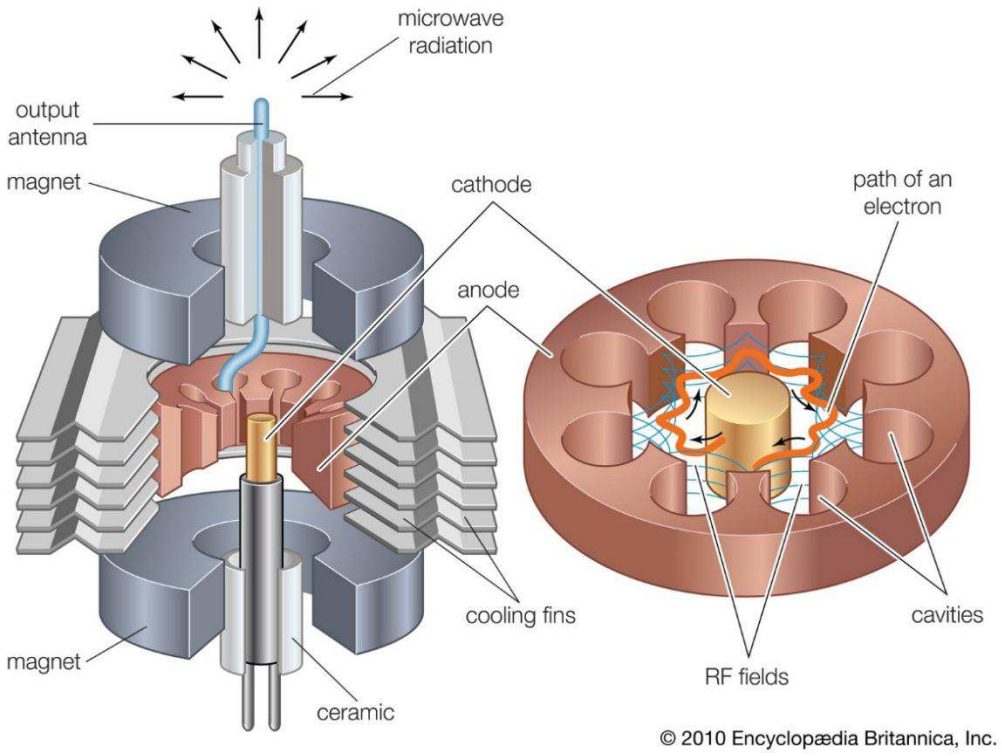

Figure 7: Motion of electrons in a magnetron (Electro Encyclopedia, 2010).

2.5.3 Wave distribution in household microwave machine

Household microwave machine that is common for the small cylindrical experiment, is a simple multimode microwave cavity with a power supply of 3KW and a frequency of 2 45 GHz.

The multimode cavity system produces low-strength electric fields. Due to its low power, the created energy from the magnetron is guided to the cavity through a

waveguide. Further on, and with the help of the stirrer, the wave emits from all directions toward the material situated inside the cavity. (Nekoovaght, 2015)

There is a verified relation between wave distribution and temperature increase, in other words, there will be high temperatures wherever there is a high concentration of waves. Besides, all of the cavity walls need to be perfect electrical conductors in order to completely reflect the microwaves (Figure 8 demonstrates the energy distribution inside the cavity). In this fashion, waves tend to penetrate the material and increase its inner temperature instantly. Because of the distance between the subject and the propagated waves as well as the conduction of the walls, microwave energy is absorbed by the material from all directions. Still, the temperature distribution is not equal in different fragments of the material. The reason can be that the heating process has produced sections with hot and cold spots.

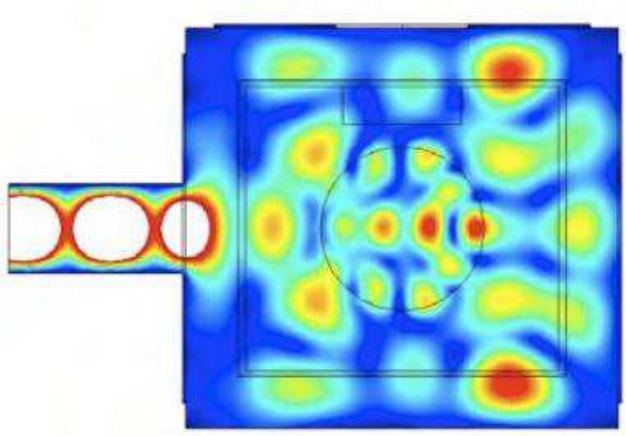

Figure 8: Computer model of a 2D slice, of a 3D electric field distribution inside a microwave oven cavity (Santos T et. al, 2010).

2.6 Types of cavity

The first type of microwave cavities is a multimode cavity, which is also the most commonly used. The multimode cavity is capable of generating low to medium heating rates at average power densities while treating a large volume of material at a time. An example of a multimode applicator is the household microwave oven. These applicators can withstand a number of high order modes concurrently. Such cavities normally include a metal box, which is as long as several half-wavelengths in at least two dimensions. This is to support a various resonant modes at any given range of frequency. The cavity walls are made of materials with high conduction properties, namely aluminum or copper, to reflect microwaves with minimal loss.

Yet, a very complex electric field pattern exists inside a multimode cavity that owns different electric field intensities at different areas. This is primarily why material positioning within the cavity affects the uniformity and efficiency of the heating process. Hence, stirrers and turntables are designed within the cavity to rotate the material and improve the heating evenness (Kobusheshe, 2010).

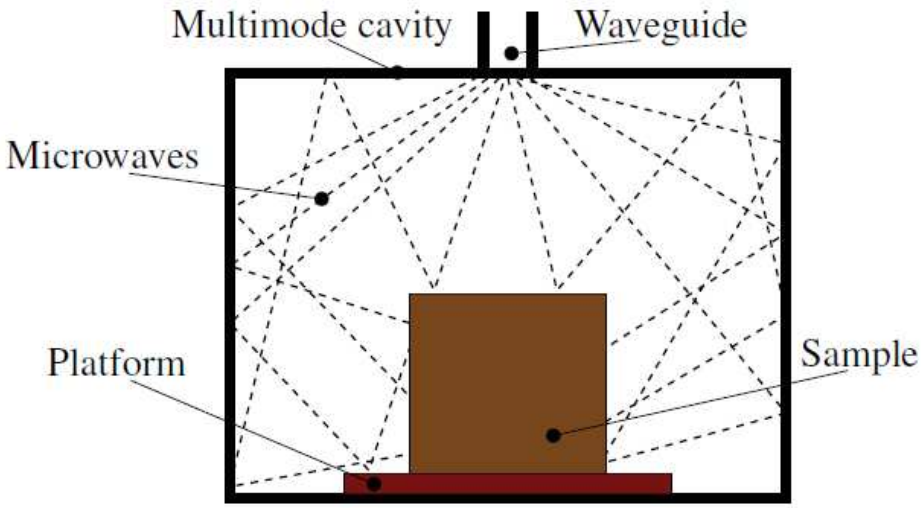

Figure 9: Structure of multimode Microwave cavity (Pickles, 2009).

Conversely, single-mode applicators withhold only one precise electric field pattern inside the cavity. A single-mode pattern is basically achieved by the superposition of the inward and reflected waves, promoting a standing wave with maximum field intensity .Thus, a single-mode cavity field pattern is far easier to predict and define than its alternative, a multimode cavity. This concept is derived from the solution of Maxwell's equations, with known boundary conditions, and highly depends on the geometry of the cavity. The material to be heated must be placed at a location which has the maximum field strength to optimize the transmission of the electromagnetic energy from the source to the material. The size of the cavity is influenced by the standing wave and as a results, the size of the single mode cavity would be in the order of one wavelength across (e.g 12.2 cm at 2.45 GHz). Having the same power applied, a single mode cavity can manage to generate a higher electric field strength in comparison to the other applicator types.Therefore, not only single mode cavities are preferred whenever high heating rates are a prerequisite, but they are also suitable for low loss material processing. (Kobusheshe, 2010)

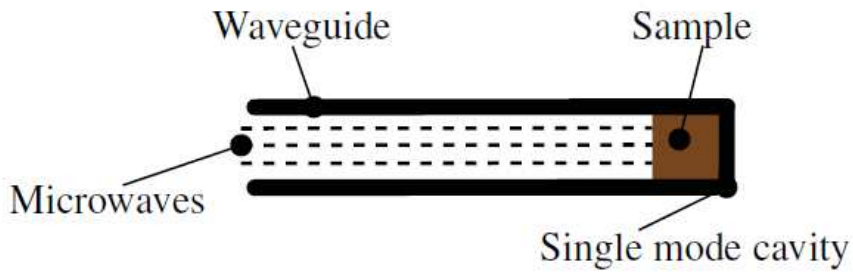

Figure 10: Structure of single mode Microwave cavity (Pickles, 2009).

2.6.1 The penetration depth

Generally speaking, the time and temperature of the heating process depend on a number of factors including composition, size, quantity, shape, density and physical state of the item. The depth of penetration of microwaves decreases when the degree of absorbency increases. The absorption of microwave radiation depends on the high-frequency **dielectric** properties of the constituents of a rock.

When microwave energy is absorbed by materials, the amplitude of the wave decreases gradually as the wave propagates through the material. If any internally reflected waves are neglected, the power density (and therefore power absorbed) falls exponentially with depth. The microwave penetration depth, D_p is defined as the distance into the material at which the power flux falls to 1/e = 0.368 of its surface value). The penetration depth is given by Equation 2:

$$D_p = \frac{\lambda_0}{2\pi\sqrt{2\varepsilon'}} \times \frac{1}{\sqrt{\left[\left(1+\left(\frac{\varepsilon''}{\varepsilon'}\right)^2\right)^{0.5}-1\right]}} \quad (2)$$

Where:

λ_0 = Wavelength of incident radiation

ε' = dielectric constant

ε'' = loss factor

The last equation shows that penetration depth increases with an increase in the wavelength (or a decrease in frequency). The penetration depth also increases with a decrease in values of ε' and ε'' .(Kobusheshe, 2010)

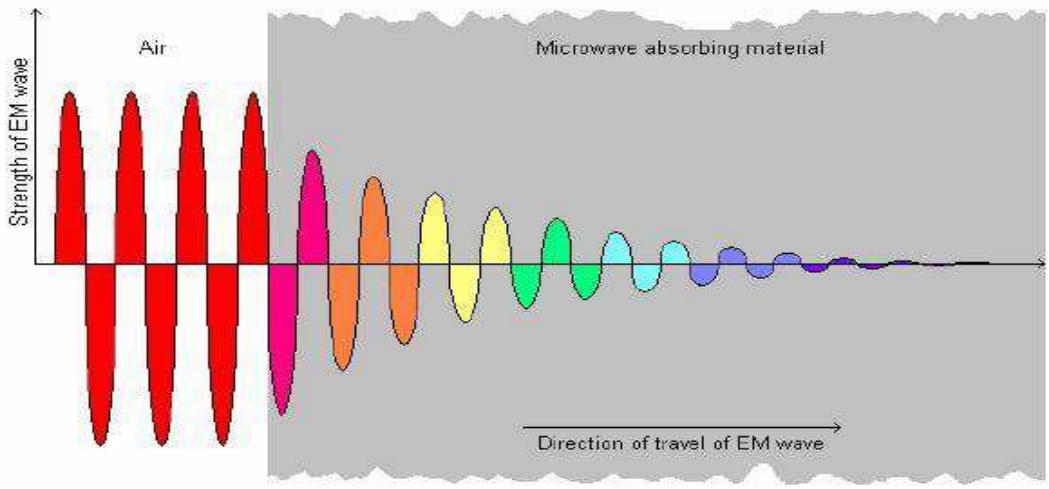

Figure 11: Attenuation of microwave energy (Scott, 2006).

2.7 Microwave vs. Conventional Heating

The conventional heating means that the heat energy induced to a material must pass through the surface and then across a temperature gradient from one point in a material to the other by either conduction, convection or radiation. Thus, the rate of heat transfer within a body is restricted by its temperature at the interface and material's thermal diffusivity. Undoubtedly, this results in uneven temperature distributions within the work piece in addition to complications in heat control as the process is inherently slow. It also leads to waste of energy while heating the sample in case selective heating is the goal. When microwave heating is applied, energy is absorbed volumetrically, resulting in rapid heating and saving more time (Sumnu et al., 2005). Microwave heating systems, therefore, operate with a much higher degree of efficiency. "In large industrial microwave ovens, this efficiency is defined as the percentage of the applied microwave energy which is dissipated as heat in the workload and can be in the region of 95% (Meredith, 1998)". The table below shows the key points of difference between microwave and conventional heating. (Kobusheshe, 2010).

Microwave Heating	Conventional Heating
Energy transfer	Heat transfer
Non-contact heating	Conduction or radiation heating
Rapid heating possible	Heating rate limited by thermal diffusion
Material selective heating	Selective heating not possible
Volumetric heating	Surface heating
Energy may be transported to material through hollow wave guide	Heat must be transmitted by medium to material causing heat loses

Table 1: Comparison between microwave and conventional heating (Kobusheshe, 2010).

2.8 Microwave Safety Considerations

Microwaves have the potential to be hazardous. This is a critical consideration point mostly because these effects may not be realized until damage to living organisms has already been done. Although the human body is designed to warn the person against excessive external heat, it gives no alarm when microwave radiation penetrates the skin and generates internal heating (Baden-Fuller, 1979).

Energy balance considerations (based on a standard man in standard conditions) suggest that a value of 10 $W.cm^{-3}$ (or 100 $W.m^{-2}$) is a safe upper limit for microwave radiations even in the exposure time is infinite. The reason behind this is the existence of thermoregulatory systems that can compensate for the absorbed power. This also means that a power level as low as 10 $W.m^{-2}$ may be considered as having no heating effect - even when extreme conditions of temperature and humidity are in place (Baden-Fuller, 1979).

Nevertheless, evidence (disputed) has proved a degree of non-thermal effects on the nervous system. It has been claimed that exposure over a period of years to power levels in magnitudes of 2 $W.m^{-2}$ will lead to disturbance in the nervous system, even though 'occupational exposure' to healthy adults suggest that there is basically no effect (Baden-Fuller, 1979)

Frequency range	E-field strength (V m21)	H-field strength (A m21)	B-field (mT)
up to 1 Hz	___	3.2×10^4	4×10^4
1–8 Hz	10,000	$3.2 \times 10^4 / f^2$	$4 \times 10^4 / f^2$
8–25 Hz	10,000	4,000/f	5,000/f
0.025–0.8 kHz	250/f	4/f	5/f
0.8–3 kHz	250/f	5	6.25
3–150 kHz	87	5	6.25
0.15–1 MHz	87	0.73/f	0.92/f
1–10 MHz	$87/f^{1/2}$	0.73/f	0.92/f
10–400 MHz	28	0.073	0.092

Table 2: Reference levels for general public exposure to time-varying electric and magnetic fields (ICNIRP GUIDELINES 1998)

3 Background of Industrial Microwave applications

The initial suggestion to use microwave heating in industrial applications was made in the forties when the first magnetrons were developed. However, the implementation took place in the fifties after extensive work on material properties. By then, the first studies on microwave exposure hazards were prepared and published.

The implementation of microwave energy covers a range of practices that can be categorized as communication applications such as telecommunication and satellite data transmission (Osepchuk, 1984), and non-communication applications for industries in which the power resembles heating. Other uses exist in the medical field which, for the purposes of this study, will not be discussed further. Nevertheless, since the beginning of 1960's, microwave ovens for home use have become available and popular. It didn't take long until some industries began using microwave power in different processes such as rubber extrusion, plastic manufacture and the treatment of foundry core ceramics. Gwarek et al., 2004, categorizes the typical areas of microwave power application as below:

- Food processing (heating, thawing, biological deactivation, quality control)
- Industrial material drying (paper, wood, explosive wood drying)
- Chemical reaction enhancement (micro-reaction control, fluidized beds)
- Melting of industrial materials (glass, rubber, sludge)
- Sintering (ceramics, metal powders)
- Plasma generation
- Mineral processing (rock crushing, comminution)

Most industrial heating systems demand a power input of 10kW, often extending it to a range between 100kW to 1MW (Meredith, 1998). Additionally, the following criteria have to be satisfied (Jones, D.A, 2004):

- A high conversion efficiency of input power to useable microwave power, quite essential as power rating escalates;
- Operation within the prearranged frequency band at all times.
- A low capital expenditure, expressed in kilowatt of output power; this factor is particularly important as the generator often comprises more than half the cost of the machine installation.
- Robustness in surviving incidents typical of the specific operation (e.g. electrical power surges and transients, arcing in the applicator and feed system, incorrect adjustment of operating conditions, vibration etc.)
- Simplicity in operation, meaning minimum user adjustable controls;
- Simplicity in maintenance, fault diagnosis and remedial plan;

Low operating expenditure, not only in electrical power consumption but also in replacing consumables (e.g. the microwave power tube). This points toward a long magnetron life.

3.1 Application of microwave in mineral industry

Industrial microwaves, are a single mode cavity capable of generating high power as a result of its robust magnetron. The maximum output power for this machine is 30 KW with a frequency of 2450 MHz. As a result of high power transmission, there is a very rapid escalation in temperature of the treated materials. For industrial microwave machines, the given energy from the magnetron is transferred directly

with the help of a long rectangular waveguide into the cavity. Since the waves travel a much longer distance inside the waveguides than in air (due to phase velocity and the cut-off frequency of waveguides), the length of the waveguide must be long enough to permit the formation of two complete cycles of waves within it. (Nekoovaght, 2015)

For industrial devices, the temperature distribution is greatly different from the household type. Through several experiments, a small area of the material was positioned directly in front of the horn antenna and then heated by microwave irradiation, indicating that the energy was directed perpendicular to the aperture of the horn waveguide. In another term, there is no corresponding wave radiating on the material and only a small area of the face, exactly below the waveguide, is affected. In any event, distribution of waves focused on the face of the material leads to temperature increase at the spot of waving and this rise will be more than that of the other layers. Figure 12 indicates the distribution of energy and temperature on the face of the material in an industrial microwave machine.

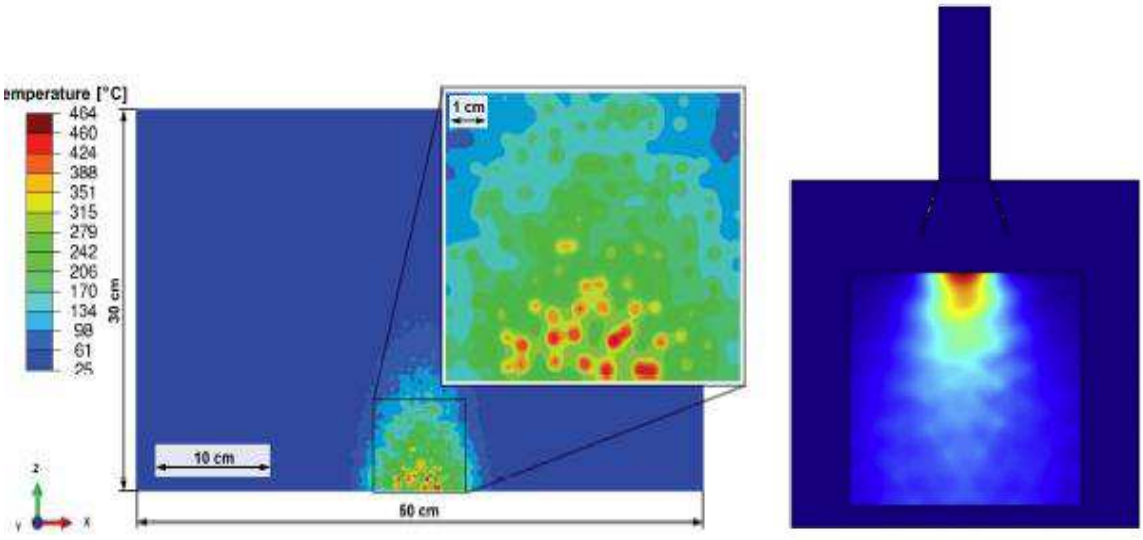

Figure 12: Temperature distribution in ◦C after 15 s of microwave irradiation (25 kW) in the 2D model rock (Left picture, Meisels et al 2015). Electric field energy propagation within the load inside the closed cavity. (Right picture, Hassani, 2016).

There exists more investigation on microwave-assisted energy in the mineral processing industry than in operations assisting mechanical excavators. These studies have been more concentrated on the influence of the energy on both crushing and liberation of valuable minerals from gangue minerals as a mineral

processing procedure. According to Walkiewicz et al. (1991) “about 50 to 70% of the amount of energy of mineral extraction is used in comminution, where the efficiency of conventional grinding is only 1%”. Walkiewicz (1991) also proved a reduction of 10 to 24% in Bond Work Index (‘a standard test to calculate the grind ability of the material”) of iron ores by treating samples with the microwave energy prior to the grinding procedure.

3.1.1 Effects of Microwave Radiation on Coal

In 1990 a low power microwave was used with the 500W power to desulphurise coal. The results showed that although the pyrite (FeS2) in coal was preferentially heated, the final obtained temperature was still insufficient for the conversion of non-magnetic pyrite to magnetic pyrrhotite. Yet an idea came around to mix the coal with NaOH or KOH, increasing the final temperature adequately to further enhance the magnetic properties of the pyrite and dissolve it along with organic Sulphur. This leads to a reduction of sulphur content of almost 70%. Later on it was indicated that the comparative work index of coal can be reduced by up to 30% in a 650W, 2.45 GHz microwave, also showed that a conventional treatment of coal improves the grinding ability to a similar extent than a microwave. Still, microwave treatment of coal brings other advantages like reducing the Sulphur and ash content along with a safer and more controllable drying mechanism (Vorster, 2001).

3.1.2 Effects of Microwave Radiation on Gold Processing

It was investigated the effects of microwave radiation within various sections of a gold processing circuit. Microwave radiation was suggested to be applied in the roasting phase for the removal of arsenic and sulphur components. Mixing the concentrate with sodium hydroxide before microwave treatment forms various soluble salts of sulphur and arsenic which means a high recovery gold. Moreover, one of the most common gold extraction practices is the carbon-in-pulp method, in which gold is adsorbed onto activated carbon. In the next steps, the adsorbed gold is removed by elution and the carbon is treated in an acid bath to get rid of its contaminants before it is regenerated in a steam atmosphere at approximately 660°C. Lastly, the re-activated carbon is returned to the CIP circuit. Even though activated carbon is regenerated in rotary kilns or vertical tube furnaces, the

granulated activated carbon can be easily heated by microwave radiation. The advantages of such a method is that the carbon can be heated more rapidly and with a better control on temperature which can possibly save some energy. Initial test work by Bradshaw indicates that microwave regeneration of activated carbon is not only economically feasible, but it also brings higher abrasion resistance to the carbon (Vorster, 2001).

3.1.3 The Effects of Microwave Radiation on Iron Production

The reduction of iron ores is very much dependent on the surface area that is available for gas-solid contact. Differential heating and the subsequent stress cracking caused by microwave radiation of minerals. Increases the surface area for contact. This is practically why microwave radiation is used in the reduction process of iron ore particles in a CO atmosphere.

Besides, it was discovered that microwave treatment at 1300 W for 6 minutes has the optimum enhancement on the reduction process and therefore, microwave pretreatment of iron ore is a valid alternative to sintering or pelletising.

In 1996 it was conducted as experiments on the reduction of iron ore with coal in a 15 kW microwave cavity with a volume of 0.06 m3 in an inert nitrogen atmosphere to inhibit reoxidation of the iron. The outcome suggested that microwave heating has a high potential to significantly reduce the reaction time when compared to conventional heating. Considering the time required for 80% of the reduction to take place where conventional case requires around 30 minutes, the microwave process only requires 7.5 minutes for a reduction of more than 75%. Additionally, one of the major advantages of using microwaves is their ability to dissipate the energy promptly throughout the whole volume of the sample. This leads to a direct heating operation in contrast with a conduction scenario as is normally the case. The final benefit would be the dust free, high energy flue gas is produced (Vorster, 2001).

3.2 Rock breakages with microwave

The mechanism behind rock breaking with microwave energy comes from the difference in thermal expansion coefficient of minerals within a rock. Still, the absorbed microwave energy also depends on the dielectric properties of these minerals.

As it was mentioned before, one of the major issues for rock breakage by microwave machine is dielectric properties (The ability of materials to absorb microwave energy). The permittivity of any rock type forming mineral is totally dependent on its mineralogy and petrography characteristics. Each mineral has its own dielectric properties, whereas the complex of several minerals together results in completely new dielectric properties. Some other parameters, such as the grain size, the mixture percentage and the type of minerals forming rocks reflect the final dielectric properties of the rock. Moreover, if the permittivity of the rock changes the dielectric properties of the rock will change significantly (Nekoovaght, 2009).

Rocks containing water have a significantly higher ability to absorb the microwave energy. In the case of a moist, low permeable material, the high internal pressure of water can cause the material to burst.A rock naturally consists of various minerals (high or low-absorbing), which have different dielectric and heating specifications (Table 3). Once the specimen is under microwave irradiation, a portion of the microwave beam is reflected from the surface of the rock and further transmitted.

Rock, Mineral	dielectric const.	Rock, Mineral	dielectric const.
Galena	18	Granite	4.8-18.9
Sphalerite	7.9-69.7	Sandstone	4.7-12
Cassiterite	23	Plagioclase	5.4-7.1
Hematite	25	Basalt	12
Fluorite	6.2-8.8	Clays	7-43
Calcite	7.8-8.5	Petroleum	2.07-2.14
Apatite	7.4-11.7	Soil	3.9-29.4
Barite	7-12.2	Water	80.36
Peridorite	8.6	Ice	3-4.3
Rock salt	5.6		

Table 3: Electrical properties of rocks and minerals (Applied geophysics 2nd edition, 1990)

A high percentage of the transmitted (penetrating) microwave beams are absorbed by the high absorbing dielectric minerals which later convert this absorbed wave of energy into heat. As the constituents of these minerals have different thermal expansion coefficients, the minerals slowly start to expand. Yet, these minerals need a larger space as they start to build up internal stresses inside every single minerals and along the grain boundaries Such thermally induced stresses cause cracks inside the rock body and inevitably result in strength reduction.

The explained mechanism is the basic process of the rock breakage involving microwaves. The technique of thermally-induced mineral expansion and the increased thermal stresses that follows can be further optimized due to the reappearance of the irradiation process (pulsed microwave systems). (Peinsitt, 2010).

3.2.1 Combination of microwave with mechanical excavation TBM

The general concept behind this idea is to irradiate the face of the tunnel with microwave energy simultaneous with boring the tunnel. This provides an opportunity for exposure of rocks to the microwave irradiation first, meaning a possible drop in rock strength, to a certain amount, within a specific depth and very much depending on the type of rock and microwave conditions. It is fairly obvious that shearing and normal forces are mainly subjective to the tunnel boring machine penetration rate, therefore, it is safe to claim that a possible weakening of the rock after exposure to microwave irradiation, can increase the penetration rate. (Nekoovaght, 2009).

4 Relation of treated rocks by microwave in different conditions with temperature and UCS

Many experiments have been done in order to achieve sufficient data for small samples when they are exposed to microwave energy.

Peinsitt (2010) carried out several experiments on 3 types of rock: Granite, sandstone and Basalt. Tested samples had a diameter of 50 mm and height of 50 mm according to SMC standard and UCS geometry .The aim of these tests was to

weaken the structure of the rocks with the new microwave energy method and prepare them for next steps (mineral processing).

Figure 13: small specimens (granite, sandstone, basalt), Peinsitt (2010).

Table 4 demonstrates the mechanical properties of the tested rock samples in an intact conditions.

	Granite	**Sandstone**	**Basalt**
Density [g/cm^3]	2.641	2.551	2.699
Load at failure [kN]	432.01	378.43	619.76
Deformation [mm]	0.477	0.458	0.610
Elastic Limit [kN]	325.49	316.54	542.45
Elastic deformation [mm]	0.300	0.342	0.544
Axial US velocity [m/s]	4335	3969	5674
Compressive strength [MPa]	211	185	325
Elastic deformation modulus [MPa]	31949	21558	30383
Fracture energy [Nm]	81.77	108.43	178.68

Table 4: Rock Parameters from UCS Peinsitt (2010).

4.1 Test preparation and procedure

The microwave device used to radiate the stone sample, is a straightforward multimode microwave with a power supply of 3200 W and a frequency of 2,45 GHz. This device, a Panasonic NE 3240 microwave, is simply accessible and regularly utilized as a household appliance. It has a supply voltage of 400V/50Hz and a power input of 4960W and 12.9 A. In order to get maximum absorption, samples should be put in the middle of the cavity.

The intact samples were heated in different radiation intervals. As previously mentioned, heating causes breakage in rocks by increasing the ionic or dipolar movements. This is the main reason why Peinsitt (2010) performed the tests first in a dry condition and afterwards in a saturated condition since the water intensifies the dipolar nature of the test specimen. Consequently, temperature and later crack propagation inside the rock will be escalated.

After the samples were geometrically prepared, they were dried for 48 hours, weighed and then soaked for another 48 hours and weighed again before the actual radiation test is performed.

4.2 Results

Temperature rate

The experiment times were 60 seconds for Basalt and 300 seconds for Sandstone and Granite. The following results belong to the Granite test samples, in which the most extreme temperature achieved for the dry stone was around 225°C. Yet, the temperature peak of the immersed stone is 302°C, meaning a 77°C shift compared to the dry rock. Figures 14 and 15 illustrate these differences.

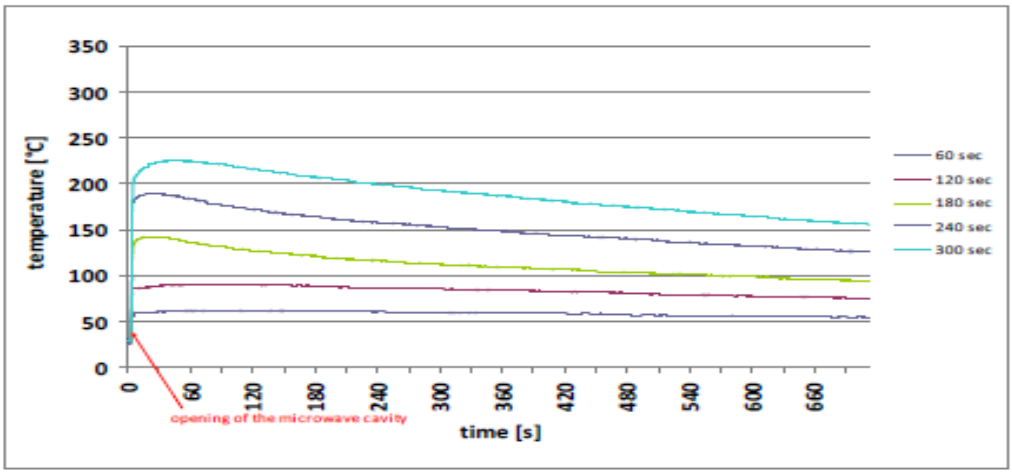

Figure 14: Temperature sequence of dry granite at different irradiation times Peinsitt (2010).

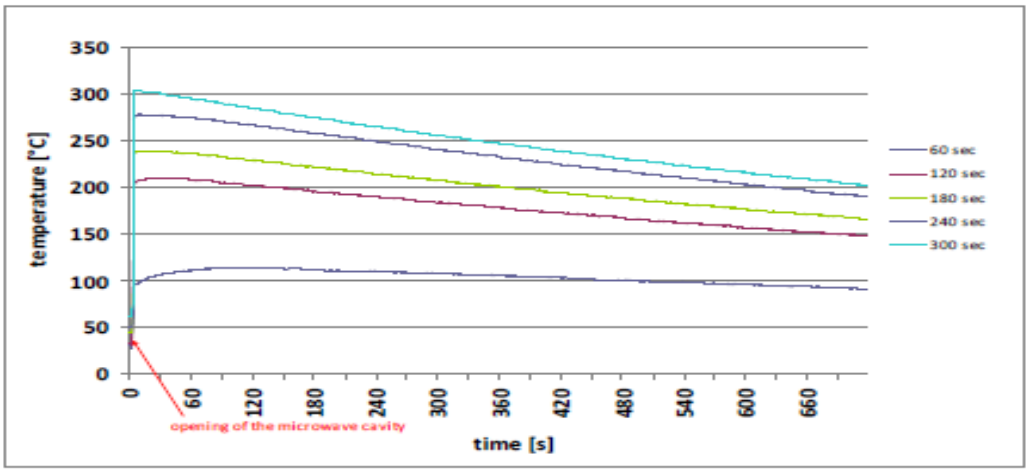

Figure 15: Temperature sequence of saturated granite at different irradiation times Peinsitt (2010).

The same temperature variations can be observed for Basalt and Sandstone samples in dry and saturated conditions. With regard to the mechanical parameters, e.g. USC, the strength of saturated rock in comparison to dry samples is decreased due to the existence of cracks as a consequence of microwave radiation.

Change in UCS values

Some experiments UCS of an intact granite sample is higher than when the sample is treated by microwaves. This reduction is in the order of 30% (Nekoovaght, 2015). Nevertheless, increasing the temperature by raising the water content of granite, has no influence on the UCS value, meaning that the UCS of the treated saturated granite is equivalent to that of the treated non-saturated one.

5 Small and large scale microwave experiments

5.1 An approach to temperature increase

As explained in the last section, Peinsitt (2010) executed the experiments on small samples in different conditions (intact and saturated rock) and the outcomes proved that the internal temperature of the rock after microwave irradiating varies depending on the mineralogy and water content. The principle of the microwave energy suggests that existence and interaction of either dipolar molecules or ions inside the sample can lead to higher frictions that warms up the rock. The aforementioned experiments focused on dipolar friction enhancements, however, it is also possible to raise the ionic interactions as a means of achieving higher temperatures.

For this purpose, salt was chosen as one of the cheapest and easiest substances that can be dissolved in water and act as the saturating fluid. Accordingly, the ionic and dipolar properties of rock can be improved. To verify this theory, 3 rock samples of Granite, Volcanic rock and Marble were selected for further investigation.

Figure 16: Samples for wave experiment (from left to right Granite, Volcanic rock, Marble).

The testing equipment used were completely similar to Peinsitt's tests. Figure 17 shows the microwave oven with a power supply of 3200 W and a frequency of 2,45 GHz.

Figure 17: Small-scale Panasonic laboratory microwave, Montanuniversität of Leoben.

Once the samples are drilled and polished, one of each type was immersed in water and saltwater solution (In addition to the dipole water molecules, ionic compounds (i.e. dissolved salts) in the material can also be accelerated by the electromagnetic field and collided with other molecules to produce heat) for 48 hours. It is clear that the weight of rocks would not be the same, yet the significant point is only the increase in temperature of the rock in order to achieve as many cracks as possible. All experiments have been performed in the same conditions for 2 minutes (they were dry before testing for 1h) with the highest power of irradiation (3.2kw) and temperature was calculated by an Infrared gun. Figures below demonstrate the data collected from tests in different conditions.

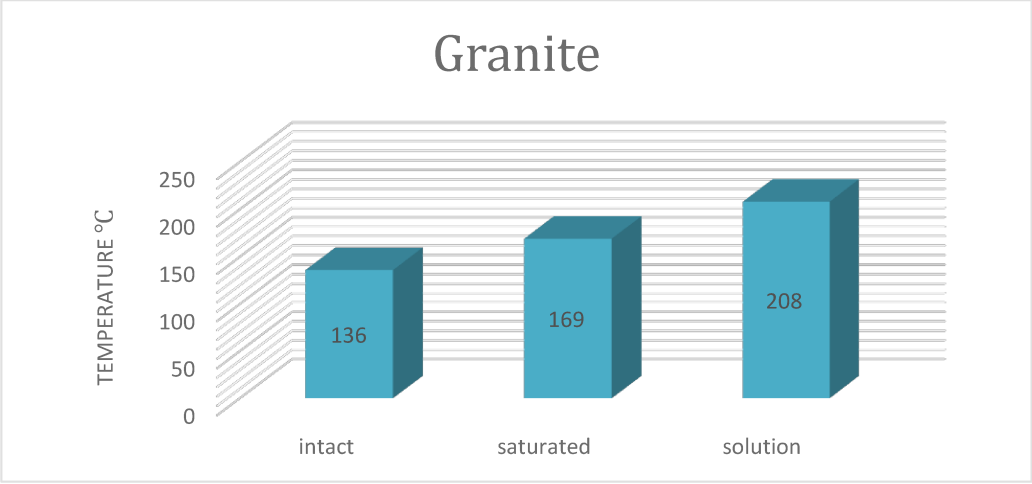

Figure 18: Temperature differential for granite in 3 modes.

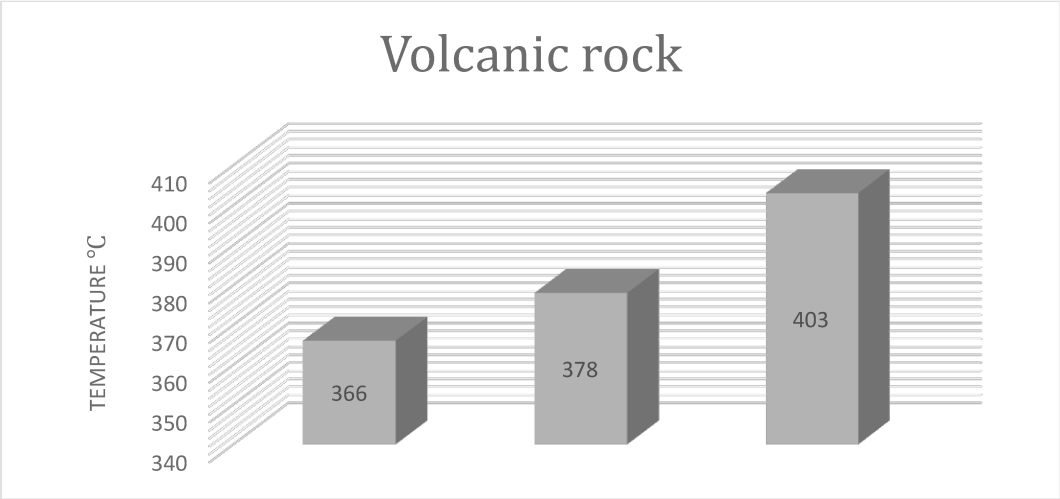

Figure 19: Temperature differential for volcanic rock in 3 modes.

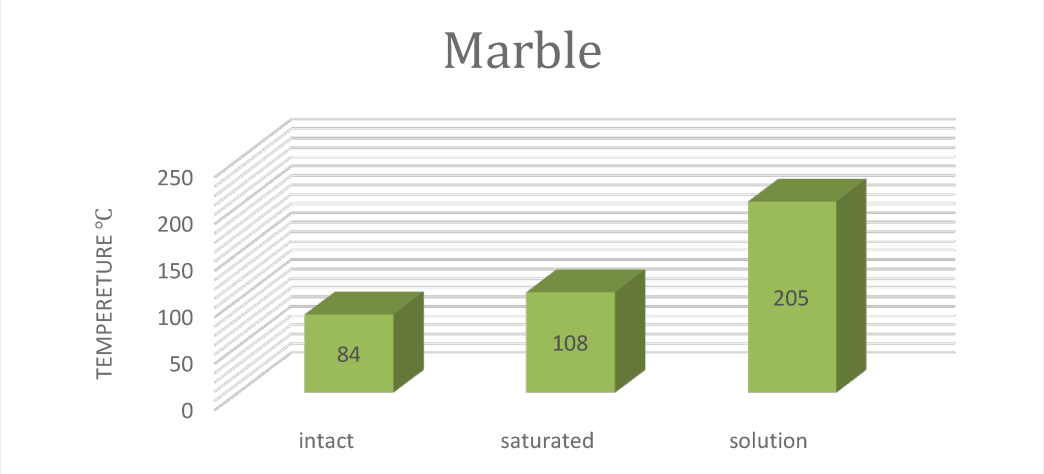

Figure 20: Temperature differential for marble in 3 modes.

As it is can be seen from the charts, the temperature is rising step by step. For Granite, the difference between intact and saturated sample is around 30 ℃ but this number doubled for solution samples.

A temperature shift of 20°C was detected for the saturated volcanic rock in comparison to the intact one. This value also doubled in the solution one. In addition, at the same time (2 minutes) there was a small explosion for solution volcanic rock that led to breakage.

In marble samples, the distinction between intact and saturated is near 20℃. Nonetheless, it increased 5 times more for solution rock. This means that the influence of the ionic part is more impressive dipolar.

Figure 21: Treated rocks at first row after a specific time and broken volcanic sample.

As discussed above, the composition of a rock sample will affect how it will be heated up inside the microwave oven. As the concentration of dissolved ions increases, the rate of heating also increases due to the ionic interactions induced by microwave.

5.2 Large scale Granites get exposed by Industrial Microwave machine

In this part of the work, the experiment on Granite and the assessment concerning the effect of microwave radiation will be described in more details. In the chapter discussing small-scale specimen.

Microwave illumination has been demonstrated as a practice for cracking various types of hard rocks, among which, it is more complicated to conduct splitting in granite. That is because of its mineralogical figures, mainly of quartz, feldspar and micas being medium to low microwave absorbers.

However, with the help of the industrial microwave machine with high power, it is feasible to create a network of cracks on this hard rock. In this section, investigation on big Granite samples will be explained. Samples were irradiated by an industrial microwave machine and the effect of microwave on this hard rock was digitized with the help of computer tomography and crack sketching.

Figure 22: 3 blocks of granite for high power microwave test.

5.2.1 Mineralogy of granite

Granite is a plutonic rock, one of the most common types of igneous rock in the crust of the Earth and is typically medium to coarse grained. It is usually found in various colors from pink to light gray. It originally includes orthoclase or microcline [(K,Na)AlSi308] and sodic plagioclase, quartz [Si02], muscovite (white mica) [K2Al4(Si,Al)802o(OH,F)4] and biotite (dark mica), amphibole, with tiny additional minerals such as magnetite [Fe304], garnet [X3Y2(Si04)3], zircon [ZrSi04], titanite [CaTiSi05] and apatite [Ca5(P04)3(F,Cl,OH)] . Seldom, the iron-rich olivine fayalite [(Fe,Mg)2Si04], can be identified in the structure.

Gray NEUHAUSER granite, chosen for the purposes of this research, and its composition is shown in table 5.

Additionally, figures 23 and 24, depict the petrographic testing on granite.

Mineralname	Vol.-%	Chemische Zusammensetzung
Quarz	24,4	SiO_2
Kalifeldspat	11,8	hier Mikroklin = $K[AlSi_3O_8]$
Plagioklas	44,8	Mischungsreihe von Na- und Ca-Feldspäten mit den Endgliedern Albit = $Na[AlSi_3O_8]$ und Anorthit = $CaAl_2Si_2O_8$
Myrmekit	1,6	wurmförmige Verwachsung von Quarz = SiO_2 und Albit = $Na[AlSi_3O_8]$
Biotit	12,0	$K(Mg, Fe^{2+}, Mn)_3[(OH, F)_2\|(Al, Fe^{3+})Si_3O_{10}]$
Muskovit	2,9	$KAl_2[(OH,F)_2\|AlSi_3O_{10}]$
Chlorit	2,1	$(Mg, Fe^{2+}, Al)_6[(OH)_8\|(AlSi_3O_{10}]$
Epidot	0,1	$Ca_2(Fe^{3+},Al)Al_2[O\|OH\|SiO_4\|Si_2O_7]$
Apatit	0,1	$Ca_5[(F,OH)\|(PO_4)_3]$
Calcit	0,1	$CaCO_3$
Saussurit	nicht bestimmbar	Gemenge aus Epidot = $Ca_2(Fe^{3+},Al)Al_2[O\|OH\|SiO_4\|Si_2O_7]$, Serizit = $KAl_2[(OH,F)_2\|AlSi_3O_{10}]$, Chlorit = $(Mg, Fe^{2+}, Al)_6[(OH)_8\|(AlSi_3O_{10}]$ und Calcit = $CaCO_3$
Erzminerale • Ilmenit • Pyrit • Pyrrhotin • Chalcopyrit	0,1	 $FeTiO_3$ FeS_2 FeS $CuFeS_2$

Table 5: Composition of Neuhauser granite (Baustoffprufstelle Wismar GmbH).

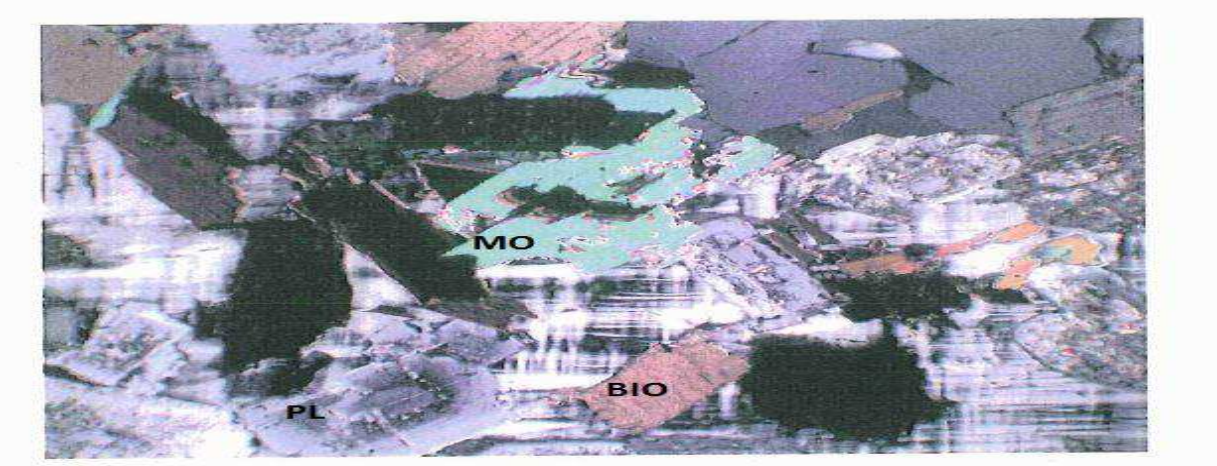

Figure 23: Microclinic with typical twin lattice grating as gore filling between biotite (brown), muscovite (green) and plagioclase (green, zoned). Picture width 2.5mm.

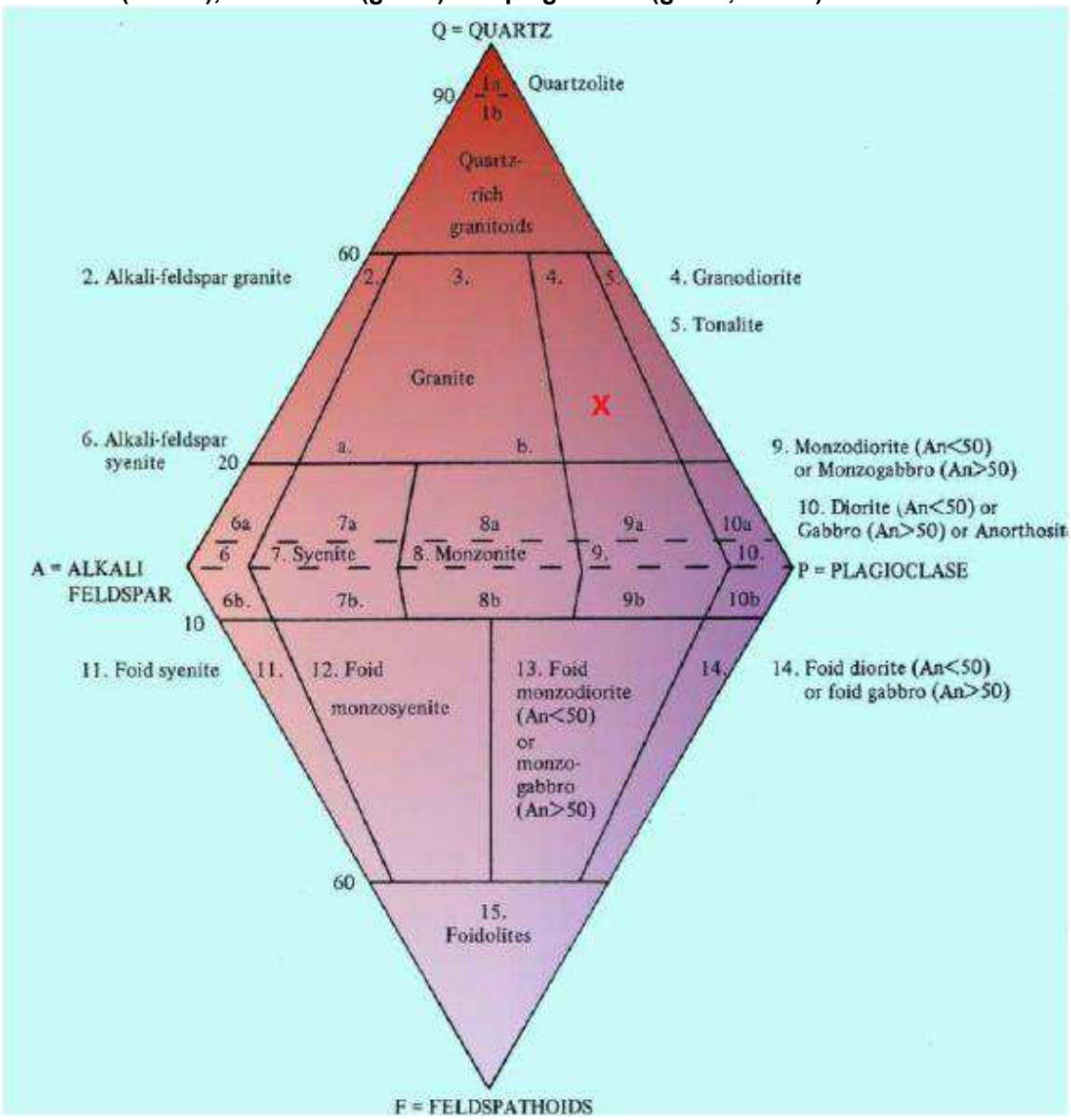

Figure 24: Classification of plutonic rocks with position of Neuhauser granite(X).

Mechanical parameters	Granite
Density [g/cm^3]	2.641
Load at failure [kN]	432.01
Deformation [mm]	0.477
Elastic Limit [kN]	325.49
Elastic deformation [mm]	0.300
Axial US velocity [m/s]	4335
Compressive strength [MPa]	211
Elastic deformation modulus [MPa]	31949
Fracture energy [Nm]	81.77

Table 6: Mechanical parameters derived through calculations after UCS.

5.2.2 Large scale microwave testing equipment and apparatus

Microwave machine

The microwave machine used for the test consists of 2 parts:

- The wave generator and waveguide which generate microwave energy and transfer it to the sample.
- A cavity box that provides a safe and confined zone during the experiment.

Figure 25 demonstrates the used microwave machine for experiments.

Figure 25: Microwave machine for large scale testing (Sandvik company).

The heart of this machine (microwave generator) is supplied by Mügge Company. The amount of output energy that its magnetron produces is 30 KW with a frequency of 2450 MHz. The magnetron is supported by an electronic bank. There also exists an automatic tuner which reduces the number of reflections. Besides, a circulator deviates the reflected wave from the system to a water load section that is in charge of protecting the very sensitive magnetron from extreme mirrored wave.

With the help of a computer, the operator would be able to adjust the time of exposure as well as the output power. Power is changeable from 10% of the total power to 100% (30KW). Cavity box was designed not only for safety requirements but also to facilitate handling of samples for test. The safety box is the most vital part in the construction of the high-power laboratory device.

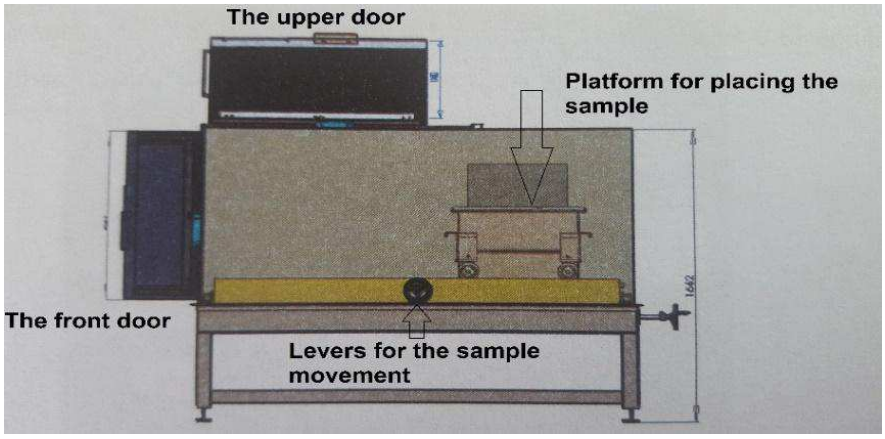

Figure 26: The safety cavity showing doors and moveable sample place.

The maximum size of rocks for operation should not exceed 30*30*30 cm^3. As it is visible from the sketch, the device is equipped with 2 large doors which facilitate rock sample insertion with either a forklift from the front door or a ceiling crane from the door on top.

Furthermore, there is a platform made of steel inside the cavity box in order to place the sample and it is able to move in x and y-direction, with 2 levers outside of the box for precise movement of the sample.

Infrared device (Temperature measurement)

This device was utilized to measure the temperature at the surface of any object prior and after being treated with microwave energy. All materials have a specific infrared emissivity value. Emissivity is a measure of the capability of a structure to

radiate infrared energy and can have a value from zero (shiny mirror surface) to 1.0 (dark body).

The surface temperature of every specimen in this test is measured by an Ahlborn MR721420 device (figure 27) directly after being treated by microwave energy. The infrared gun is capable of measuring the minimum, maximum and average temperature emitted from the specimen and displays the values in different units on the screen.

Figure 27: Infrared device for temperature measurement of samples.

Microwave radiation measurement

It is already clear that microwaves are dangerous to the human body; thus, to avoid leakage of the wave from the cavity box, doors of the industrial system are supported by a spring sealing. Additionally, during exposure, a special apparatus has been designed to control the circumference of the doors and make sure there is no leakage of the wave from the inner part of the machine to the outside.

Figure 28: Microwave radiation leakage measurement.

Penetrating spray

One of the oldest and simplest non-destructive tests on materials is ‘liquid penetrant testing’. The earliest experiments go back to the 19th century where kerosene and oil mixture used as the spray material. This technique is often used to reveal surface discontinuities as the colored or fluorescent dye pours out of the flaw. The procedure is built on the ability of the liquid to be drawn into any discontinuity within a clean surface by capillary action. After a certain amount of time has passed (commonly known as ‘dwell time’), the extra penetrant is cleaned for a surface and a ‘developer’ is applied. This acts as a blotter that draws the penetrant from the discontinuity to reveal its presence.

Computer tomography

The Austrian Foundry Institute (ÖGI) in Leoben has two computed tomography systems from Phoenix | X-ray company in operation (Figure 29). The provided non-destructive three-dimensional view into the "interior" opens up a completely new possibility for material research, component development and process optimization.

The investigation method is independent of the material and can, therefore, be applied to metallic and ceramic materials, plastics, materials from the refractory and construction industries, as well as composite materials.

Figure 29: The two CT systems at ÖGI Leoben.

In the field of foundry, or in other terms in ‘casting applications’, there is an increasing interest in the three-dimensional, non-destructive examination of the often complex geometry of components. With the help of computer tomography, it is possible to detect the classic cast defects, such as pores, voids, inclusions, microstructures loosenings and the like. The advantage of this method is that compared to the radiation test (radioscopy), smaller errors can be presented with better contrast. In addition, conclusions can be drawn about the geometry and position of the discontinuities.

In the CT examination, the object to be examined is irradiated by an X-ray source and rotated 360° step by step (Figure 30). The X-rays passing through the object are detected by a digital surface detector and reconstructed with the help of a high-performance computer to a three-dimensional model of the object. The model can then be visualized and analyzed depending on the task in hand.

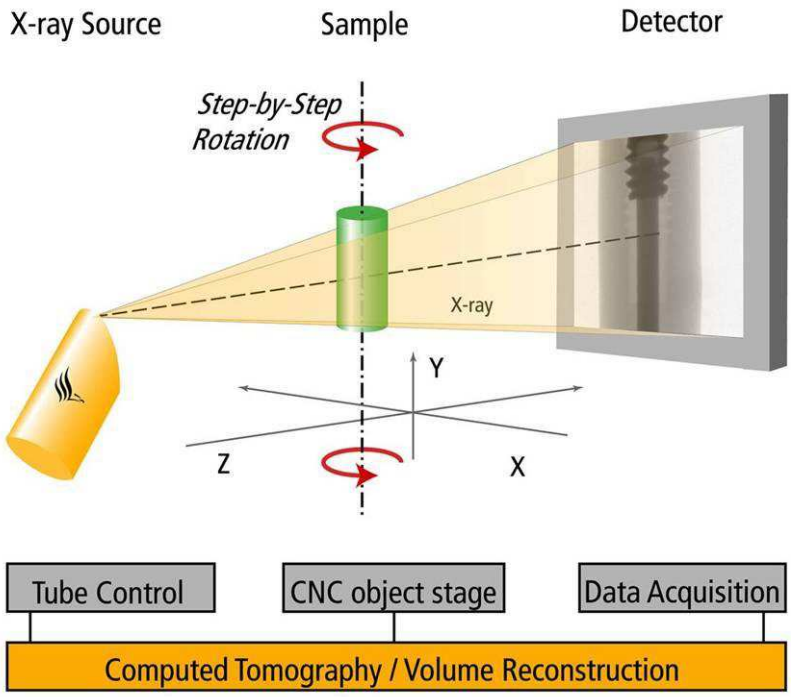

Figure 30: Principle of a computer tomography with x-ray tube, sample manipulator, and detector.

With the aid of the CT, it is possible to comprehensively verify the predictions of the numerical simulation on the real cast. For instance, in classical casting simulations, the casted regions are indicated with regard to their tendency to porosity as a result

The computed tomography (CT) investigations were performed on a Phoenix X-ray v|tomex c equipped with a 240 kV cone-beam microfocus X-ray tube and a GE DXR flat panel detector with 1000x1000 px and 14-bit dynamic range. For the volume reconstruction, a modified Feldkamp algorithm was used for a filter-back projection as implemented by the system supplier.

Most modern CT machines take continuous pictures in a helical (or spiral) fashion rather than taking a series of pictures from individual slices of the material, same as what the original CT machines did. Helical CT has several advantages over older CT techniques: it is faster, produces better 3D pictures of areas inside the body, and is able to detect small abnormalities more accurately.

5.2.3 Methodology of experiment

As mentioned above the treated sample was Granite which is one of the hardest rocks and is almost non-microwave absorbing. The dimension of each cube was 30*30*30 cm with around 180 kg weight. The first cube (Cube A) was placed on the steel platform into the cavity box by the help of a crane from the top door.

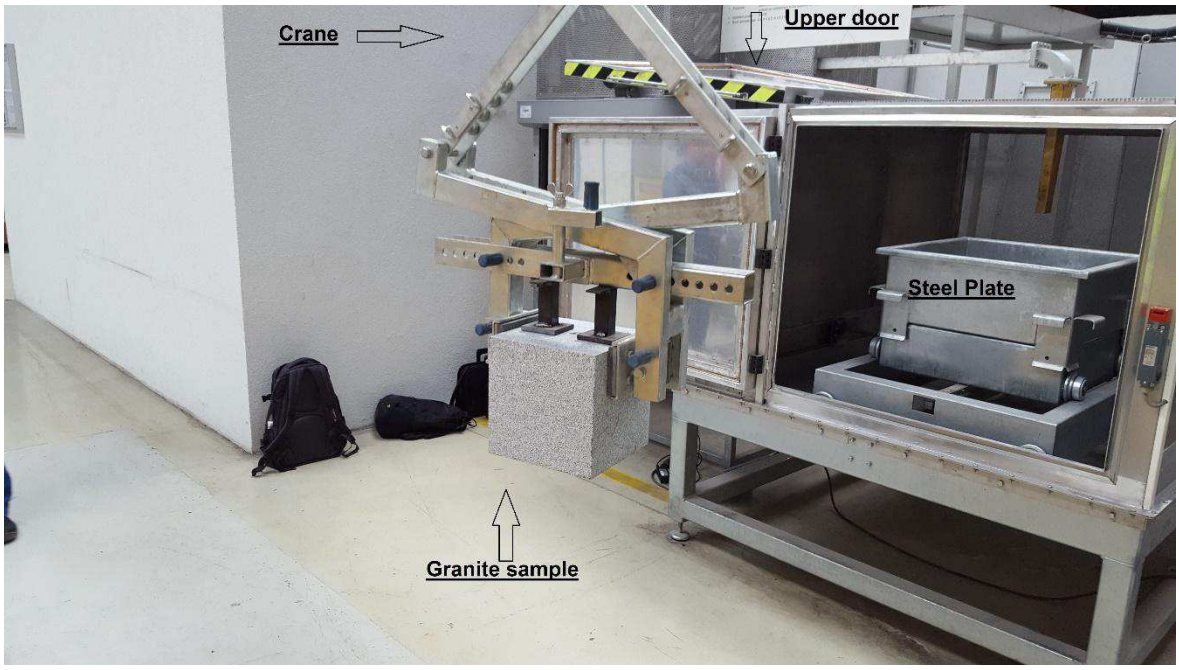

Figure 31: Cavity box and operation of Inserting sample inside it.

Sample was settled exactly below the waveguide in the center of the cavity box by means of the movement lever, so that there was only a 2 cm gap between the waveguide and the rock. Later the doors were closed properly and by using the special computer application, the power was switched on to 50% for 5 minutes. Transferred (15KW) and reflected (50W) energy was then presented on the screen of computer.

After 80 seconds, a minor fracturing sound was heard and the machine was stopped manually. The temperature of the rock was then measured by the infrared gun and a value of 358 ℃ was recorded. Moreover, 2 short longitudinal cracks were observed on the surface. Besides, during operation, the whole device was checked continuously by the microwave leakage measurement.

For the second test, the irradiating power did not alter (15KW transferring, 50W reflecting). At 80 seconds, the operation was interrupted because of another

fracturing sound but the temperature of rock sample was recorded as 600℃. Also, a small hole was formed at the irradiation spot and a black liquid appeared as the material melted on the surface.

The same rock was later prepared for implementation of the third exposure time at another radiation spot on the surface. An equivalent power was supplied and within 90 seconds, fracturing occurred at pick of 600℃. Figure 32 illustrates the surface of the cube A with the 3 induced waves upon it.

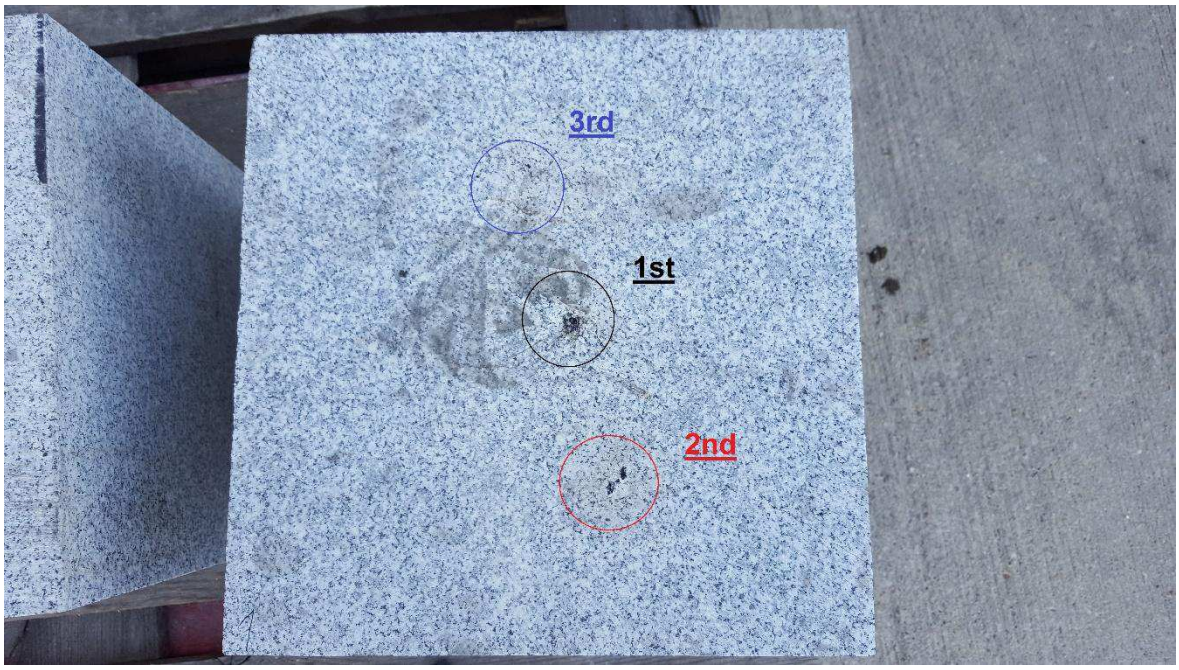

Figure 32: Surface of the first sample (A) with melted holes after 3 times 15KW microwave radiation in 90 seconds.

Second granite cube (Cube B) was inserted into the cavity in the same manner. In this test, the utilized power was similar to the first test (50% of total power).The sample was situated in the middle of the cavity and waveguide was exactly focused on the center of the rock.

Figure 33: Placing the cube on platform and position of the waveguide on the sample.

15KW of the induced wave was transferred with 50W begin the reflection wave after 120 seconds. Again the fracturing point has represented the end of the test, so the machine was shut down and the temperature was written. Infrared gun recorded the same degree for the second cube (600 ℃).

The test resulted in a very tiny hole in the place of radiation with the depth of around 5 mm. The constituting material of the hole was melted as a result of high temperatures on the surface. 2 extensive longitudinal cracks were also formed on the face for which the initiation point was the melted hole with the direction being towards the edge and sides of the rock sample.

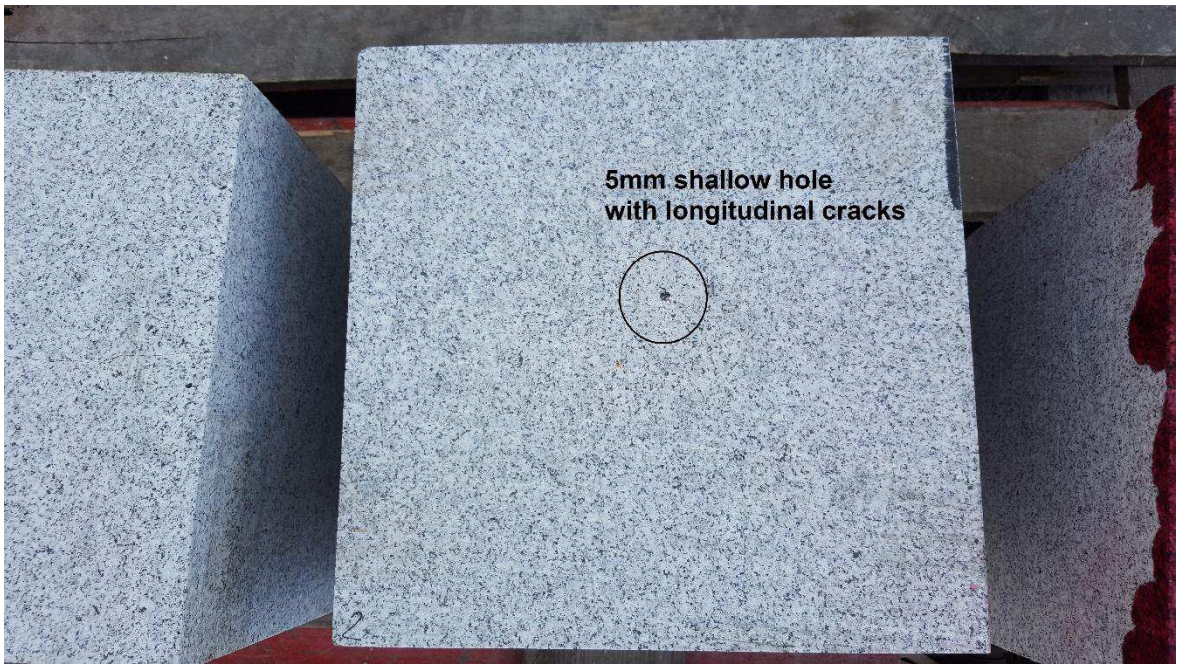

Figure 34: Second cubic (B) with a shallow hole on its surface after exposure.

To end with, the third granite cube (Cube C) was inserted into the cavity. Here, the magnetron power was raised to achieve a more wide-ranging fracture on the surface. Selected energy for this task was 60% of 30KW for 120 seconds (20KW sending, 50W receiving wave). After 90 seconds, machine turned off immediately after a tiny breakage sound was heard on the surface of the rock. The temperature recorded at that time was 600℃.

In comparison to the prior samples, not only burned hole was a bit bigger but also cracks on the surface were thick enough to recognize them very clearly. The pattern of crack propagation was also similar to the latest runs; Radial cracks initiating from melted hole to the edges and sides.

Figure 35: Face of Cube (C) with crack network and hole on it radiated by 20KW microwave.

5.2.4 Primary tasks before digitizing

As it was previously mentioned, the aim of this project is proving the effect of microwave on hard rock granite along with demonstrating the network of cracks inside the rock by means of microwave irradiation. Nonetheless, it was essential to prepare these samples for computer digitizing. All 3 granite samples were exposed to the microwave machine and later tests fulfilled in the laboratory.

Preparation steps before computer digitizing are as follows:

- Penetrating spray
- Drilling
- Computer tomography

Penetrating spray

For identification of the cracks on the surface of the granite samples, penetrant spraying was conducted. As explained in last pages, spraying distinguishes the structure of induced cracks which are a bit larger and wider than the natural one. As it can be seen from the picture below, there are 3 exposed spots highlighted by penetrant spraying on the surface of Cube A and 1 spot on Cube B and C.

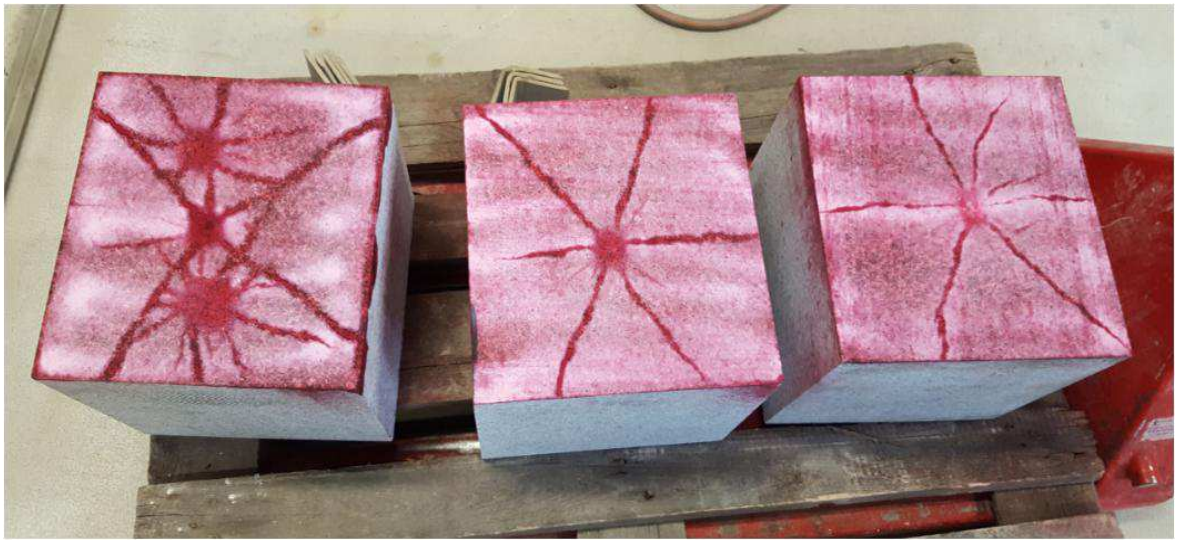

Figure 36: Surface of cube A, B and C after penetrating to highlight the cracks (from left to right).

According to the photo above, it could be distinguished that microwave power on the surface creates a small fracture which leads to a series of cracks. For all samples, cracks are in longitudinal form with a preference to travel to the corners and sides. More investigation and illustration of this pattern of cracks inside the rock led to the decision to cut Cube A perpendicular to the exposed face and then implement penetrant spray to simplify crack detection. Following pictures demonstrate the full steps of this operation.

Observing the cross-section of the cut area, it was realized that the wave had heated up the surface of the rock and generated horizontal cracks. Yet, from the point of irradiation, vertical cracks have been extended downward. To be more detailed, it is essential to capture pictures from all layers of the rock. To achieve this goal, computer-tomography is the best solution. Next step is to drill a core in the granite sample surrounding the fracture initiation spot.

Figure 37: Cutting the cube A along the radiation spots.

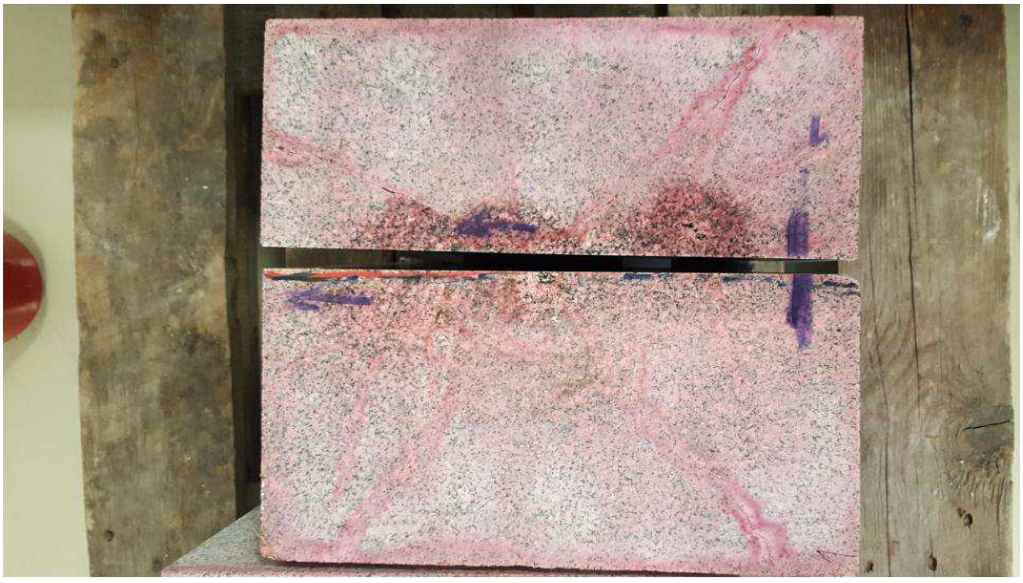

Figure 38: Top view of cube A after cutting in laboratory.

Figure 39: Side view of cut cube A and penetrating the inner side.

Core drilling

The further investigation concerning cracks inside the samples was accomplished by doing core drilling in Cube C with the highest radiation power. With the help of this core, not only it is possible to comprehend the pathway of cracks by penetrant spraying but it was also feasible to take x-ray photos from the core in order to capture detailed information. Drilling was conducted with high precision from the center of the sample so that the spot of irradiation and the center of the core would almost overlap. The diameter of the core was 10 cm with a height of 20 cm. Drilling and core penetrating are presented in pictures below.

Figure 40: Preparing core for Computer Tomography.

It is important to note that the bottom of the core was cut for a more efficient tomography operation as no cracks could be observed in the bottom 10 cm.

Computer tomography

The ÖGI Company in Leoben was responsible for doing CT on this project's core samples. The cylindrical core sent for CT was from the last granite block which was irradiated with the highest microwave power of 20KW. The process took 3 days to complete. Several pictures were received from up to down (top view) as well as from one side to the other (side view) with each individual picture demonstrating the surface of the core.

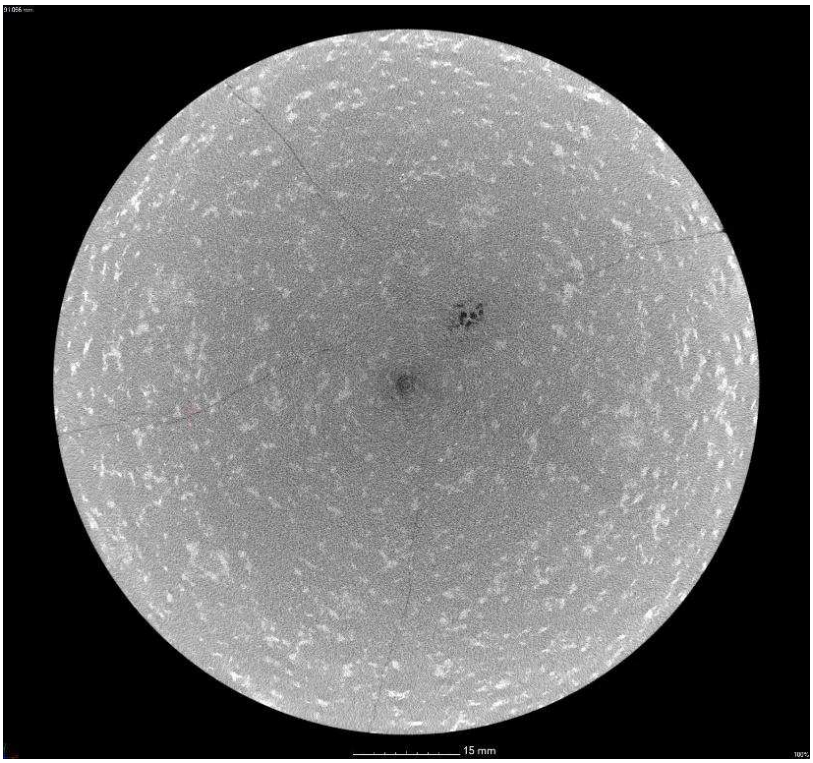

Figure 41: Top view of core taken form CT with 10cm diameter.

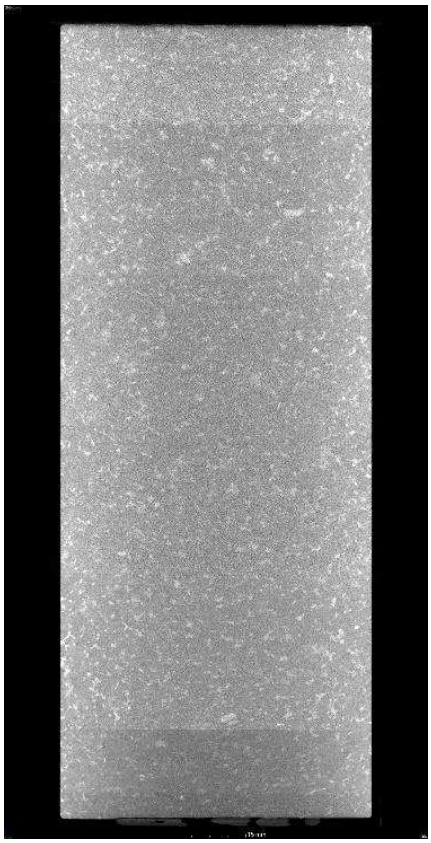

Figure 42: Side view of core taken from CT with 10cm width and 20cm heigth.

5.2.5 Crack digitizing

Captured images at the ÖGI demonstrated the top view and the side view of the drilled core, with each photo being taken every 0.05 mm from top to down as well as side to side. The software used for digitizing the cracks was AutoCAD 2016. The first selected picture of the top view showed the layer that was around 2mm below the real surface due to the bad resolution of the first few photos. The selection of layers for crack digitizing went on for every 2 mm until 10 cm into the depth of the core where the cracks disappear. In other words, the distance between any two images that were taken for digitizing was 2 mm. Each picture or layer was differentiated by specific colors to illustrate all cracks within that layer. As the cracks were sketched, it became evident that there was no connection between the cracks since the spot of radiation was damaged during waving. Figure 43 presents the first layer of a top view of the core with a network of cracks.

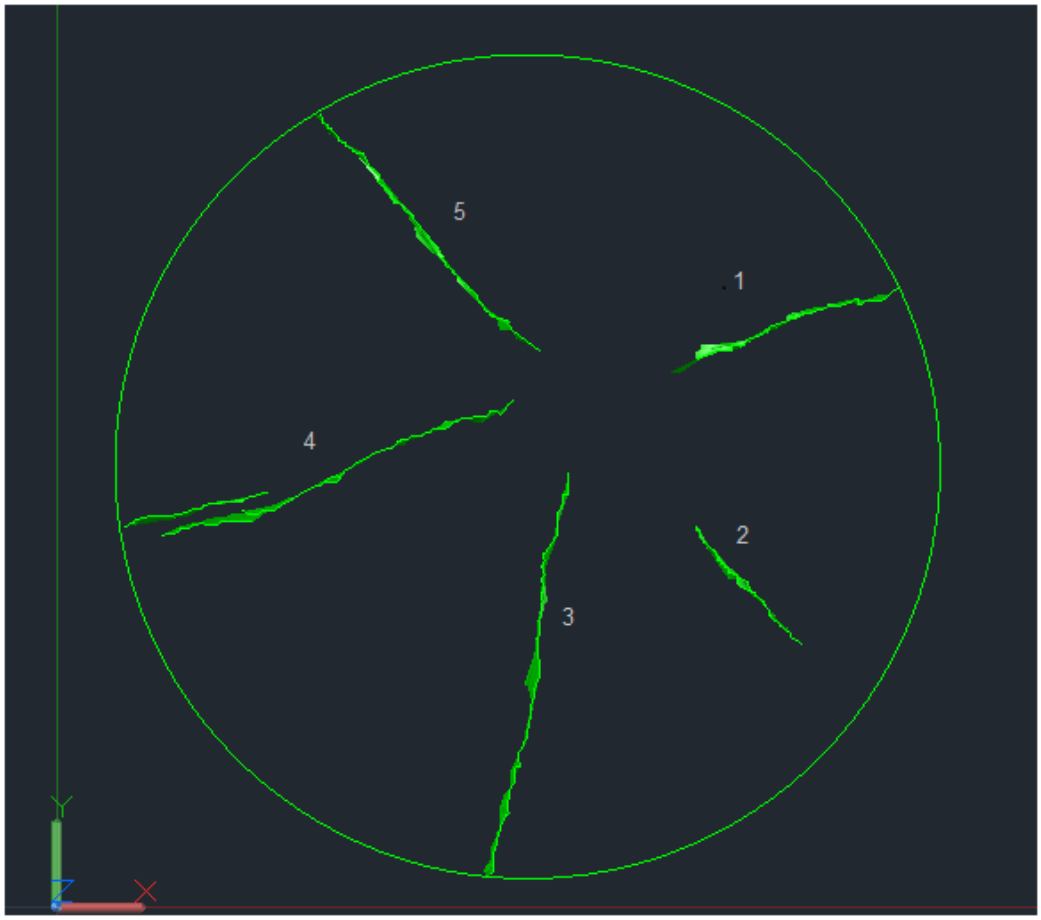

Figure 43: First layer of top view 2 mm below the surface with radial cracks.

The same task was carried out until all cracks disappeared, picture 44 shows the entire crack distribution from the surface to the depth (10 cm). Going deeper, the length of the horizontal cracks also turned out to be shorter and shorter until the depth of 10 cm below the surface where horizontal cracks seized to exist. Moreover, the thickness of the cracks was reduced when traveling downwards from the surface. As noticeable from the previous picture, there were 5 cracks on the surface. Specifying the cracks on the first layer from 1 to 5 (clockwise), the shortest one (number 2) terminated in the third layer around 6 mm below the crust.

The digital sketch also displays that cracks 1 and 4 continued until the end of digitizing whereas cracks 3 and 5 stopped extending at depths of 34 mm and 64 mm respectively. In addition, based on Figure 43, there could be a connection between crack 1 and 4 with a possibility of them being one continuous radial crack and the tiny radiation spot as that gap. On the other hand, it can be figured out that the orientation of cracks is not straight and regular, their distribution along the depth is somehow in a zigzag mode. Moreover, the initiation point for all of the cracks up to 12 mm below the face is nearly alike. So it could be interpreted that the intensity of the microwave power is more or less constant until 1 cm below the surface and from this level, it started losing its energy.

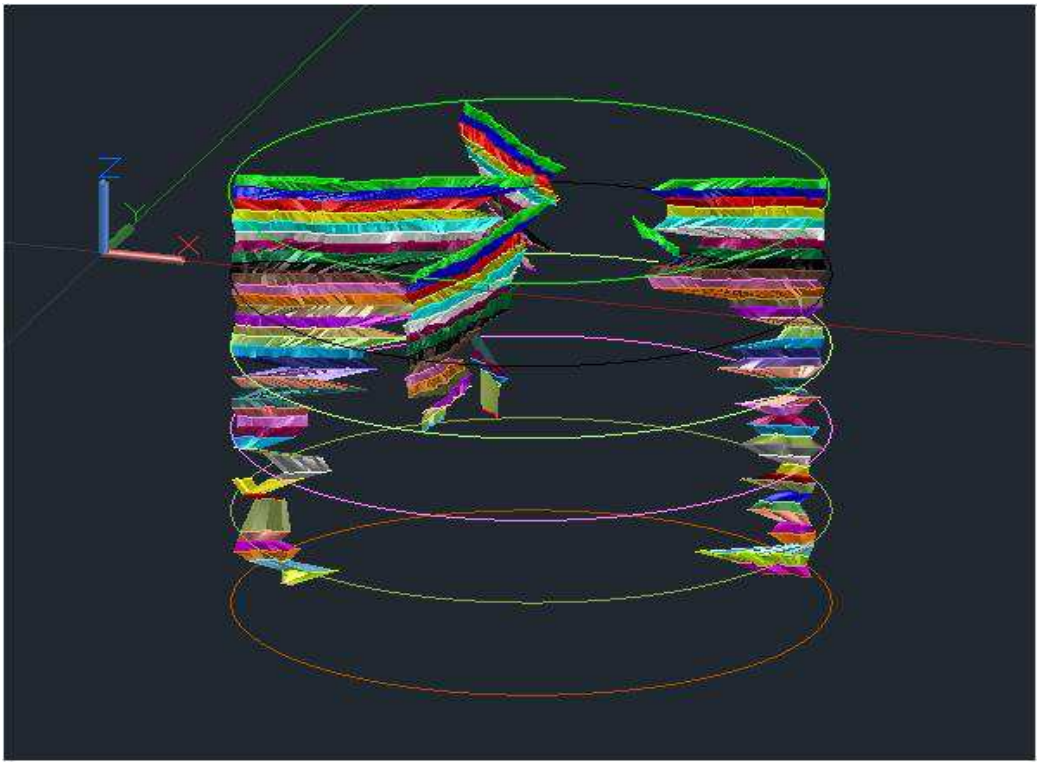

Figure 44: Digitized core with whole radial cracks from surface till 10 cm below.

The next step after analyzing the top view images, was digitizing the vertical advancement of the cracks which has been carried out by observing the photos of CT in a side to side fashion, starting from the face of the core at one side and ending at the other side. The resolution was equal to the top view photos and they were similarly captured every 0.05 mm. Considering the cylindrical core, the zone of cracks ranges from 0 to 10 cm (diameter of the cylindrical core) with the height of 20 cm. The first sketched plane is presented in figure 45.

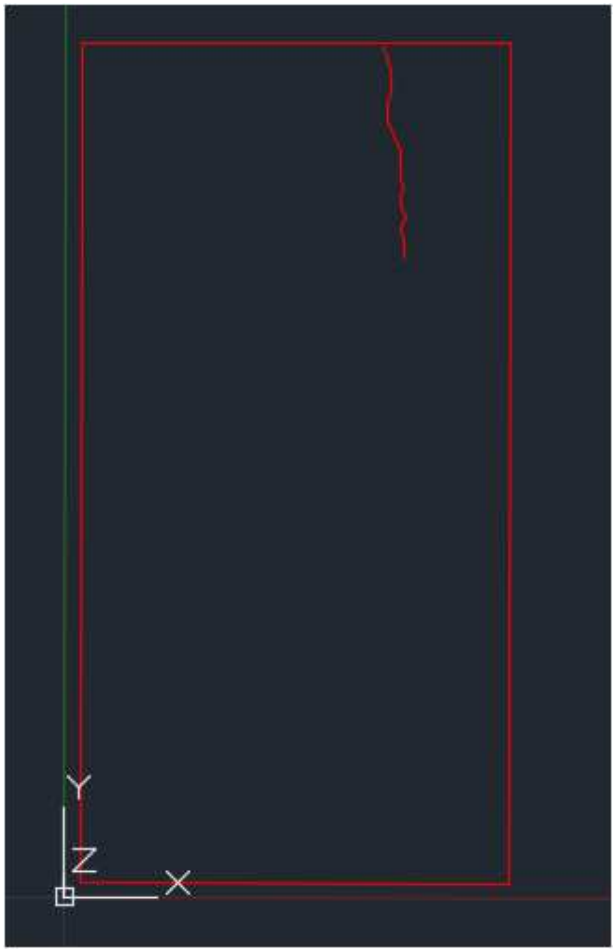

Figure 45: Side view of the core with the formation of a vertical crack (10 cm width and 20 cm height).

Similar to top view, there was also a 2 mm distance between selected planes for drawing side view sketches. In other words, the first picture can be labeled as ‘0’ right at the sidewall and the following pictures continue every 2 mm going toward the core to the other wall ‘50’. Interestingly, the vertical cracks on both core faces were longer in comparison with cracks in the middle. Besides, during digitizing, a number of horizontal cracks were discovered in some planes. Moreover, no vertical

crack discovered from planes between 22 mm and 44 mm. Figure 46 shows the final schematic of side to side sketching including both vertical and horizontal cracks.

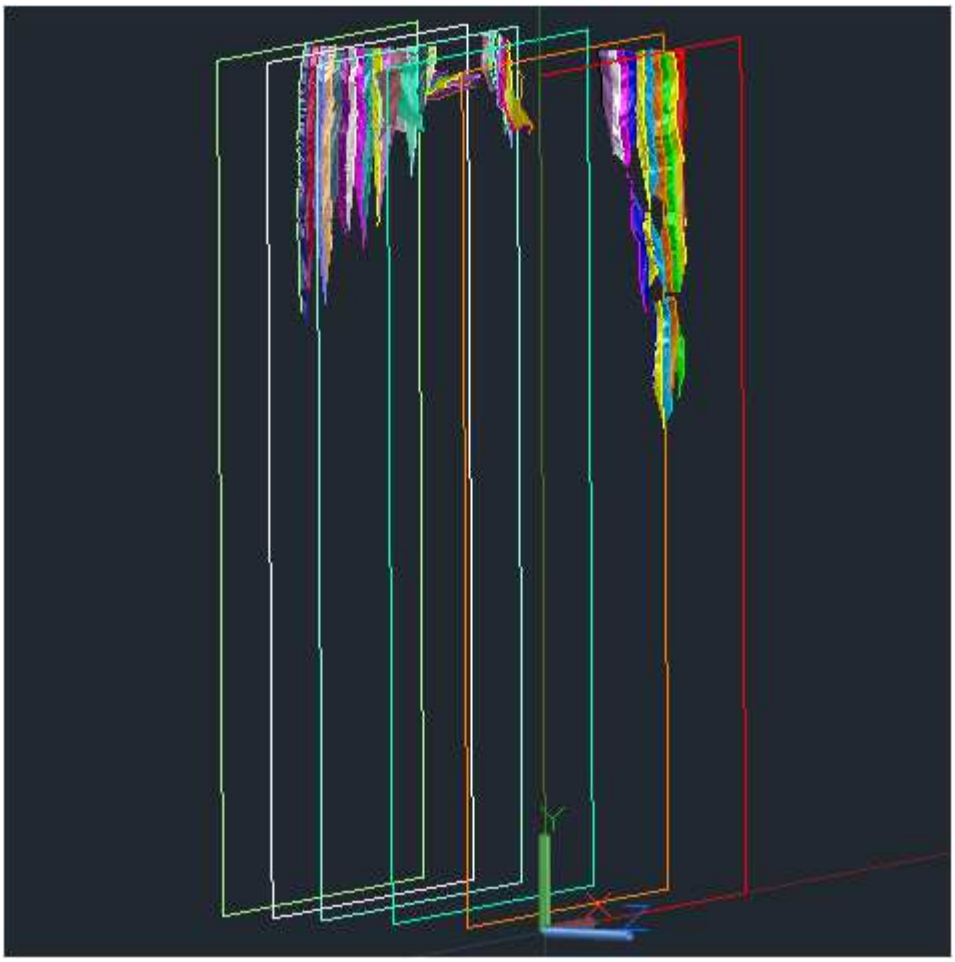

Figure 46: Side view with complete vertical and horizontal crack (side to side).

Finally, these 2 patterns were overlaid on each other, combining digitized cracks from top view with all cracks in side view to have a fully detailed model of the granite cylinder containing the full crack network. This process was carried out by combining the X, Y and Z axis of individual cracks and layers. For simplicity, the final sketch model was presented in the format of a top view image, which according to figure 47, owns some special features with regard to cracks-overlaying:

1. Increase in the length of cracks even at lower levels.
2. A horizontal connection between cracks 4 and 5, 12 mm below the surface.
3. At a depth of near 10 cm, the presence of cracks (crack density) in side view is more prominent than the top view ones.

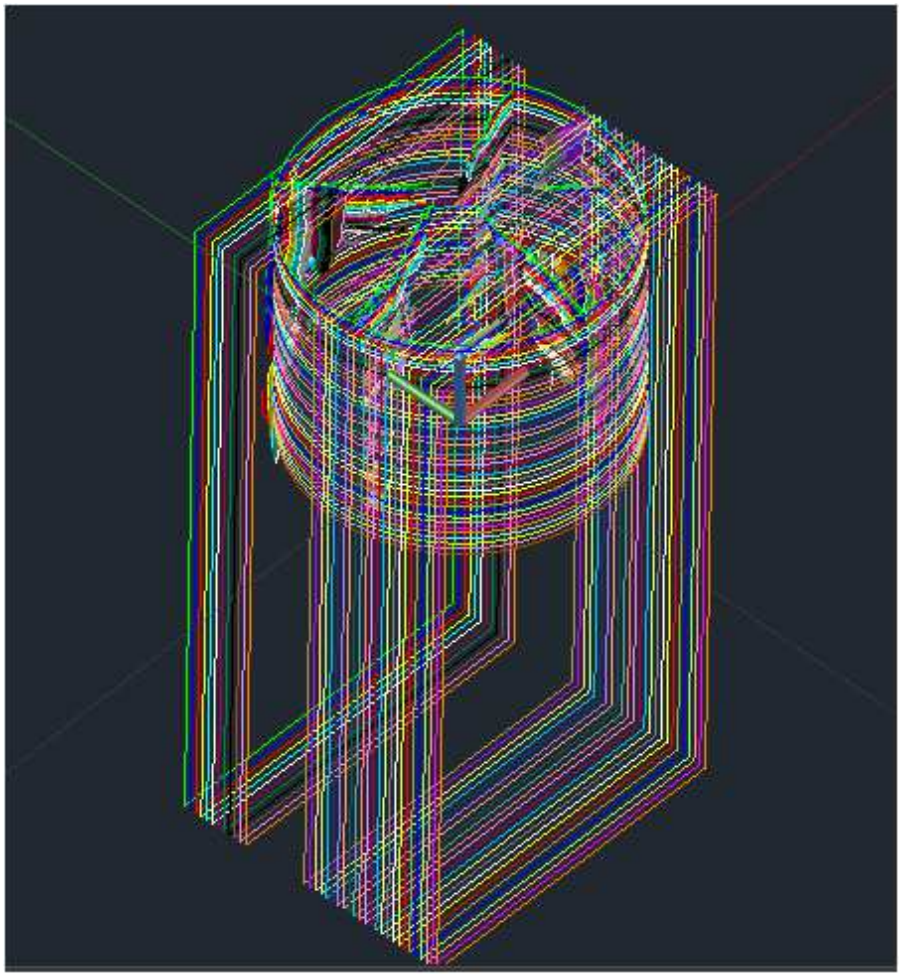

Figure 47: Overlaid pattern Top view and Side view.

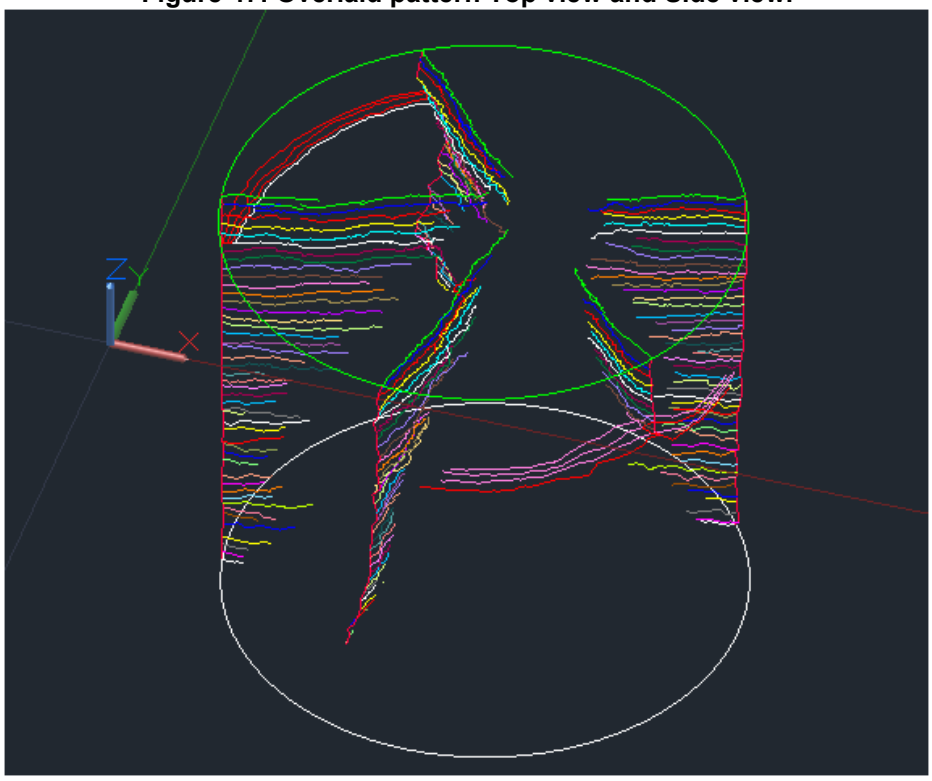

Figure 48: Schematic of cracks after overlaying with 10 cm diameter and 10 cm height.

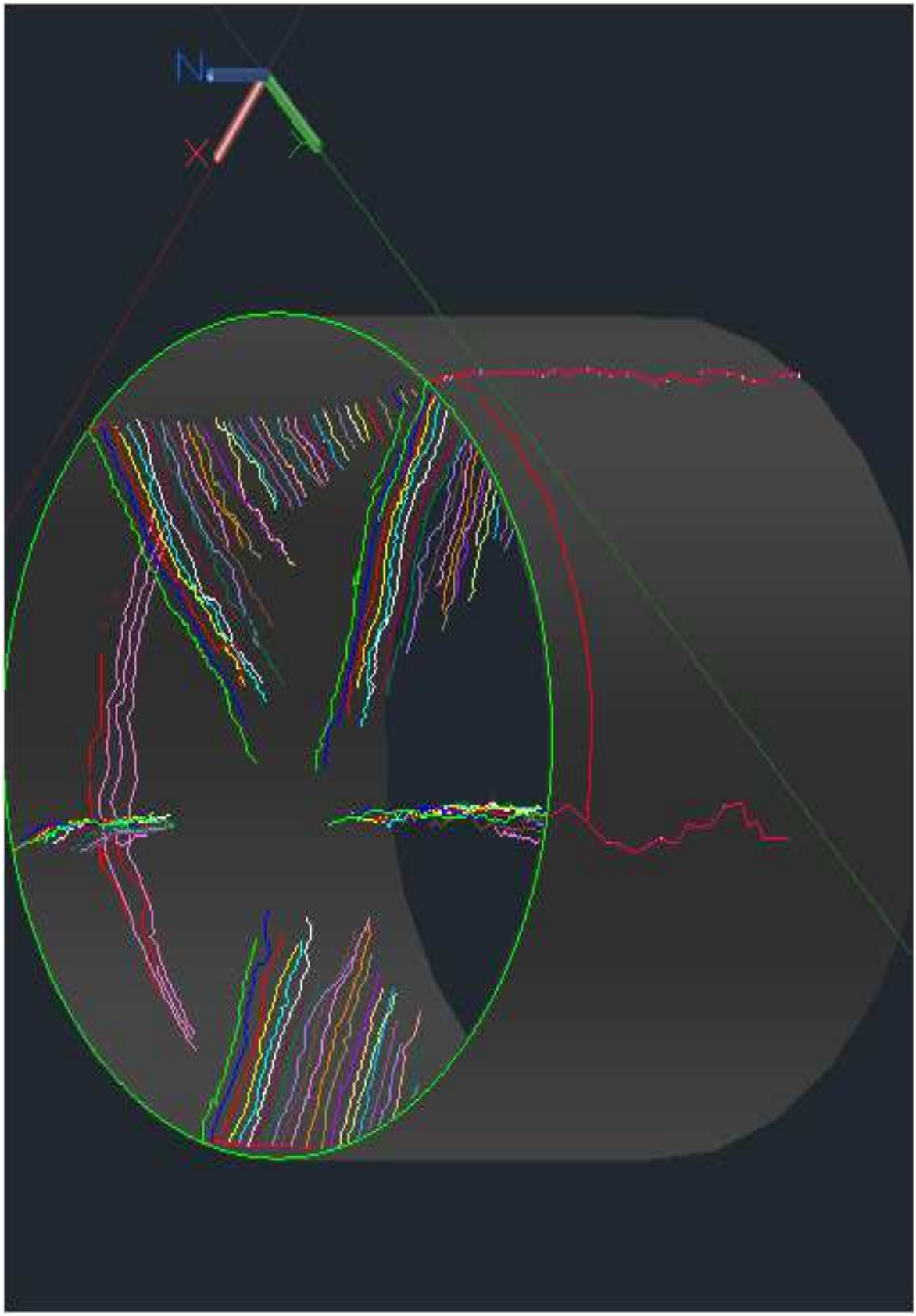

Figure 49: Final Schematic of treated core with all digitized cracks within 10cm diameter and 10 cm height cylinder.

5.2.6 Digitizing of cracks for small cylinder

As explained in the last section, all existing cracks inside the core, from the surface to 10 cm below, were digitized after CT to evaluate their orientation and distribution. Unfortunately, in this case, due to the poor resolution of data (as pictures), the spot of radiation could not be clearly assessed.

To resolve this challenge, a new core with a smaller diameter was drilled on the original cylinder. Drilling was performed with the diameter of 2.5 cm surrounding the radiation spot with the intact height of 20 cm. The small core was sent to the ÖGI Company for CT as well. Identically to the big core, two sets of photographs from the top view and the side view were obtained. The resolution was unchanged and each picture was taken at 0.05 mm intervals. Figure 50 depicts the newly drilled core from the big cylinder.

Figure 50: Drilled small core (2.5 cm diameter) with the center of the radiation spot.

Using AutoCAD, the density of cracks around the spot of radiation was precisely drawn. From the top, the first selected photo for this task was 1.5 mm below the surface to have a brighter resolution. Furthermore, the area of the core was divided into 24 sections to better illustrate the location of the cracks (Figure 51). Whatever has been digitized, were the tiny cracks which could be distinguished as a result of

microwave radiation, not from the geological events. Around 5 mm was the diameter of the tiny hole without any cracks.

During the drawing phase, it was understood that there is a distinction among cracks with respect to their thickness. Different cracks were classified into 3 groups: a blue one with 55-65μm thickness, the red one with 40-55μm thickness and white one with 30-40μm thickness. One of the aims of this categorization was to estimate the distribution of cracks in small scale and figure out their density when moving into depth.

To fulfill this task, 3 layers from top view were chosen. The first layer, as mentioned before, can be found 1.5 mm below the surface while the second and third layers were located 5 mm and 10 mm below the surface.Next, all 3 types of cracks were outlined and counted in each individual section.

As can be seen in figures 52, 53 and 54, blue cracks which are the longest and the thickest ones, spread more on the first layer and towards the edge of the core than to the center.

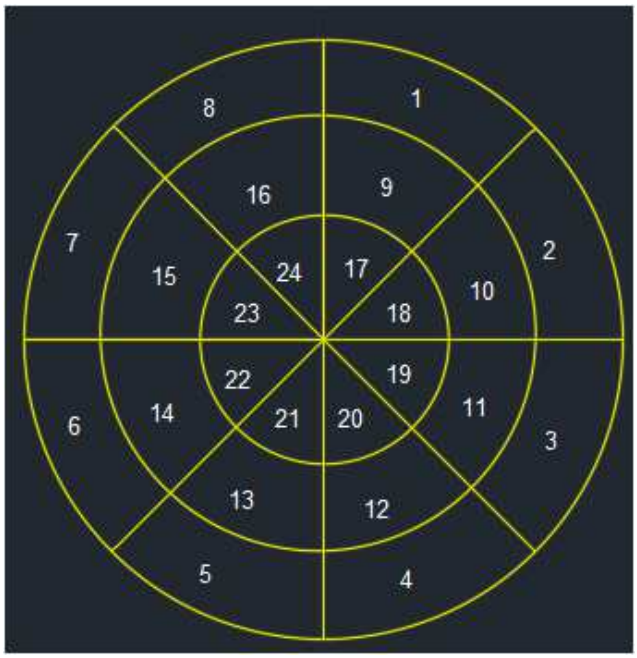

Figure 51: Division of the face of the small cylindrical core into 24 sections for clarifying the crack density.

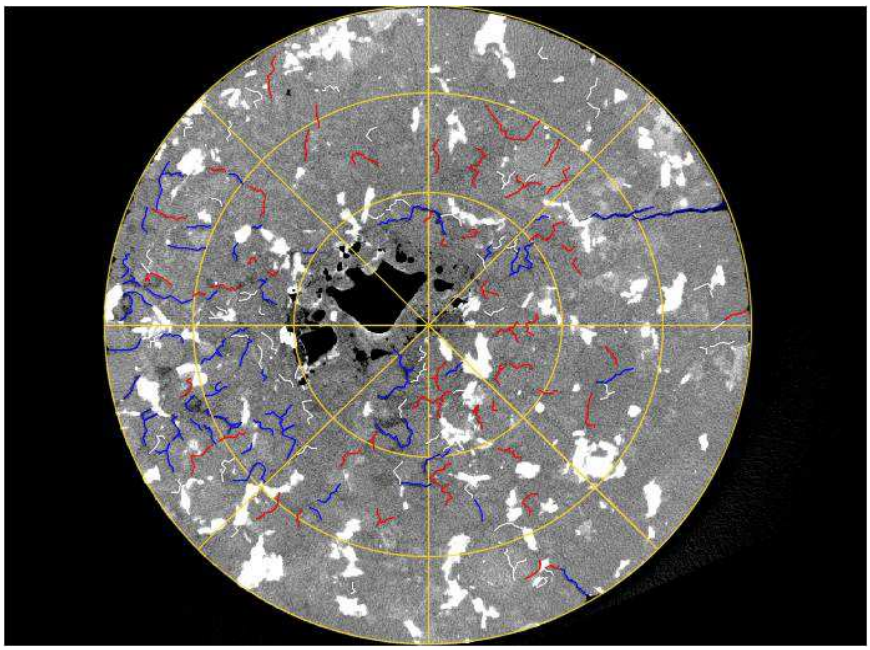

Figure 52: Top layer for the small core with 1.5 mm below the surface (2.5cm diameter).

	Blue with 55-65µm thickness	Red with 40-55µm thickness	White with 30-40µm thickness	
Section 1	0	0	3	3
Section 2	2	1	1	4
Section 3	0	0	3	3
Section 4	1	2	4	7
Section 5	0	1	2	3
Section 6	13	4	4	21
Section 7	15	4	5	24
Section 8	0	2	3	5
Section 9	0	10	3	13
Section 10	2	4	0	6
Section 11	2	4	2	8
Section 12	1	5	3	9
Section 13	4	5	2	11
Section 14	16	1	5	22
Section 15	6	5	5	16
Section 16	0	3	1	4
Section 17	2	3	3	8
Section 18	3	4	3	10
Section 19	0	6	0	6
Section 20	1	6	3	10
Section 21	5	2	3	10
Section 22	0	0	0	0
Section 23	0	0	0	0
Section 24	3	0	3	6
Sum	76	72	61	209

Table 7: Crack density in the first layer of the top view (1.5 mm).

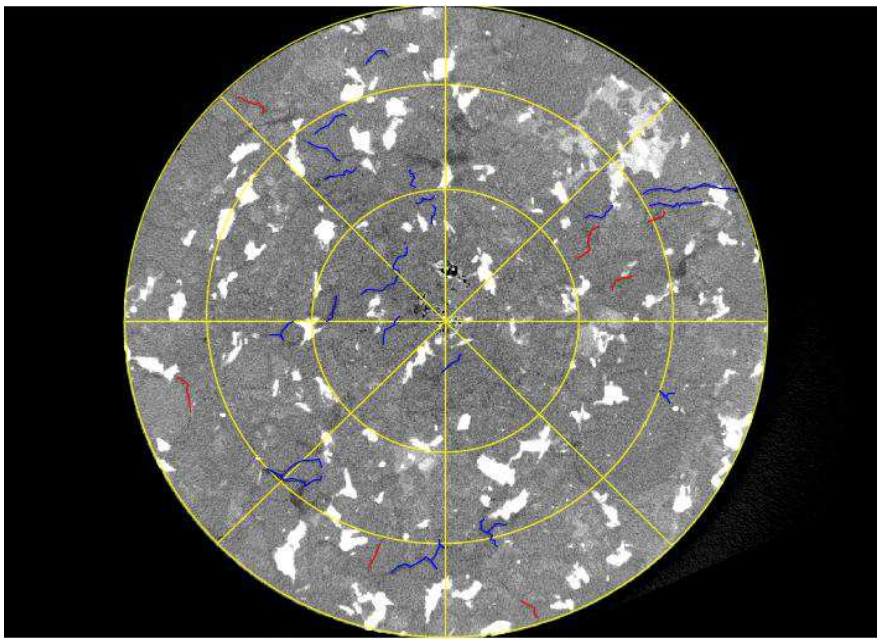

Figure 53: Top layer for the small core with 5 mm below the surface (2.5cm diameter).

	Blue with 55-65µm thickness	Red with 40-55µm thickness	White with 30-40µm thickness	
Section 1	0	0	0	0
Section 2	2	1	0	3
Section 3	1	0	0	1
Section 4	0	0	0	0
Section 5	2	1	0	3
Section 6	0	1	0	1
Section 7	0	0	0	0
Section 8	1	1	0	2
Section 9	0	0	0	0
Section 10	1	2	0	3
Section 11	0	0	0	0
Section 12	3	0	0	3
Section 13	4	0	0	4
Section 14	3	0	0	3
Section 15	0	0	0	0
Section 16	5	0	0	5
Section 17	0	0	0	0
Section 18	0	0	0	0
Section 19	1	0	0	1
Section 20	1	0	0	1
Section 21	0	0	0	0
Section 22	1	0	0	1
Section 23	3	0	0	3
Section 24	3	0	0	3
Sum	31	6	0	37

Table 8: Crack density in the second layer of the top view (5 mm).

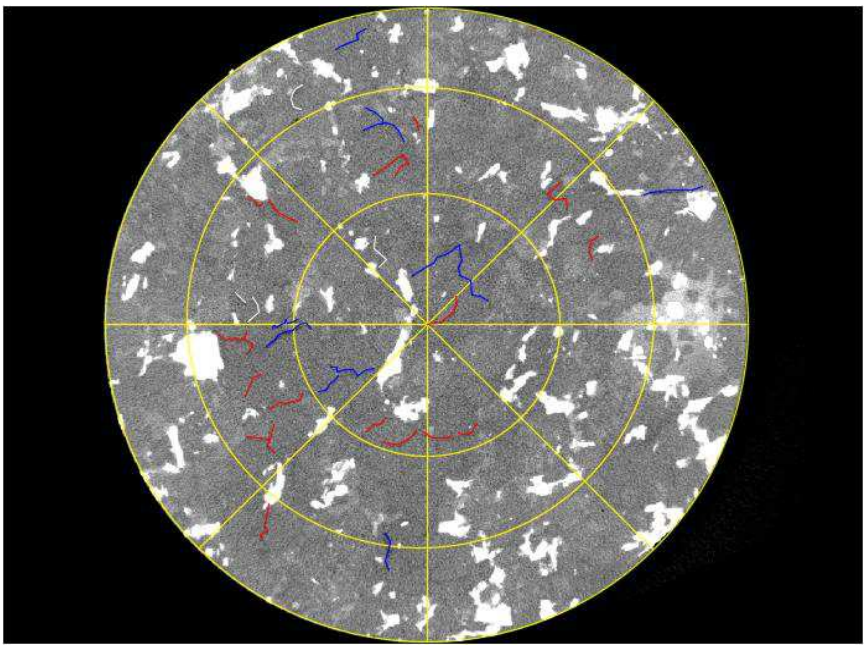

Figure 54: Top layer for the small core with 10 mm below the surface (2.5cm diameter).

	Blue with 55-65µm thickness	Red with 40-55µm thickness	White with 30-40µm thickness	
Section 1	0	0	0	0
Section 2	1	0	0	1
Section 3	0	0	0	0
Section 4	0	0	0	0
Section 5	1	2	0	3
Section 6	0	0	0	0
Section 7	0	0	0	0
Section 8	1	0	1	2
Section 9	0	1	0	1
Section 10	0	2	0	2
Section 11	0	0	0	0
Section 12	0	0	0	0
Section 13	0	0	0	0
Section 14	1	6	0	7
Section 15	2	2	2	6
Section 16	4	3	0	7
Section 17	3	0	0	3
Section 18	1	2	0	3
Section 19	0	0	0	0
Section 20	0	2	0	2
Section 21	0	2	0	2
Section 22	3	0	0	3
Section 23	0	0	0	0
Section 24	3	0	2	5
Sum	20	22	5	47

Table 9: Crack density in the third layer of the top view (10 mm).

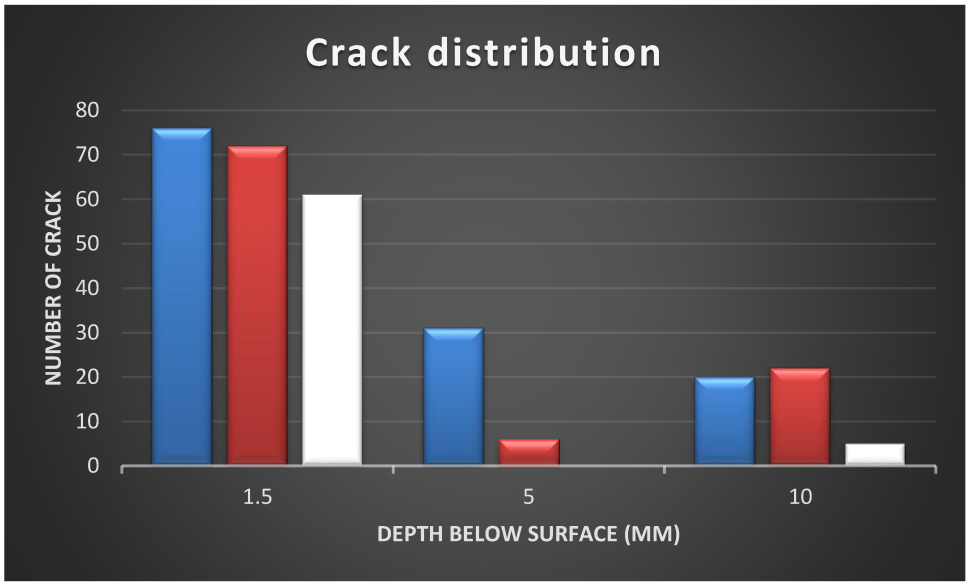

Table 10: Crack distribution (3 types of crack) of the top view in 3 layers.

Comparing the photos of crack distribution, it is evident that the crack density decreases with depth, especially in the case of blue cracks which are the longest and thickest. In the first layer (1.5 mm below the surface), the number of all 3 types of cracks is quite the same. However, there is a significant gap between blue cracks and white cracks in the second layer, where the sum of all blue cracks is reduced to two times less and white cracks have totally disappeared. There is also a giant fall in the quantity of red cracks.

In the third layer with a depth of 10 mm, the total amount of cracks is surprisingly more than the second layer as the density of the red and white cracks have raised. Despite that, the number of blue cracks have decreased.

From the side view, the same procedure was conducted. 3 images were selected from the collection of CT photos for clarification of the crack network in a planar manner. The first plane was designated at the middle, and the second and third one 6mm far from either side walls (Figure 55).

The gridding, sketching and counting procedures were the same as that of the top view, the one and the only difference were just the grid geometry which in this case was rectangular. The face of each individual plane was partitioned into 36 small rectangular blocks with the height of 5.4 mm and width of 4.1 mm. Cracks were once again classified into 3 groups based on their thickness: blue ones with 50-60µm thickness, yellow ones with 40-50µm thickness and white ones with 30-40µm thickness. The middle plane and its crack system are shown in figure 56 with the result of the crack counting.

Most of the thickest cracks were concentrated on the first horizontal row which is up to 5 mm below the surface. Moving gradually into the depth of the core, the cracks become shorter and thinner and the number is reduced while, this trend acts the opposite for white cracks.

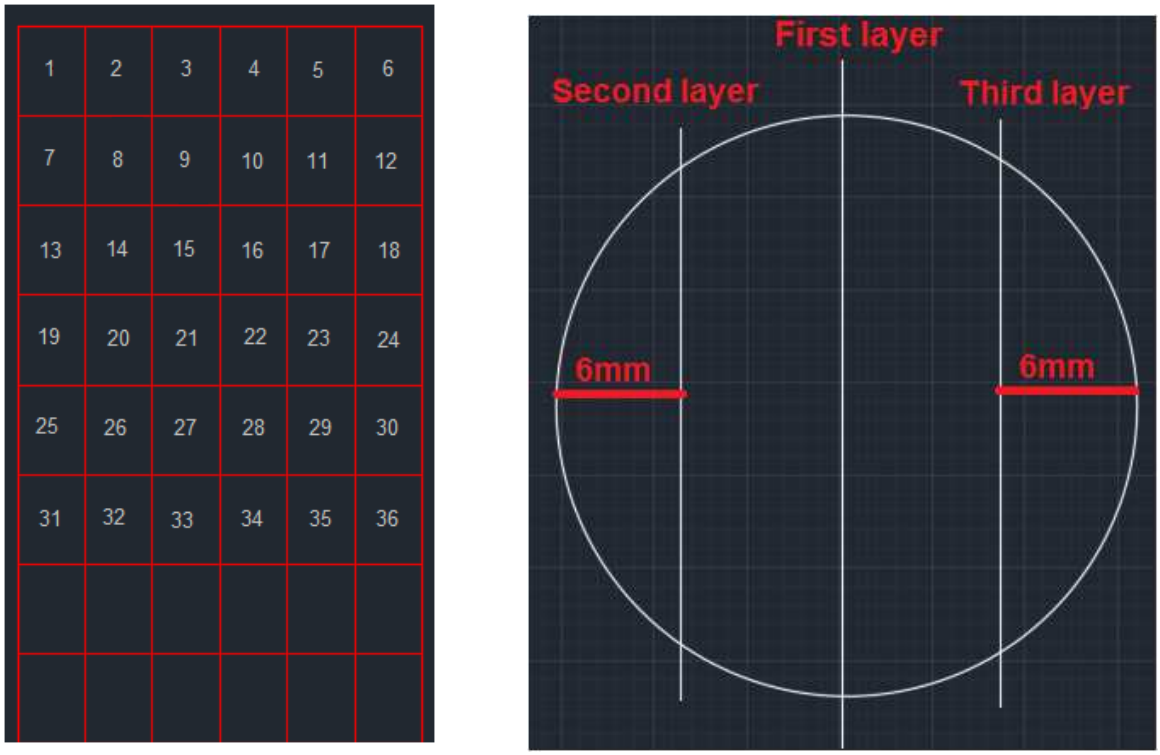

Figure 55: Division of the side view of a small cylindrical core into 36 blocks for clarifying the crack density (left) and selected planes for digitizing (right).

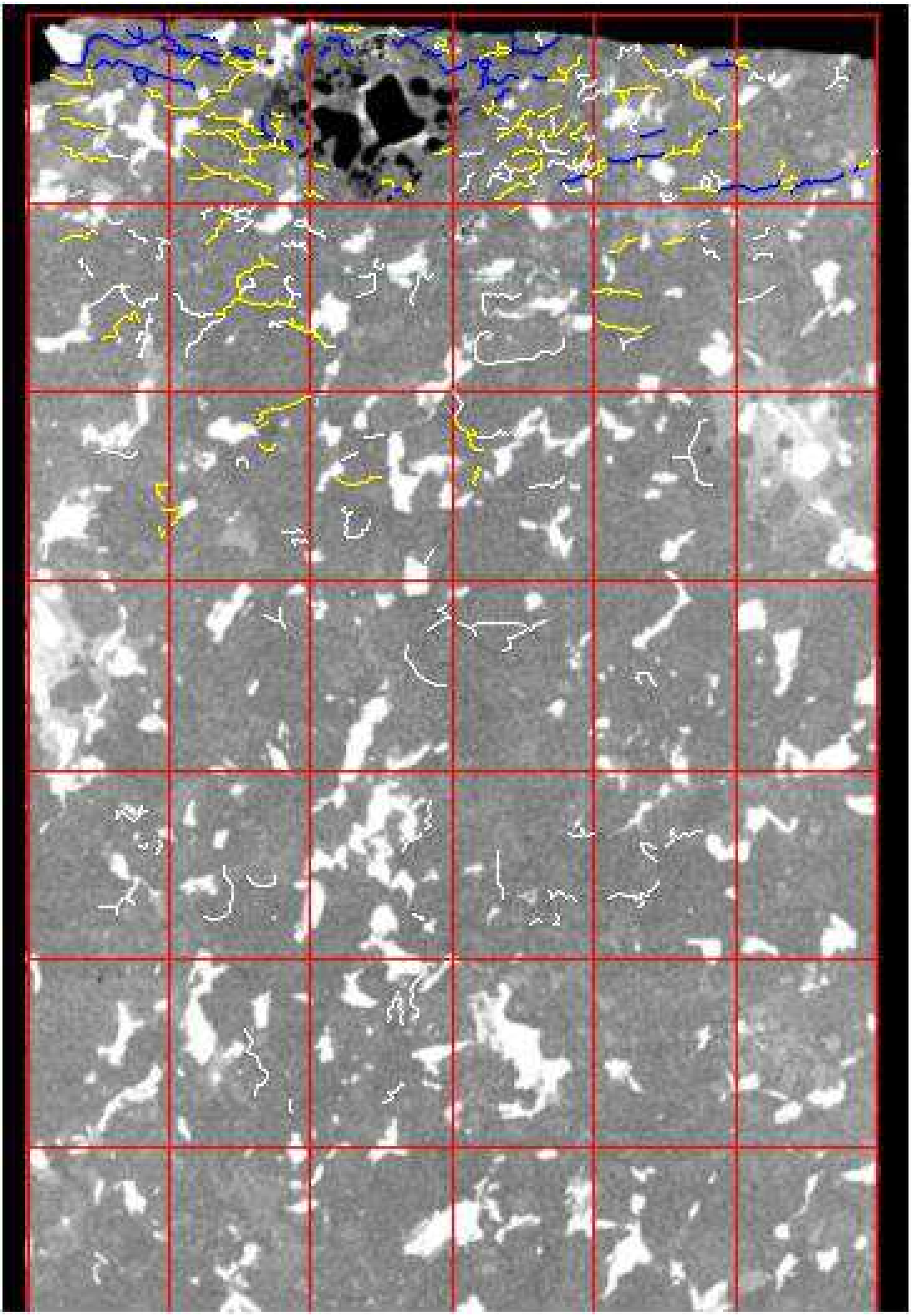

Figure 56: Side photo with 2.5cm width from the middle of the core (first plane) with sketched cracks.

	Blue with 50-60µm thickness	Yellow with 40-50µm thickness	White with 30-40µm thickness	
Block 1	3	4	2	9
Block 2	8	16	0	24
Block 3	7	8	2	17
Block 4	11	17	22	50
Block 5	5	12	8	25
Block 6	4	5	5	14
Block 7	0	2	11	13
Block 8	0	6	11	17
Block 9	0	0	5	5
Block 10	0	1	5	6
Block 11	0	5	4	9
Block 12	0	0	3	3
Block 13	0	2	1	3
Block 14	0	5	3	8
Block 15	0	1	5	6
Block 16	0	2	3	5
Block 17	0	0	2	2
Block 18	0	0	0	0
Block 19	0	0	0	0
Block 20	0	0	1	1
Block 21	0	0	3	3
Block 22	0	0	3	3
Block 23	0	0	1	1
Block 24	0	0	0	0
Block 25	0	0	6	6
Block 26	0	0	2	2
Block 27	0	0	3	3
Block 28	0	0	5	5
Block 29	0	0	4	4
Block 30	0	0	0	0
Block 31	0	0	0	0
Block 32	0	0	2	2
Block 33	0	0	4	4
Block 34	0	0	0	0
Block 35	0	0	0	0
Block 36	0	0	0	0
SUM	**38**	**86**	**126**	**250**

Table 11: Crack density in the center of the side plane

- Block size 5.4*4.1mm
- Crack existence only in 6 rows, depth from the surface to 32.4mm.
- The length of cracks varies from 0.23mm to 2.8mm.

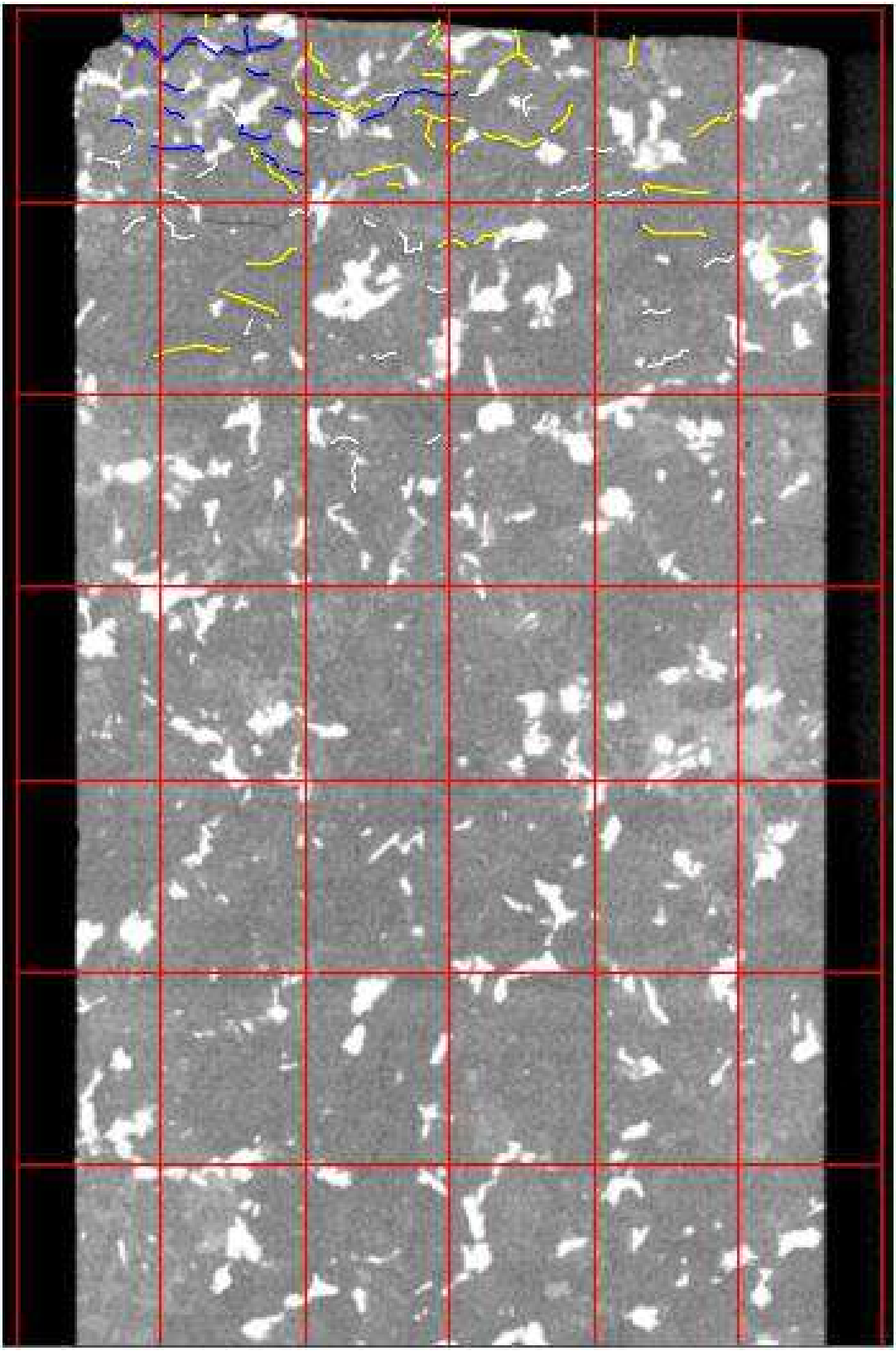

Figure 57: Side photo (20mm width) with 6 mm far from the side (second plane).

	Blue with 50-60μm thickness	Yellow with 40-50μm thickness	White with 30-40μm thickness	
Block 1	2	1	2	5
Block 2	11	3	3	17
Block 3	4	10	2	16
Block 4	1	7	3	11
Block 5	0	3	2	5
Block 6	0	0	0	0
Block 7	0	0	1	1
Block 8	0	3	3	6
Block 9	0	0	4	4
Block 10	0	2	1	3
Block 11	0	1	3	4
Block 12	0	1	0	1
Block 13	0	0	0	0
Block 14	0	0	0	0
Block 15	0	0	3	3
SUM	**18**	**31**	**27**	**76**

Table 12: Crack density for the second plane.

It is considered that the width of 2 planes (second and third) is smaller than the first one but the size of gridding is equal. As it can be seen from the data for the second plane, distribution of blue cracks is only in the first row moreover, propagation of all 3 types of cracks has been reduced and the 3rd row is the limit of this crack spreading.

In comparison to the first plane, there was a significant fall in a number of yellow and white cracks for this plane (2^{nd}). But, spreading to the depth was reduced only for 1 row till the second row.

Propagation of white cracks in depth (2^{nd}) has been decreased substantially in which, this value was double in the first plane. In another meaning, white cracks have been spread out till 6th row and 3rd row in the middle and second plane respectively.

The number of the total cracks has decreased as well. That figure for 2^{nd} plane is 3 times smaller than first one. However, it should be considered that the width of second and also the third plane is minor than the middle one due to placing in the vicinity of the side walls.

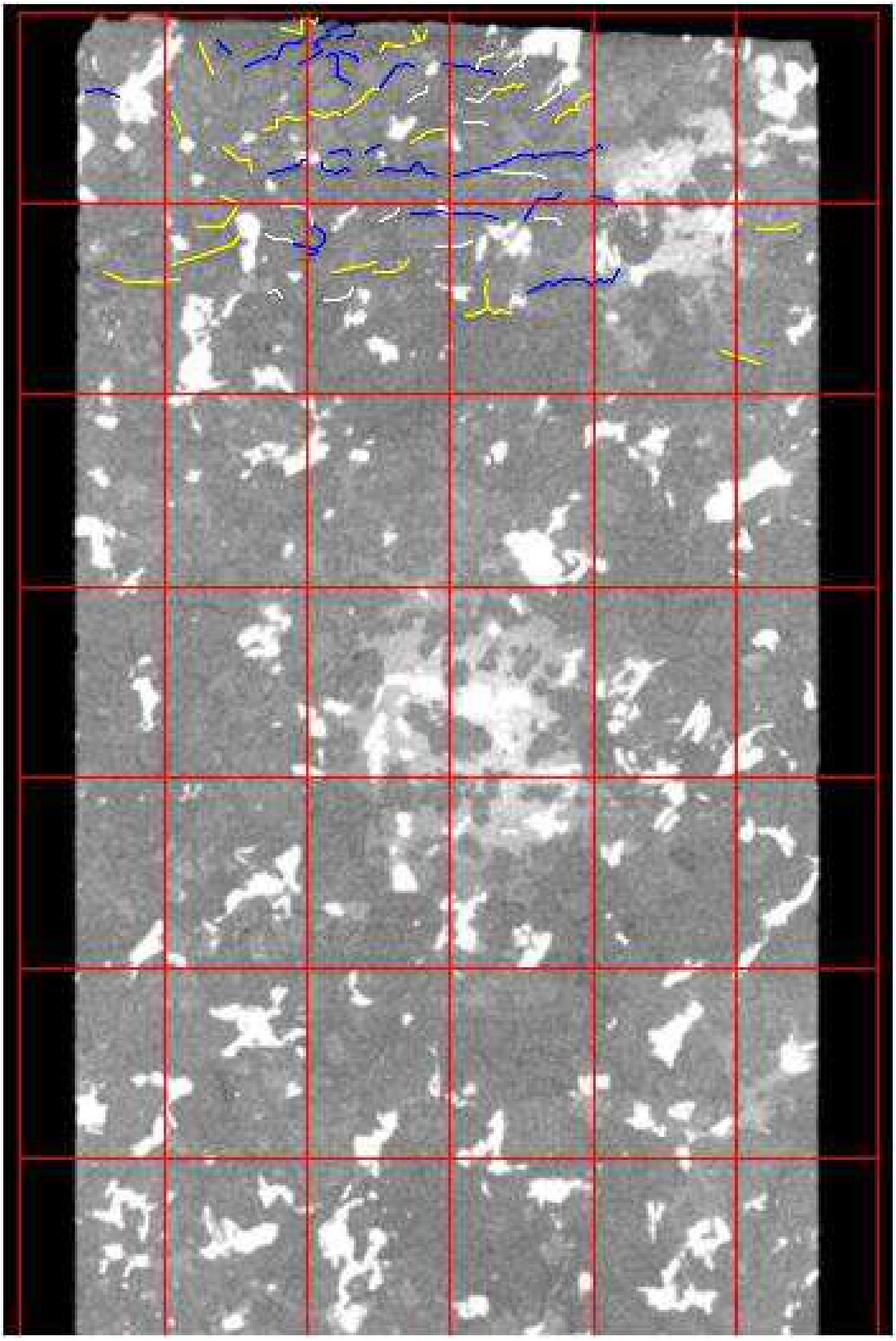

Figure 58: Side photo (20mm width) with 6 mm far from the side (third plane).

	Blue with 50-60μm thickness	Yellow with 40-50μm thickness	White with 30-40μm thickness	
Block 1	1	0	0	1
Block 2	3	5	0	8
Block 3	9	6	1	16
Block 4	2	2	5	9
Block 5	1	0	0	1
Block 6	0	0	0	0
Block 7	0	1	0	1
Block 8	1	3	3	7
Block 9	3	2	4	9
Block 10	3	2	2	7
Block 11	2	1	0	3
Block 12	0	2	0	2
SUM	**25**	**24**	**15**	**64**

Table 13: Crack density for the third plane.

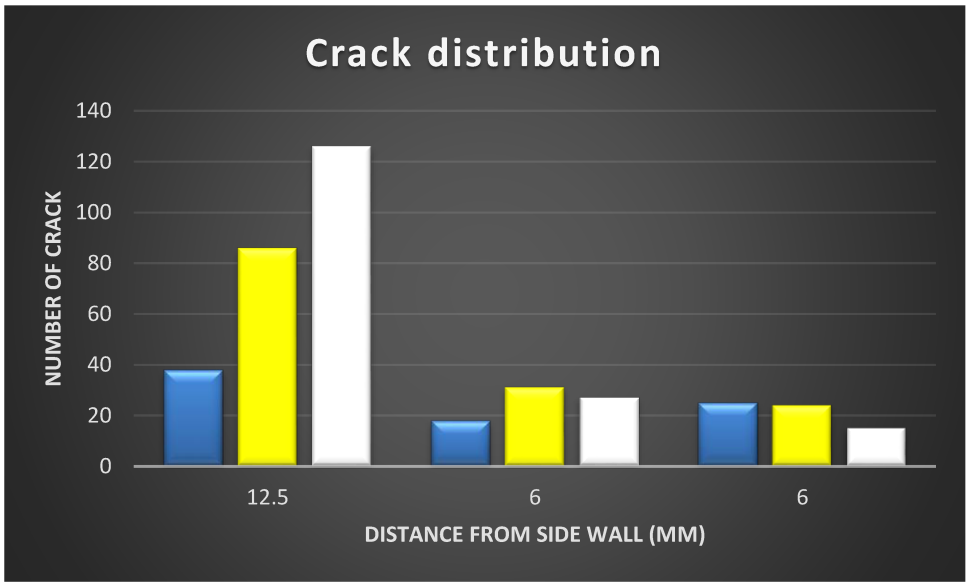

Table 14: Crack distribution (3types of crack) on side selected platforms.

For the third plane in comparison to the second one, the number, as well as the depth of crack density for blue cracks, has raised. However, the limit of crack propagation has come to the 2nd row.

Even though both planes have the same distance from the nearest walls, the total amount of cracks for the third plane is small. In addition, there is a decrease for both white and yellow cracks for this plane (3rd).

6 Discussion and Results

A large number of tests have been carried out over the years to verify the effect of electromagnetic waves on rock breakage. Most of such experiments were conducted on small-scale samples and low-power magnetrons. The main focus of these tests was to weaken the key mechanical properties of the rock, such as UCS, and enable its rupture. As discussed in the earlier chapters, the internal temperature escalation of a rock would lead to the initiation of cracks and reduction in its strength.

The aim of this project was to analyze the breakage of Granite rocks in large scale with a microwave power up to 30 KW. Based on the test results and the digitizing the appeared radial cracks as well as the density and distribution of the micro-cracks in areas near the wave and rock collision spot, it is claimed that according to the experiments of Meisels et al (2015) (Figure 59) and Nekoovaght (2015) (Figure 60), The absorbed power density from rock is just concentrating on the face and some layers below the surface, in addition, temperature distribution by going into the depth is decreasing.

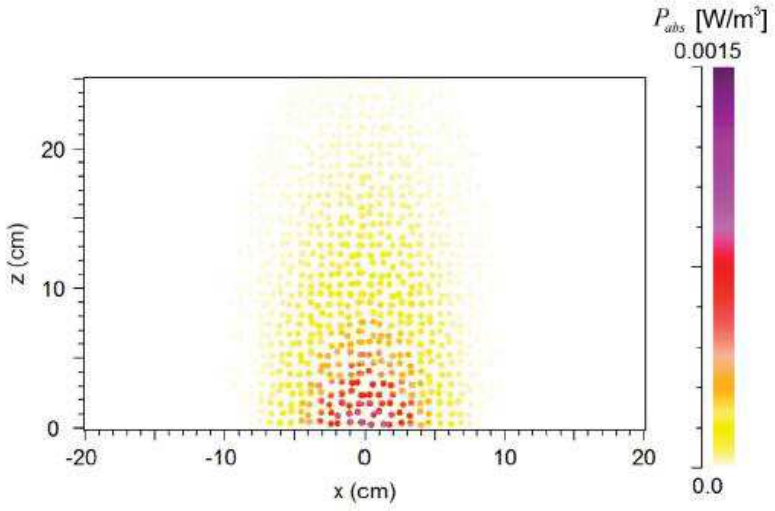

Figure 59: 2 Dimensional model of absorbed power density. The microwave source is at Z=-1 cm and radiates in the positive Z direction. The thickness of rock in direction of propagation is from Z=0 cm to Z=30 cm (Meisels et al 2015)

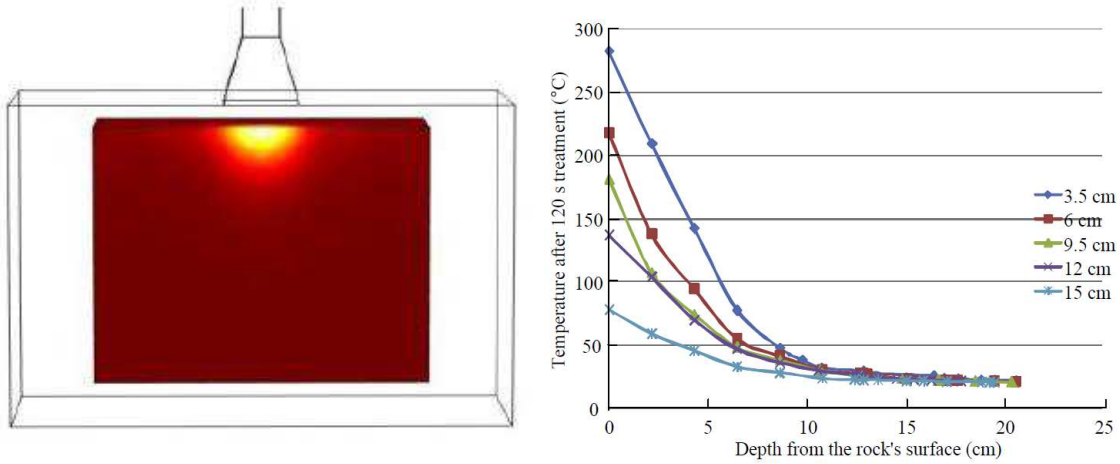

Figure 60: Left picture: Zone affected by microwaves on the surface of the block in front of the antenna and right picture: temperature vs. depth into the stack of rock slabs after 60 s of microwave treatment at six distances from the antenna and 10 kW power. (Nekoovaght 2015).

By means of small scale digitizing, it is assumed that crack propagation specifies the temperature distribution and finally the zone of absorbed power allocation. Based on figure 61, the volume of absorbed power by Granite is like a cone in which, there are high power and crack density near to the surface in comparison to the depth. The height of this cone is around 35mm. In another meaning, as granite is a bad wave absorber rock, it can be seen that the wave has penetrated only 3.5 cm into the rock.

Moreover, it can be concluded that due to the concentrated nature of the waving action and the extremely high temperatures at that zone (collision spot), the formation of cracks occurs at the surface until a certain point in the depth of the core where the shock wave eventually dies. This mechanism leads to the creation of uniform cracks starting right at the waving spot.

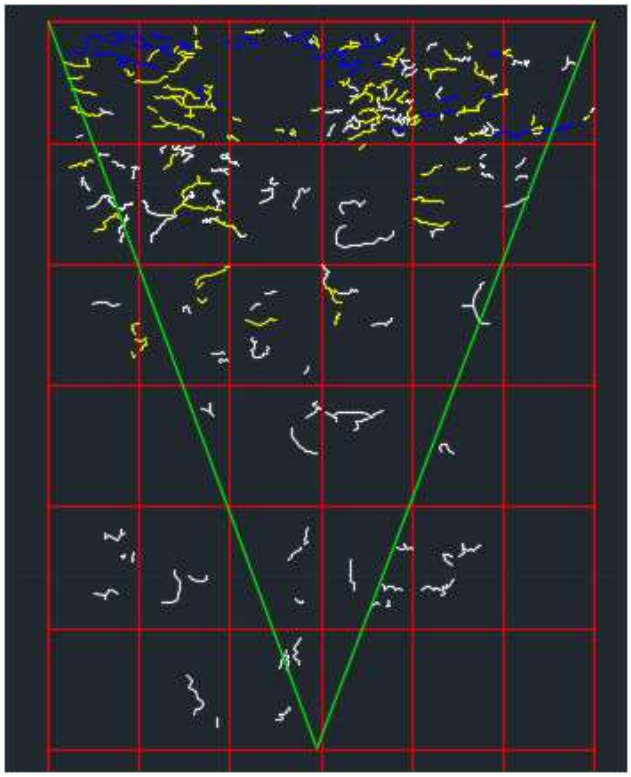

Figure 61: Absorbed power according to the micro crack density in a small cylinder (25mm width and 32.4 mm height)

Taking the experiment procedure into account, radial cracks disappeared at 10 cm below the surface whereas, microwave just could penetrate up to 3.5 cm to the depth. Therefore, there must be a stage between waving and crack formation that can be interpreted as a small thermal fracture taking place at the surface where the wave collides into the rock.

In addition, according to the micro cracks and radial cracks formation, it is assumed that the mode of crack generation is to some extent similar to the explosion. By definition, ‘explosion’ is an occurrence resulting in a sudden increase in volume and rapid release of energy. The theory of explosion suggests that as a result of the high radial compressive stresses in the vicinity of the borehole, an intense shear stress field develops close the borehole. In the shear failure zone, the rock is harshly crushed. The crushed zone is tracked by a severely fractured zone. In this zone, the crack density is very high and the damage is extreme. The action of the reflected stress waves from the free surface causes circumferential cracks reflects back into the rock mass in the form of tensile wave and leads to tensile stress concentration at tips of initiated cracks from the borehole and results in further propagation of

fractures. Therefore, tensile stresses which are concentric to the borehole cause local radial cracking.

Briefly, when an explosive is charged into the hole, a blast zone (Figure 62) is generated in the vicinity of the explosion on account of extreme radial pressures that supersede the strength of the rock. In this phase, zone 1, or crushed zone, happens when granular cracks exist, zone 2, or fracture zone, occurs at a short distance from the blast hole and contains radial cracks and finally, in Zone 3, or fragment zone, the rock will splinter to pieces and separates from its origin.

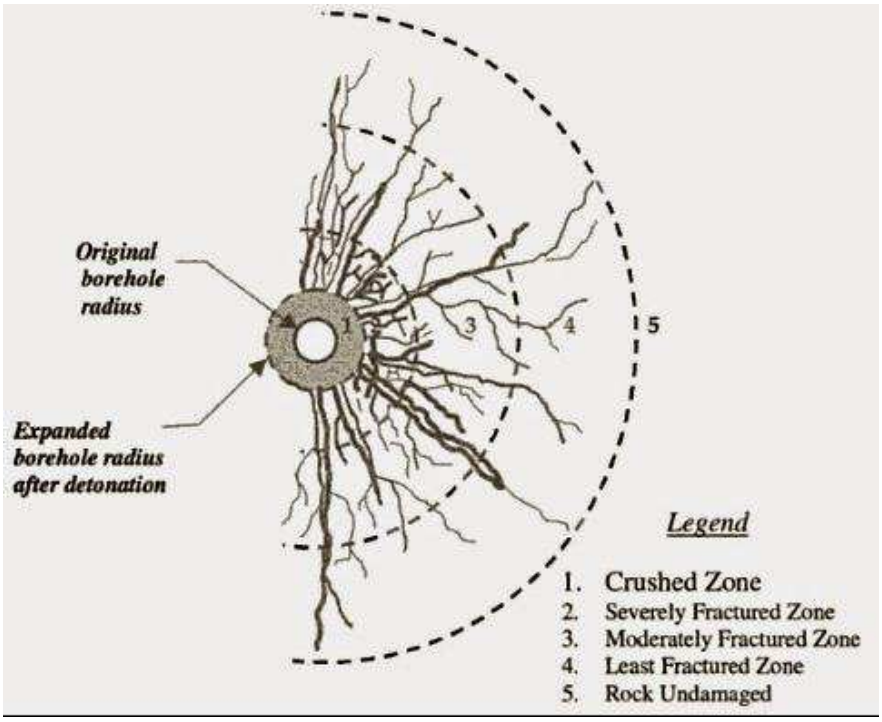

Figure 62: Crack formation by the explosion.

Consequently, the waves act as a heating power that it concentrates on the surface of granite and increases the temperature up to the maximum threshold (according to the thermal expansion coefficient of Granite), causing a thermal fracturing to take place that scatters pieces of the broken rock and creates a small hole in the size of 5 mm. In the performed experiments, the shock from fracture produces the same zone: Zone 1 (crushed) could be observed in a diameter of 2.5 cm around the waved spot (Figure 63) and Zone 2 (fractured) with longitudinal or radial cracks shaped right after it (Figure 64). Creation of Zone 3 was avoided due to safety reasons and to prevent the formation of hazardous fragments. Because if waving was being

continued, there could be high temperature in sample and at the end to some extend explosion would occur with rock flying. To further elaborate, with overlaying of crushed zone photo from CT and fracture zone, it could be seen that the initiation of longitudinal or radial cracks is completely from micro cracks zone.

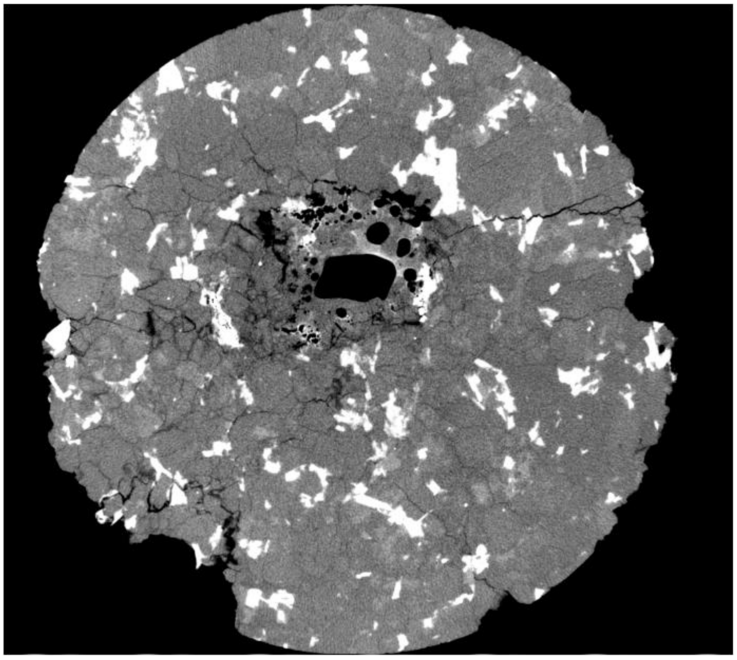

Figure 63: Top view (2.5cm diameter and 1mm below the face) of the Crushed zone by microwave (20KW) on Granite.

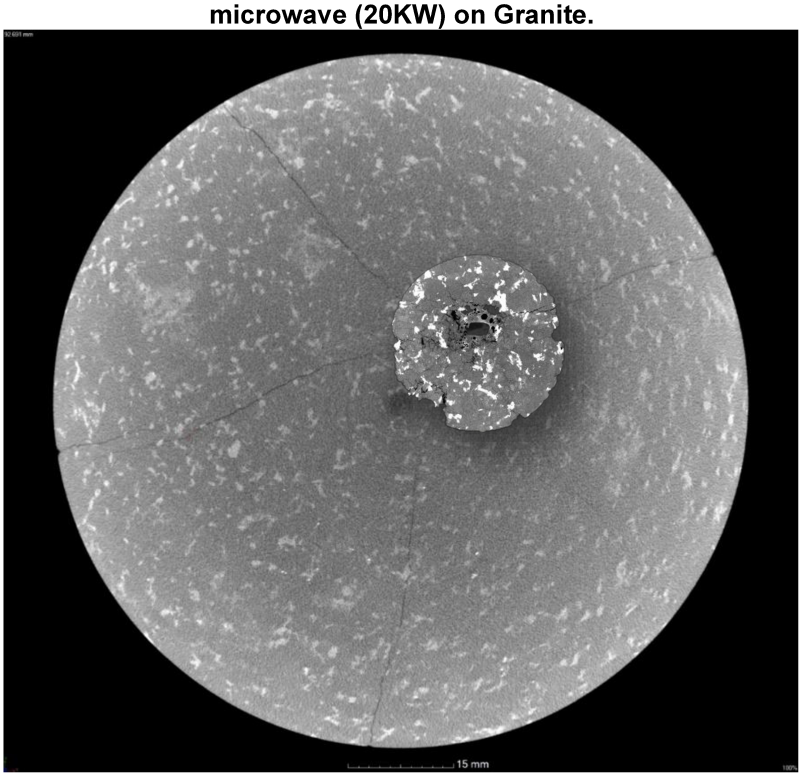

Figure 64: Top view (10 cm) mixing with crushed zone and radial cracks generated by microwave (20KW) on Granite.

The digitized model shows that the created cracks are not a consequence of heat generation. Microwave increases the temperature and volume at the collision spot, triggers a thermal fracture on the surface and the cracks start to form all the way through the sample by means of wave propagation, not heat generation.

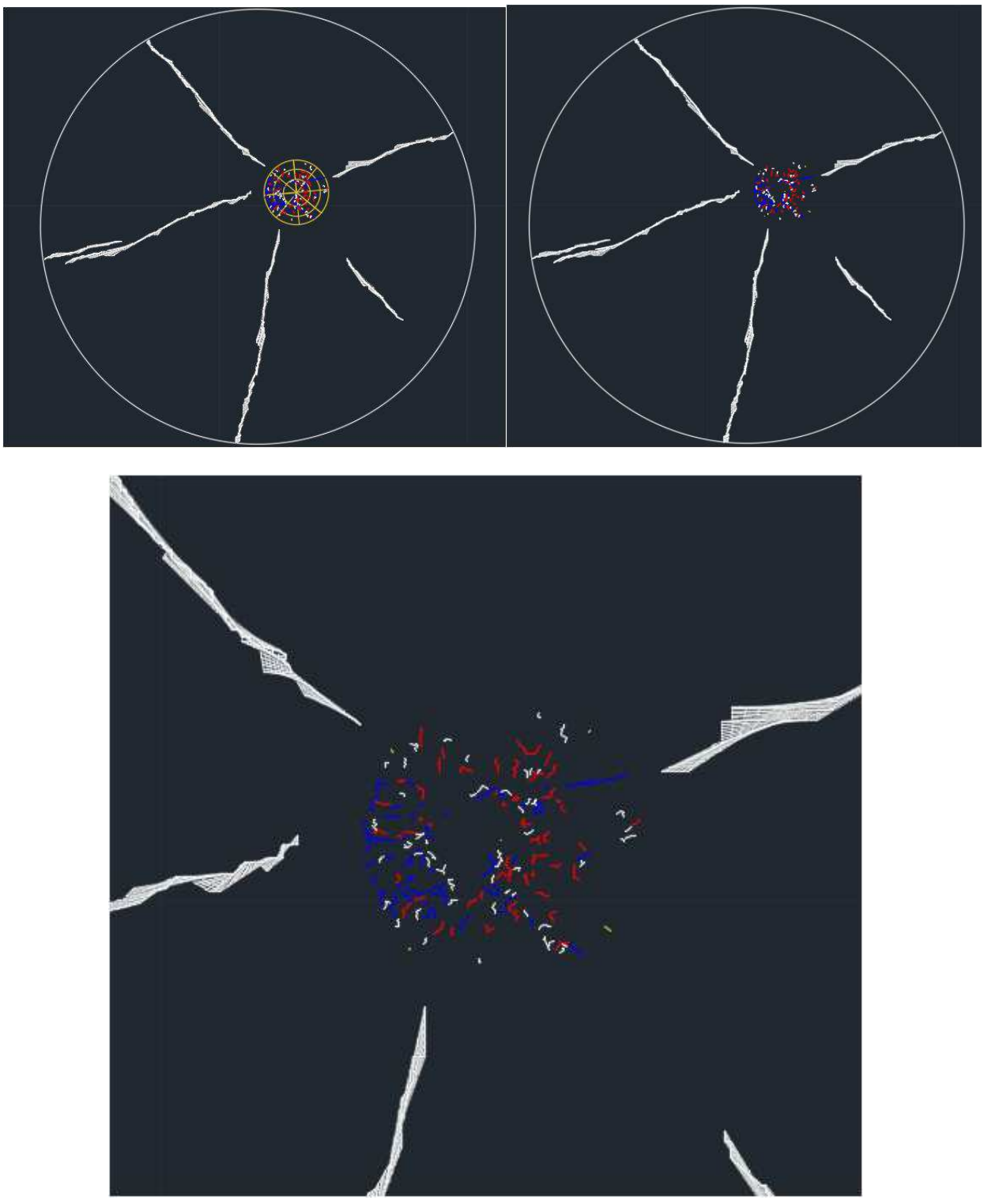

Figure 65: Digitizing of cracks in crushed zone and fracture zone with micro crack and radial crack generated by microwave (20KW) on Granite.

The procedure of crack formation could be compared by another method of rock fragmentation. Indenters, in which an indenter is settled down on the face of a sample and by pushing this toll gradually rock breakage occurs. In detail, rock deforms elastically at the initial loading stage. Then tensile cracks are initiated around the indenter and propagate. The rock under the intender are compressed into failure and crushed zone very slowly comes into begin. With increasing the loading behavior of crushed zone will be finished and transferred to another condition, in this case side cracks initiated from crushed zone. In this way by increasing the power behind intender each steps appears respectively. In another meaning, by means of a specific loading crushed zone comes out and next zone with longitudinal cracks occurs after implementing the high load on intender. (H. L Liu et al 2002)

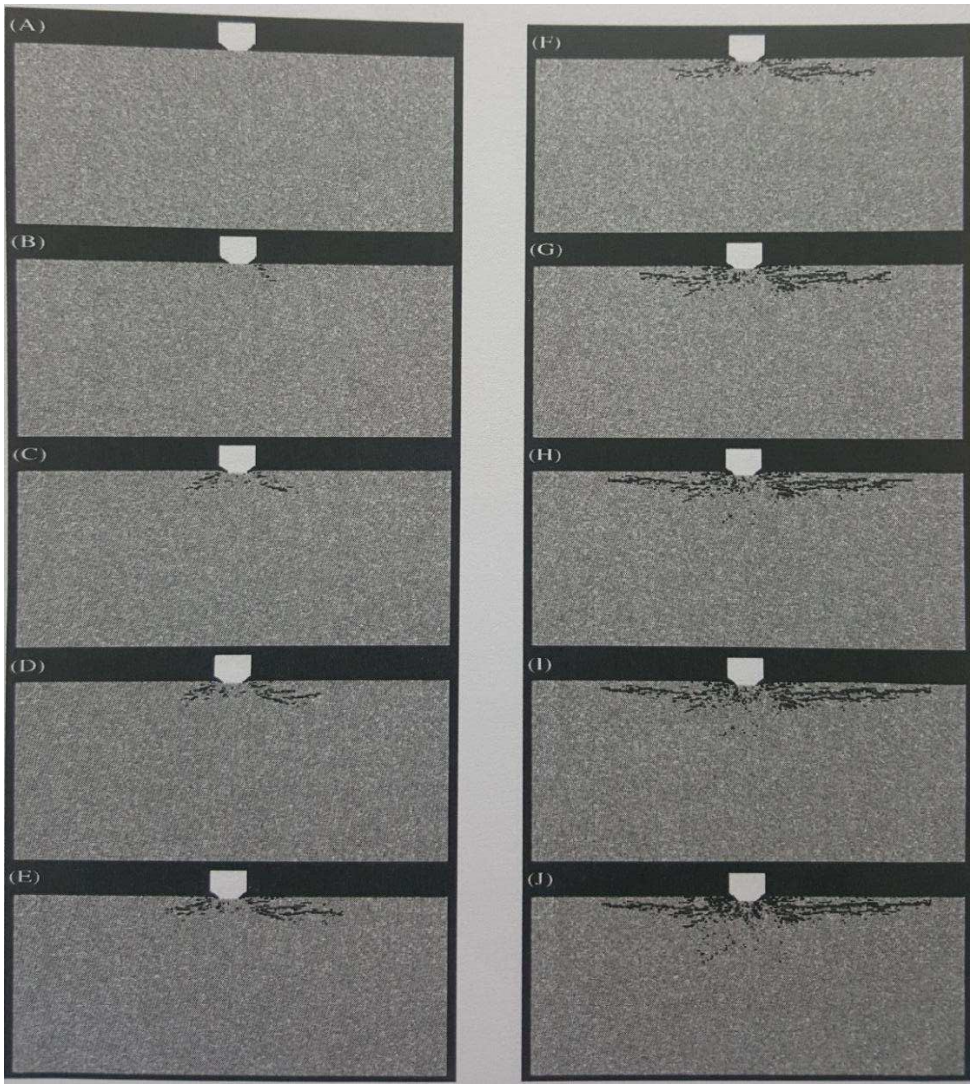

Figure 66: Rock fragmentation process induced by an indenter. (H. Y. Liu et, al 2002)

To have these 2 zones (crushed zone and fracture zone) simultaneously, it was suggested to have the high load behind the indenter from the beginning. In another meaning, instead of small load to get crushed zone and then raising this power to catch next zone, a very high pressure acted on the face of a sample. For this experiment not only there was no proper crushed zone but also the direction of fragmentation was different. So it is concluded that to get zones for rock breakage, load must be applied step by step with the help of indenter.

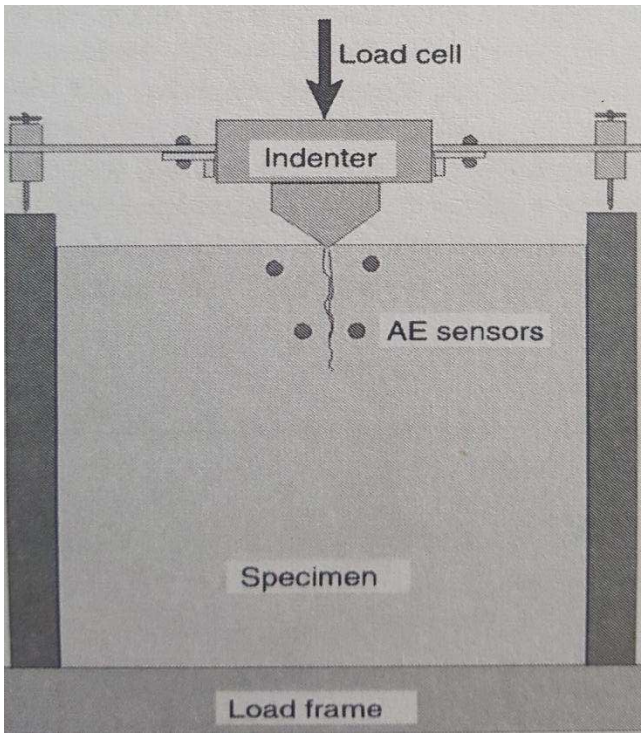

Figure 67: Rock breakage by high pressure indenter (L. H. chen et al, 2006)

With the help of these experiments, it could assumed that the result of the rock breakage at the end of first test is somehow similar to wave treated granite (there are crushed zone and fractured zone at the end) but there is a difference in steps of procedures. As discussed before crushed zone and fracture zone in wave treated sample occurs at the same time or maybe with very tiny delay. However, this trend for indenter needs to happen in 2steps by increasing the load of indenter.

Finally, it could be concluded that rock breakage by explosion, indenter and waving create the somehow the similar ending with having separated zoned on the sample. However, according to what described above this procedure to some extend between explosion and waving is equal and happens very quickly in a row.

7 Conclusion and Recommendation

Based on what was described in sections above, one of the most effective methods to break rock and create cracks is microwave irradiation. This wave, by increasing the friction between the molecules of rock, raises up the temperature until special threshold. Afterward, this heating as well as molecular interactions causes crack formation inside the rock.

As it was discussed, in small-scale experiments, the water content is one of the most effective parameters that can increase the temperature of the sample in comparison to an intact one. Water intensifies the molecular interaction within the sample, however, by adding salt, ionic interaction increases as well. Therefore, a saturated sample with a mixture of salt receives more microwave, hence, temperature escalates until a maximum rate which is required for fracture creation in rock samples.

For the large-scale block (Granite), a different irradiating machine was utilized; a high power industrial microwave, as opposed to the domestic machines, in which radiation was not comprehensive and focused on the surface of the sample.

Samples were exposed from the surface as microwave radiated only toward one spot right under the antenna (spot microwaving). This wave heated up the sample to 600 °C while cracks were being generated simultaneously on it.

Based on a sketch drawn from the data taken by computer tomography, it was figured out that there was a small hole as a result of the wave that caused thermal fracturing on the surface. The shock of this fracturing process created micro cracks and radial cracks around the spot of collision.

It could be confirmed from the digitizing that crack propagation in the household microwave is related, to the increase of temperature. Additionally, in an industrial microwave and considering its influence on granite, raising the temperature is a source for thermal fracturing on the surface and this phenomenon later generates the following cracks inside the block.

In summary, the processes of rock breakage by high power microwave are:

1. Microwave radiation.
2. Increasing the temperature of the small area of the surface under the antenna.
3. Generation of Thermal fracturing on the surface of the sample.
4. Propagation of micro and radial cracks.

Recommendation:

Rock breakage and creating crack could decrease the rock parameters for the next process. By implementing microwave radiation on the face of the rock before blasting, not only there will be time-saving for drilling phases but also it may reduce the amount of used explosive in boreholes. Moreover, as a result of the crack network, it can be calculated for drilling less hole for the explosion. This could be applied to the face of hard rock in tunneling to weakening it before blasting.

8 Bibliography

Baden Fuller AJ, (1979), Microwaves : an introduction to microwave theory and techniques, 2nd Edition, Pergamon, Oxford, ISBN 0 08 024228 6

Esen S., Onederra I., Bilgin H.A, (2003): Modelling the size of the crushed zone around a blasthole, International Journal of Rock Mechanics & Mining Sciences

Food and Environmental Hygiene Department (FEHD) of the Government of the Hong Kong, (2005).

Giancoli DC, (1988): Physics for scientists and engineers, 2nd Edition.

Gwarek, W. K and Celuch-Marcysiak, M. (2004). A review of microwave power applications in industry and research. Proceedings of 15th International conference on Microwaves, Radar and Wireless Communications.. p. 843 - 848.

Hartlieb Ph, (2013): Investigations on the effects of microwaves on hard rock. PhD thesis, Montan university of Leoben.

Hassani F, Nekoovaght P.M (2012): Microwave assisted mechanical rock breaking. Department of Mining and Materials Engineering, McGill University, Harmonising Rock Engineering and the Environment – Qian & Zhou (eds) © 2012 Taylor & Francis Group, London, ISBN 978-0-415-80444.

Hassani F, Nekoovaght P.M, Gharib N, (2015): The influence of microwave irradiation on rocks for microwaveassisted underground excavation. Journal of Rock Mechanics and Geotechnical Engineering.

Hassani F, Nekoovaght P.M. The development of microwave assisted machineries to break hard rocks. Department of Mining and Materials Engineering, McGill University.

Hassani F, Nekoovaght P (2016): The influence of microwave irradiation on rocks for microwave assisted underground excavation. Journal of Rock Mechanics and Geotechnical Engineering.

Jacob J, Chia L.H.L and Boey F.Y.C, (1995): Review of thermal and non-thermal interaction of microwave radiation with materials. Journal of materials science, p. 5123-5327

Jones D.A (2004): Understanding Microwave Treatment of Ores. PhD thesis, University of Nottingham. p. 15-20

Kobusheshe J. (2010): Microwave enhanced processing of ores. PhD thesis, University of Nottingham. p. 25-40

Linn H, Möller M. (2005) Dielectric heating: http://www.linn-high therm.de/fileadmin/user_upload/pages/about_us/download/publications/ white_papers/Dielectric_heating.pdf

Meisels R, Toifl M, Hartlieb P, Kuchar F, Antretter T (2015): Microwave propagation and absorption and its thermo-mechanical consequences in heterogeneous rocks. International Journal of Mineral Processing.(Volume 135,)

Meredith, R. (1998) Engineers' Handbook of Industrial Microwave Heating. The Institution of Electrical Engineers, London.

Nekoovaght P. (2009): An investigation on the influence of microwave energy on basic mechanical properties of hard rocks. Master thesis, The Department of Building, Civil and Environmental Engineering. p. 50-60

Nekoovaght P. (2015). Physical and mechanical properties of rocks exposed to microwave irradiation. PhD thesis, The Department of Building, Civil and Environmental Engineering. p. 1-10

Osepchuk, J. M. (1984). A history of microwave heating applications. IEEE Transaction microwave theory and techniques. p. 1200 - 1227.

Peinsitt, T. (2009). Demonstration of the feasibility of weakening rocks with microwave techniques. Master thesis, Graz University of Technology, Graz.

Pickles, C. A. (2009). Microwaves in extractive metallurgy: Part 1 – Review of fundamentals. Minerals Engineering. p. 1102–1111.

Propagation of an Electromagnetic wave, the physic classroom http: http://www.physicsclassroom.com/mmedia/waves/em.cfm

Rostami J: Mechanical rock breakage section. SME (Third edition)

Santos T., L. C. Costa, M. Valente, J. Monteiro, J. Sousa. (2010): 3D Electromagnetic Field Simulation in Microwave Ovens: a Tool to Control Thermal Runaway, 1Physics Department, University of Aveiro, 3810-193 Aveiro,

Scott, G. (2006): Microwave pretreatment of a low grade copper ore to enhance milling performance and liberation. Chemical masters of science in engineering, Stellenbosch University. p. 1-50

Stuchly S.S. Stuchly M.A., (1983): Industrial, scientific, medical and domestic applications of microwaves, IEE Proceedings, vol 30, p. 480 – 500

Sumnu, G., Sahin, S. & Da-Wen, S. (2005) Recent Developments in Microwave Heating. Emerging Technologies for Food Processing. London, Academic Press.

Telford, W.M.; Geldart, L.P.; Sheriff, R.E. Appleid geophysics 2nd edition, 1990.

Toifl M, (2016): Numerical study of microwave induced stress and damage formation in heterogeneous rocks. PhD thesis, Montan university Leoben.

Vorster W, (2001): The effect of microwave on mineral processing, PhD thesis, University of Birmingham.

Walkiewicz, J.W.; Clark, E. and McGill, S.L. (1991). Microwave-Assisted Grinding. p. 239 - 243.

Whittaker BN, Singh RN, Sun G. (1992). Rock fracture mechanics principles, design and applications.

9 List of figures

10 List of tables

11 List of abbreviations

ÖGI	Österreichisches Gießerei Institut
CT	Computer Tomography
ms	millisecond
MHz	Mega Hertz
GHz	Giga Hertz
W	Watt
KW	Kilowatt
MW	Megawatt
RF	Radio Frequency
ucs	Uniaxial Compressive Strength
CAI	Cerchar Abrasivity Index
SMC	Sandvik Mining and Construction
TBM	Tunnel Boring Machine
A	Ampere
MPa	megapascal
Nm	Newton Meter
°C	Celsius
µm	micrometer
cm	Centimeter
f	Frequency range

Appendix

A: Processes of crack digitizing for big cylinder:

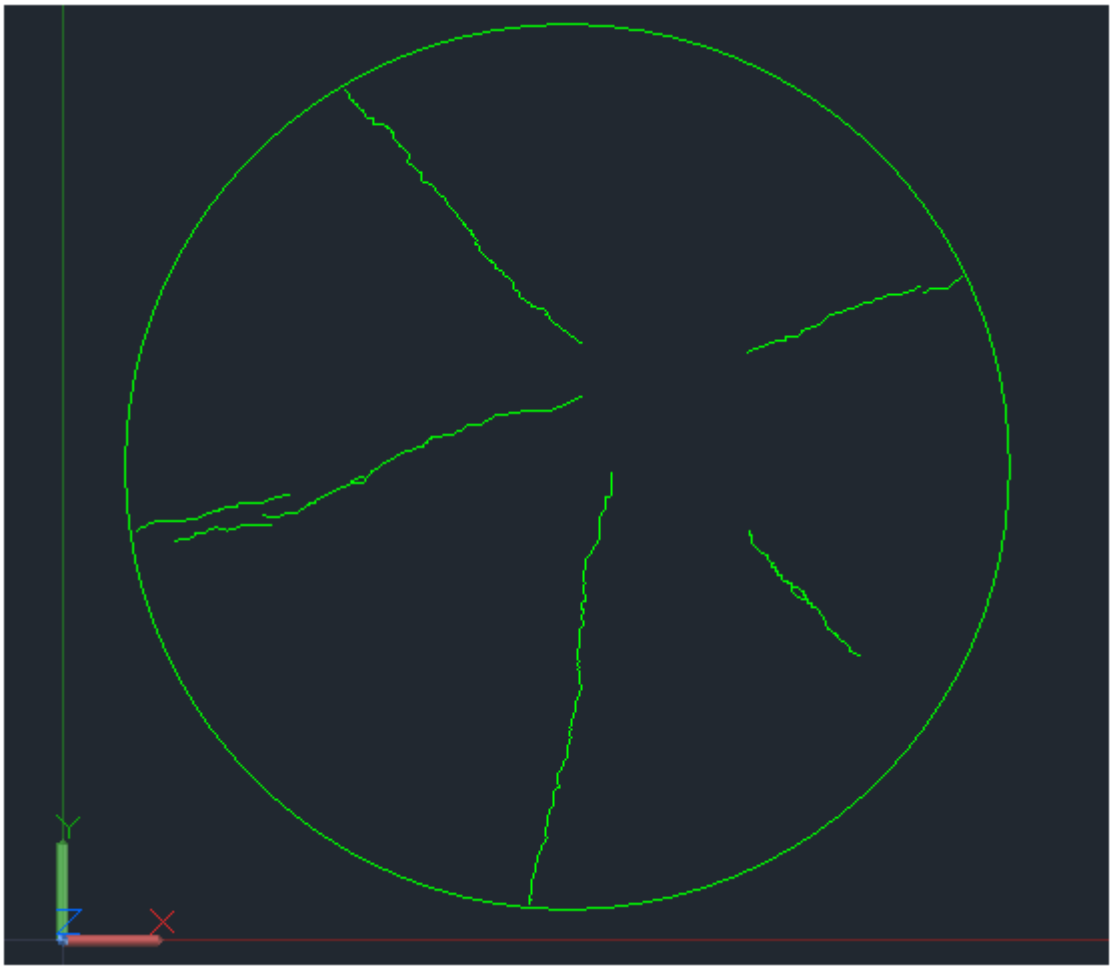

Figure A 1: Simulation of radial cracks on top view

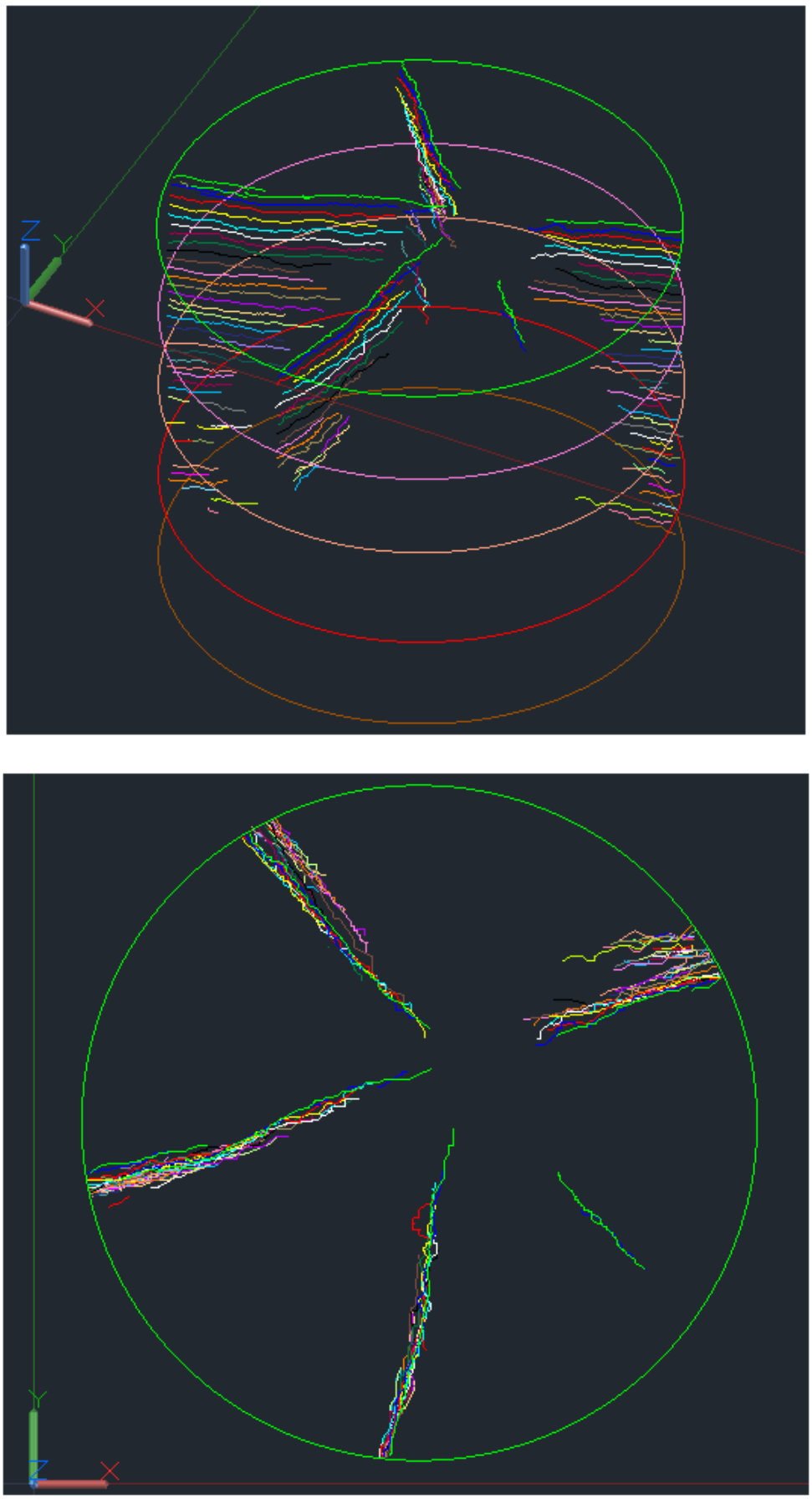

Figure A 2: Simulation of all radial cracks on top view.

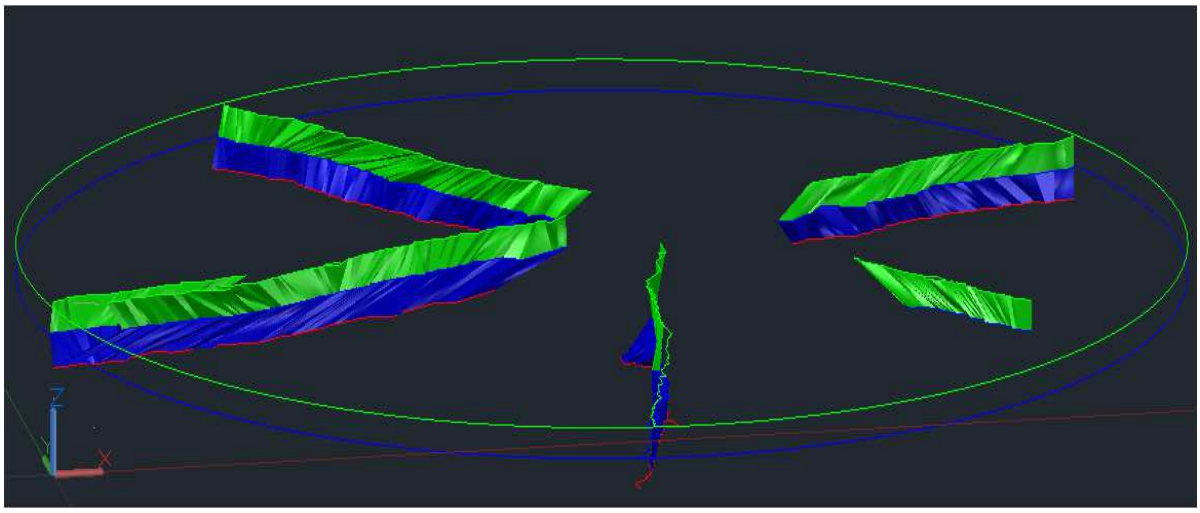

Figure A 3: Cracks connection by creating solid surface.

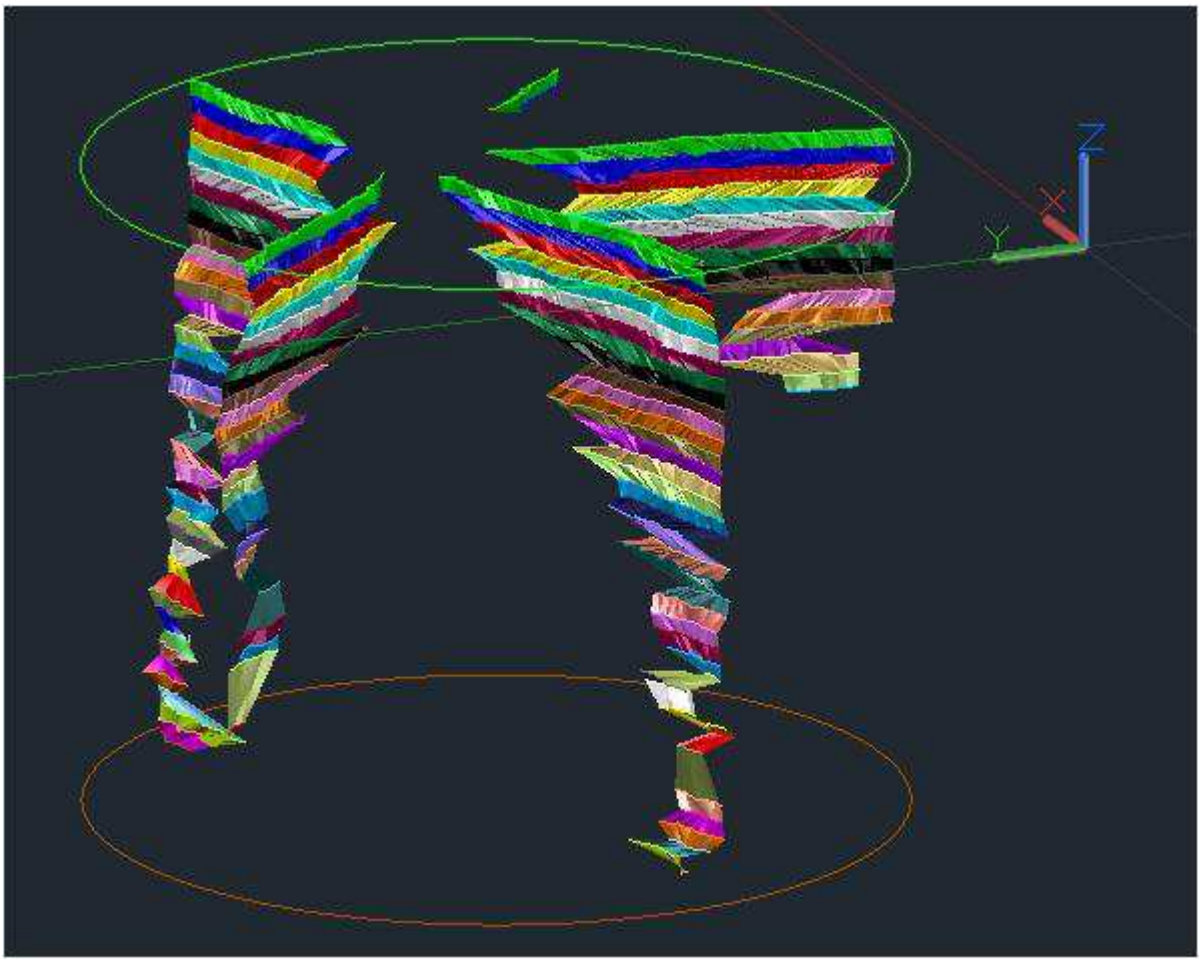

Figure A 4: Simulation of all horizontal cracks with solid surface connection between cracks.

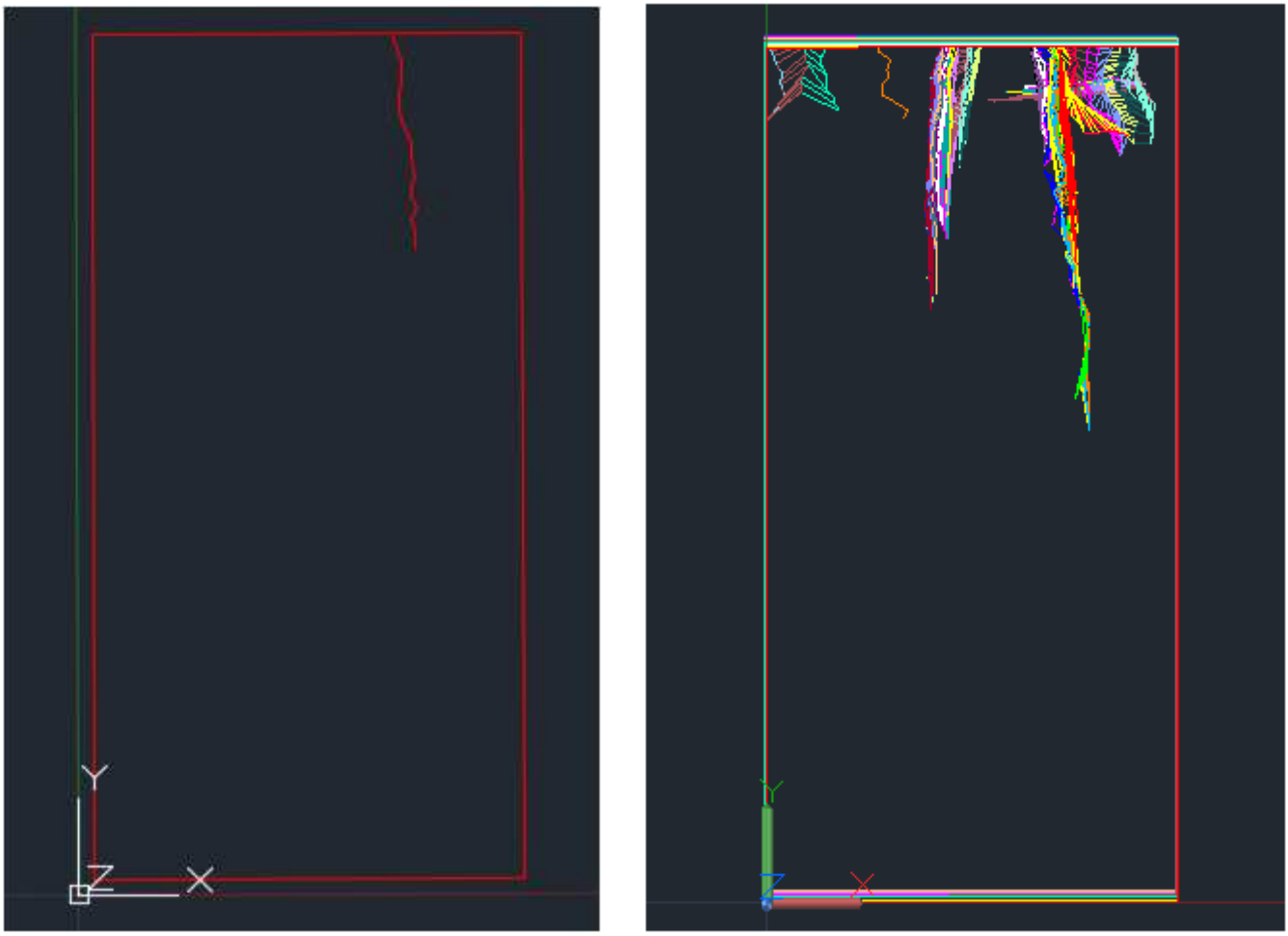

Figure A 5: Digitizing the vertical cracks form front view of drilled core.

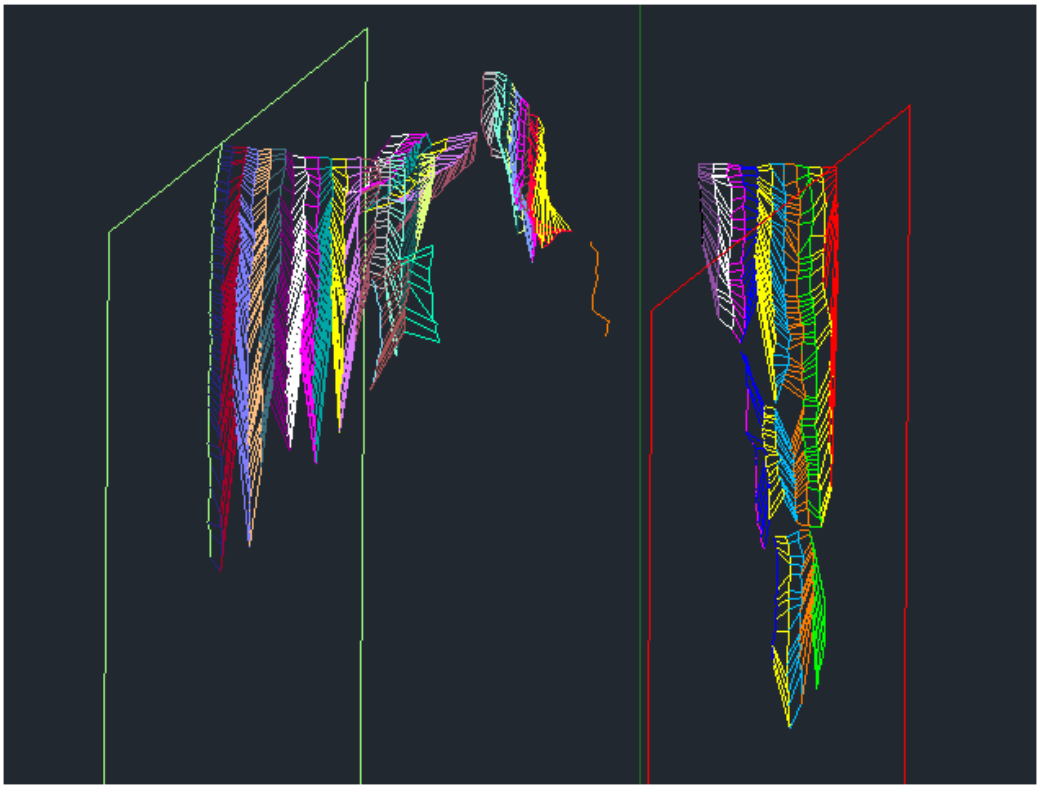

Figure A 6: Crack connection by creating network surface.

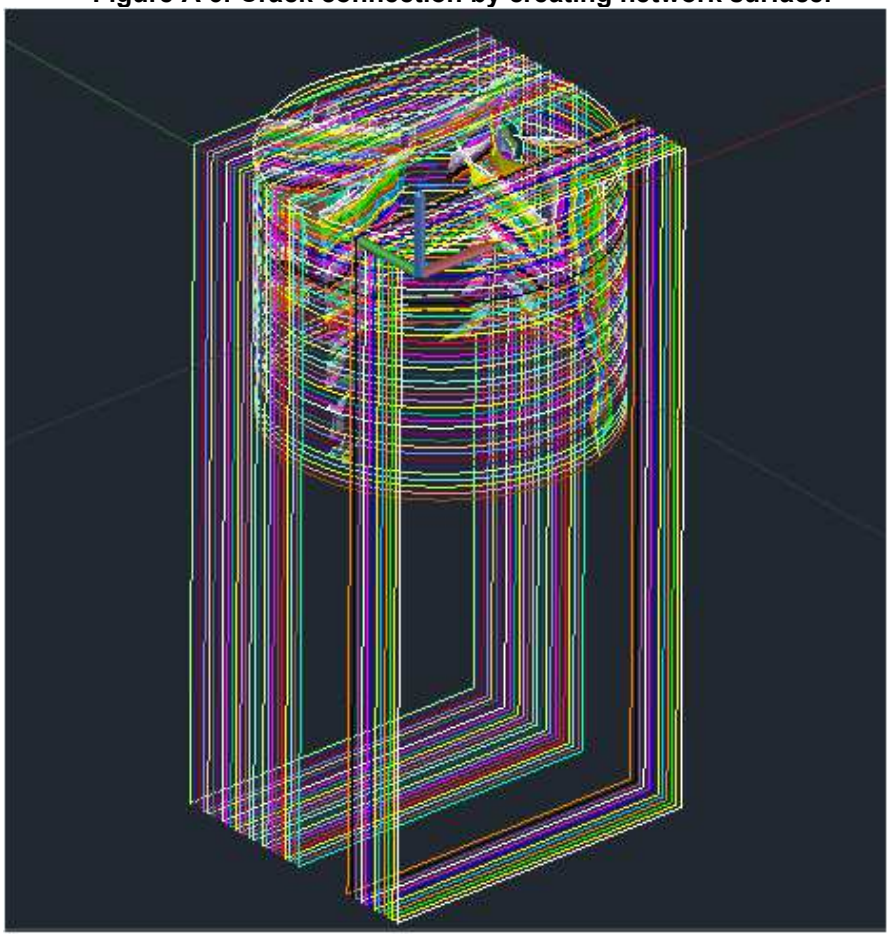

Figure A 7: Overlaying the top view and the front view including all cracks.

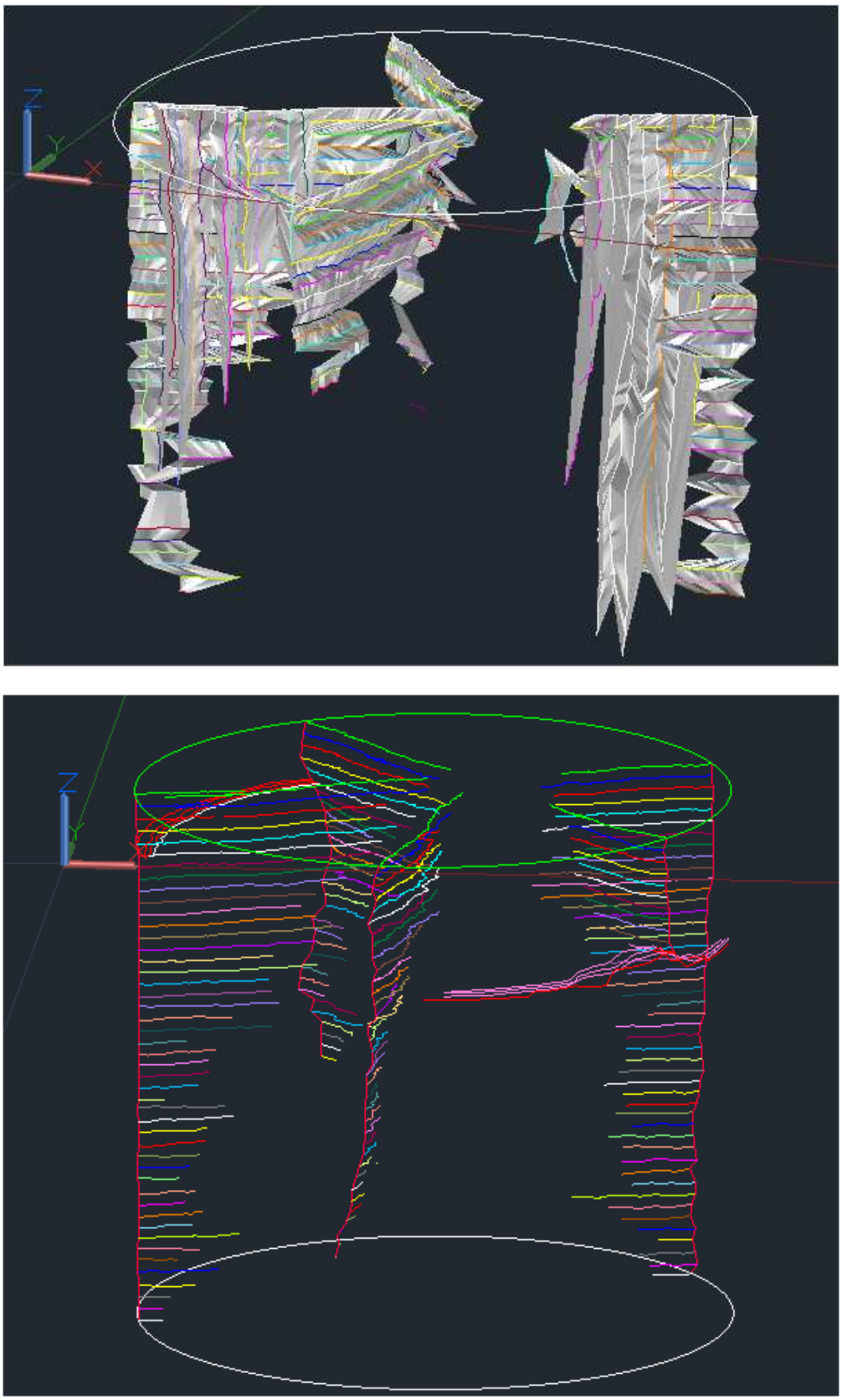

Figure A 8: Mixing the vertical and the horizontal cracks to have a constant crack network.

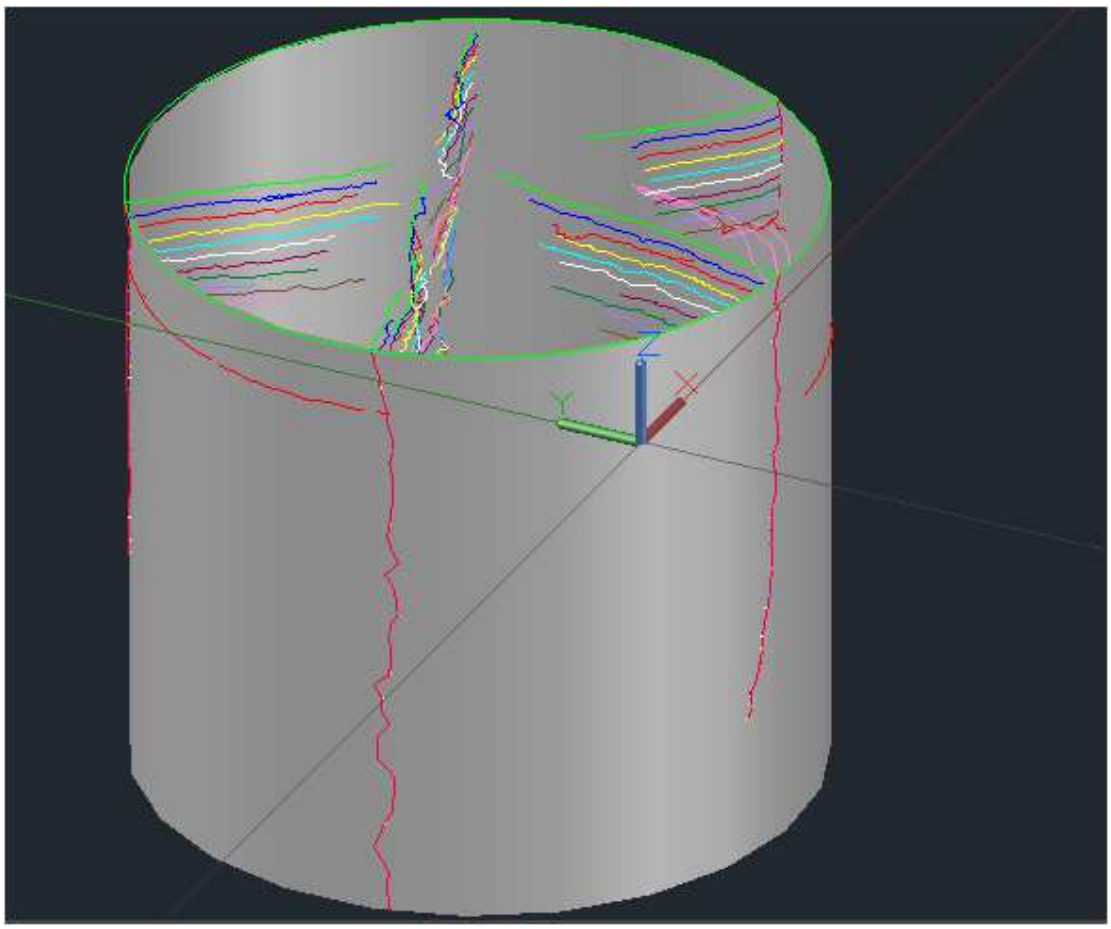

Figure A 9: Simulation of treated core by microwave contains all cracks.